**Title**
Engineering of Glycosaminoglycans for Anti-Inflammatory Tissue Engineering Applications



**Author**
Nguyen, Michael Binh

**Publication Date**
2022

Peer reviewed|Thesis/dissertation

Engineering of Glycosaminoglycans for Anti-Inflammatory Tissue Engineering Applications

By

MICHAEL NGUYEN
DISSERTATION

Submitted in partial satisfaction of the requirements for the degree of

DOCTOR OF PHILOSOPHY

in

Biomedical Engineering

in the

OFFICE OF GRADUATE STUDIES

of the

UNIVERSITY OF CALIFORNIA

DAVIS

Approved:

Alyssa Panitch, Chair

Julie Liu

Kent Leach

Committee in Charge

2022

# Acknowledgements

The past five years of my life working on my dissertation research have been a long and sometimes stressful journey, and it all wouldn't have been possible without the support of everyone around me. My family, my friends, my collaborators, my mentors, and my funding sources all contributed to where I am today.

I would like to first thank my parents Khanh-Ngoc Nguyen and Dien Nguyen for all they have done for me throughout my entire life. Throughout my doctoral studies, they have supported and encouraged me, and always pushed me to keep on going despite how difficult work got. I also want to thank my sister Kaitlyn "Architectural Wunderkind" Nguyen and James "Master of the Electrolytic Arts" Nguyen for their support during this process as well. All the times we laughed together or argued about stupid stuff like the sandwich status of clam chowder bread bowls or the quality of Cars 2 helped to make my time as a graduate student more bearable.

None of this work would have been possible without my extremely supportive research mentor Dr. Alyssa Panitch. Through her mentorship over the years, I have grown as a researcher in this fascinating field of tissue engineering and glycobiology. Not only did she teach me how to conduct research, but she always encouraged me when results were bad and celebrated with me when results were good. In addition, I also want to thank Dr. Julie Liu and Dr. Kent Leach, whose input into my work has been invaluable in pushing my research forward. My lab mates in the Panitch lab, both past and present have been a great help to my growth as a scientist as well. Dr. Tanaya Walimbe and Dr. Nelda Vázquez-Portalatín took time out of their own research schedules to help teach me how to conduct experiences, and their instruction has helped me get to where I am now. In addition, Dr. Vanessa Dartora, Dr. Tima Dehghani, Dr. Marcus Deloney, and soon to be doctors Hark Sodhi, and Laney Casella were all more than willing to help whenever I had questions, and their help has been invaluable.

My friends, both in and outside the department, have made this graduate student life more bearable, especially when times got rough. Fellow BMEGG members Shahin Shams and Robert Gresham have both provided critical assistance with my research when I needed last minute supplies or equipment as well as been there when I

needed someone to complain about research too. My friends outside the department, Blake Vilchez, Nathan Yoshino, Tait Weicht, Jason Huang, Brian Knight, and the other members of the Michael Squad Michael Ragone and Michael Stokes have made these five years so much more enjoyable.

Finally, I would like to thank my funding sources for their support in my research: NIH Training Grant in Cardiovascular Sciences and the Schwall Family Fellowship.

# Abstract

Proteoglycans are a class of biomolecules that play an important and ubiquitous role in the body, with their roles ranging from maintaining tissue mechanical properties to regulating cell signaling. Many of these functions are carried out by the glycosaminoglycan (GAG) chains that decorate the proteoglycan core protein, with glycans chondroitin sulfate (CS), dermatan sulfate, and heparan sulfate regulating growth factors and water content through their negatively charged polysaccharide chains. Additionally, the free-floating GAGs heparin and hyaluronic acid (HA) play important roles in tissue function, such as modulation of enzymes and supporting cell mobility. Because of their important biological roles, as well as their relatively simple structure, multiple easily accessible reactive moieties, and commercial availability, many groups have sought to GAGs for biomedical applications.

In this dissertation, we explore the engineering of GAGs to suppress inflammation, starting with a study regarding the balance of the chemical modification of GAGs and the perseveration of their bioactivity. Here, we discuss the fabrication of hydrogels from thiolated CS (CS-SH) and thiolated HA (HA-SH), demonstrating how increased thiolation of these GAGs impairs their recognition by hyaluronidase and GAG-targeting peptides, suggesting reduced biorecognition. Subsequent studies build off these findings, with these DPN hydrogels employed in the context of osteoarthritic joint inflammation. Articular chondrocytes encapsulated in GAG DPN hydrogels demonstrated a suppressed inflammatory response, as shown through reduced secretion of pro-inflammatory cytokines and reduced proliferation. Finally, the GAGs CS and heparin were conjugated with collagen targeting peptides to prevent platelet activation following endothelial denudation. The spacer sequence and C-terminal modification of the peptides were optimized to improve conjugation efficiency and collagen binding ability, improving the effectiveness of the peptide-glycan molecule. Overall, these studies serve as groundwork studies for the engineering of GAGs in the contexts of the prevention of inflammation through balancing the modification of GAGs for increased functionality with the preservation of the potent bioactive signals from the GAG themselves.

# Table of Contents

# List of Figures

# List of Tables

# 1. Introduction

### 1.1: Significance of Proteoglycans and Glycosaminoglycans

Proteoglycans (PGs) are a class of biomolecules comprised of a protein core with one or more glycosaminoglycan (GAG) side chains attached[1]. GAGs themselves are polysaccharides comprised of a repeating disaccharide structure, usually a uronic sugar and amino sugar. GAGs can be either be sulfated or unsulfated. Sulfated GAGs include heparin, heparan sulfate (HS), chondroitin sulfate (CS), dermatan sulfate (DS), and keratin sulfate (KS), with most sulfated GAGs being found attached to a core protein in a PG. In contrast, hyaluronic acid (HA) is the only unsulfated GAG as is found as a free-floating component of the extracellular matrix (ECM), not attached to any core protein[1].

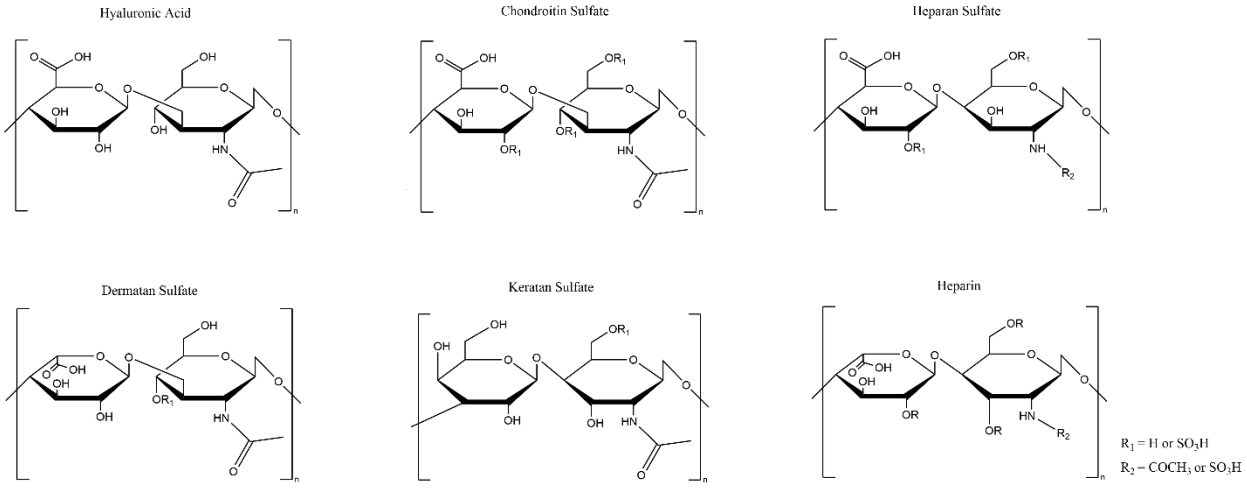


*Figure 1.1: Structure of glycosaminoglycans hyaluronic acid, chondroitin sulfate, heparan sulfate, dermatan sulfate, keratan sulfate, and heparin*

PGs are found throughout the body and play important roles in proper tissue function, with the form and core protein sequence dictated by this function. PGs can be roughly divided into several

categories: HA-binding modular PGs, modular PGs that do not bind to HA, and small leucine-rich PGs (SLRPs) [1,2]. Modular PGs that binding to HA, also known as hyalectans, consist of a central domain decorated with GAG chains flanked by a HA binding domain and a lectin binding domain[1]. This central domain can be decorated with a wide range of GAG chains, spanning three to one hundred. In contrast, modular non-HA-binding PGs will vary more in their form and sequence. Finally, SLRPs are relatively small PGs that contain leucine-rich repeat units in their core protein[1]. PGs exist as both extracellular and cell membrane bound molecules. While the function of cell membrane bound PGs generally revolves around cell-matrix interactions, the roles of extracellular PGs is more diverse. These functions can be generally broken down into four categories: modulation of tissue mechanical properties, regulation and protection of the ECM, sequestration of proteins, and regulation of cell signaling (figure 1). In most of these cases, this function is carried out by or in part by the GAG chains attached to the protein core.

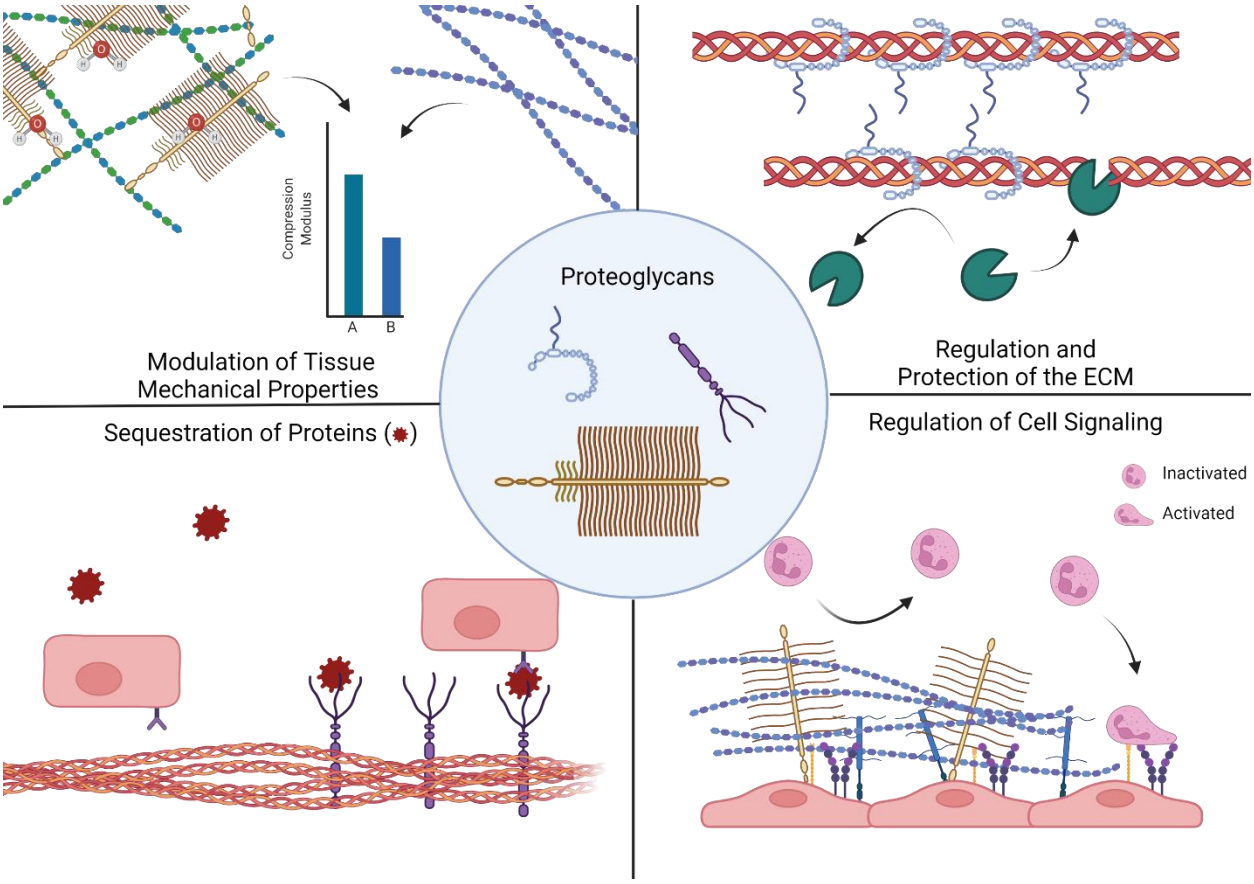

*Figure 1.2: Functions of Proteoglycans (created with biorender.com)*

Modulation of mechanical properties by PGs is often mediated through the attached GAG chains, as these negatively charged polymers are able to mediate the uptake and retention of water into the tissue. In the case of the hyalectan aggrecan, its large number of GAG chains and HA binding domain maintain a high water content in cartilage, endowing compressive strength through osmotic pressure[3,4]. Regulation and protection of the ECM is commonly done through PG binding to ECM components, such as how the SLRPs decorin and biglycan bind to collagen fibrils through their protein core[5,6]. Binding to collagen accomplishes two significant tasks: directing fibril formation and orientation and protecting against degradation[5–7]. By binding to a collagen fibril, the attached DS chain(s) will act as a spacer, aligning and orienting the collagen fibrils properly[8–10]. Furthermore, the bound PGs and their GAG chains block collagenases including matrix metalloproteinases (MMPs), preventing unnecessary degradation of collagen[7,11–13]. For the sequestration of proteins, PGs such as perlecan bind to growth factors like vascular endothelial growth factor (VEGF) through its HS chains while the PG core is anchored in the basement membrane of various tissues[14]. This can create gradients of growth factors to direct cell function and chemotaxis[14–17]. Finally, the GAG chains of PGs can modulate cell signaling through physically blocking cell-cell interactions. This can be seen in the glycocalyx, a PG rich region that lines the endothelium, where the PGs and GAGs that make it up prevent leukocytes from interacting with the underlying endothelial cells, preventing their activation[18–20]. As such, GAGs and PGs play a key role in a myriad of different functions throughout the body.

**1.2: Articular Cartilage**

One tissue where the importance of PGs and GAGs is well apparent is articular cartilage. Articular cartilage is a tissue primarily comprised of collagen type II, HA, and PGs such as aggrecan and biglycan[4,21]. Aggrecan is a large PG comprised of protein core decorated with ~60 KS chains and ~100 CS chains.

Aggrecan is immobilized in cartilage through a link protein that tethers it to HA and forms large aggregate complexes with HA and collagen[4]. Through its large number of sGAG chains, aggrecan promotes the retention and uptake of water in cartilage, giving cartilage its compressive strength and shock absorbing capabilities. In addition to aggrecan, other PGs are present in cartilage[4]. Biglycan and decorin are comprised of a collagen binding core protein with either one or two DS chains attached, in the cases of decorin and biglycan respectively[4,12]. These PGs regulate collagen fibril formation and protect against degradation through this collagen binding activity along with their attached GAG chain[12].

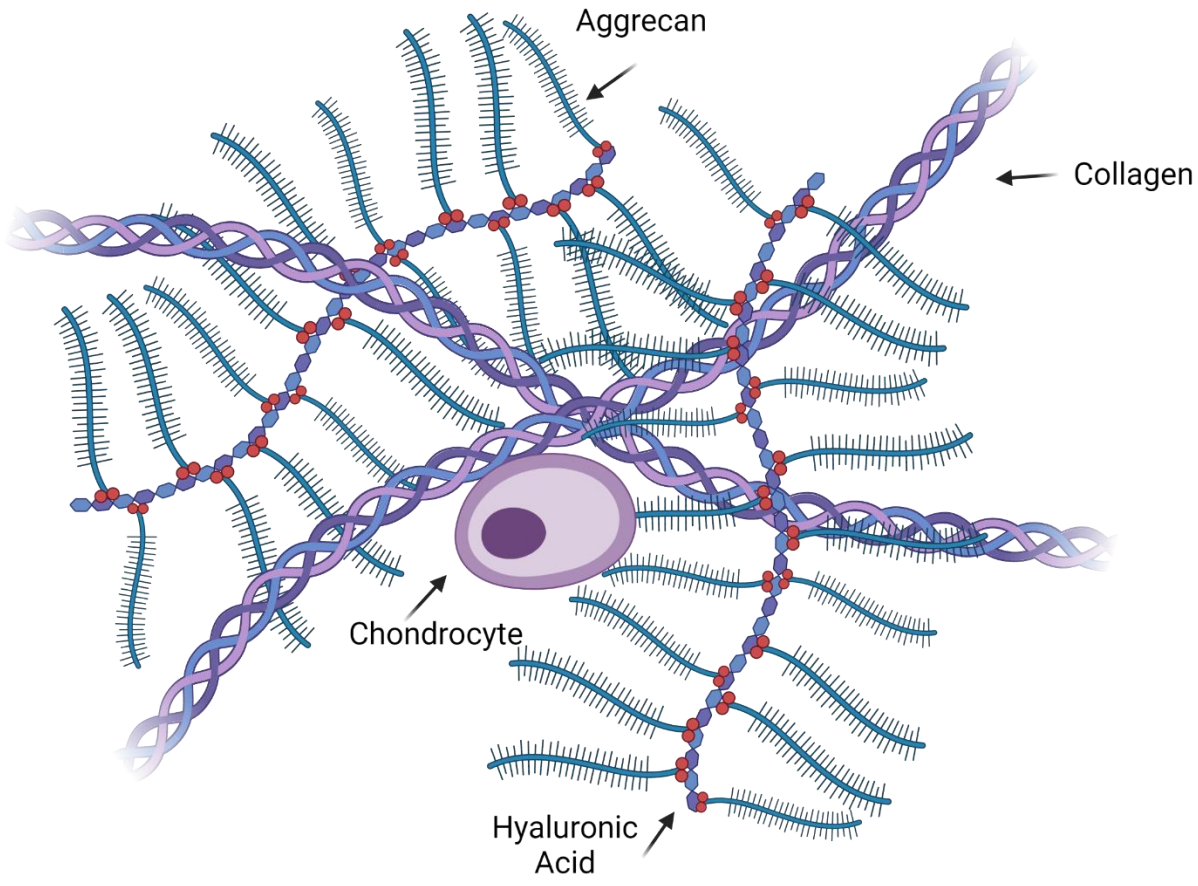


*Figure 1.3: Structure of cartilage extracellular matrix (created with Biorender.com)*

Cartilage is populated by resident chondrocytes and is avascular, with the nutrients required being delivered through diffusion from the synovial fluid[22]. These chondrocytes are responsible for the maintenance of the cartilage ECM through a tightly regulated cycle of the turnover of ECM components. In contrast with many other tissue types, cartilage is relatively sparsely populated by cells, with differentiated chondrocytes having limited proliferative capabilities[23]. As such, significant damage to cartilage is rarely healed by the body due to the poor regenerative capacity of chondrocytes[23,24].

### 1.2.1: Osteoarthritis

Osteoarthritis (OA) is a degenerative cartilage disease characterized by the loss of cartilage through its degradation. Under normal physiological conditions, the remodeling and turnover of cartilage components is well regulated by the resident chondrocytes[25]. However, under OA conditions, this homeostasis is disrupted and chondrocytes shift to an increased catabolic state, resulting in the gradual degradation of the articular surface. This degradation is carried out through increases in the production of collagenases such as MMP13[26] and aggrecanases such as the ADAMTS family[27]. In addition, it is believed that the HA turnover that occurs in healthy cartilage is disrupted, leading to loss of HA and the aggrecan tethered to it[28,29], though the mechanism of this HA degradation is still debated[30–33].

#### 1.2.1.1: Inflammation in Osteoarthritis

While previously thought of as a condition that arises due to mechanical wear of the cartilage, the current understanding of OA is that pro-inflammatory cytokines such as interleukin 1α and 1β (Il-1α, Il-1β)[34], tumor necrosis factor alpha (TNF-α)[35], and oncostatin M (OM)[36] play a significant role in the pathogenesis of OA. While the inflammatory response is not as robust the one seen in rheumatoid arthritis, low grade inflammation can be seen in both the articular cartilage and the synovium[37,38]. In particular, inflamed synovial fibroblasts and macrophages contribute to the inflammatory process and disease progression through the secretion of additional pro-inflammatory cytokines like Il-1β and TNF-α

into the synovial fluid[39–41]. Additional vascularization of the synovial lining will also bring in additional immune cells, further perpetuating the inflammatory cascade[42].

Inflammation of the articular cartilage is propagated through several factors, including the pro-inflammatory cytokines secreted by synovial cells, pro-inflammatory cytokines secreted by the chondrocytes themselves, and the products of the cartilage matrix destruction. When stimulated to a pro-inflammatory state, chondrocytes will secrete Il-1[43], Il-6[44], Il-17[45], and Il-18[46] which in turn can further induce inflammation in surrounding cells. Other chemokines such as reactive oxygen species (ROS)[47] and lipids such as prostaglandin E2 (PGE2)[48] are secreted in response to the inflammation and can further promote an inflammatory phenotype. In addition, chondrocytes also express cell surface receptors that are activated in response to certain matrix molecules known as damage associated molecular patterns (DAMPs). In particular, the toll like receptors (TLRs) TLR2 and TLR4 as well as discoidin domain receptor 2 (DDR2) can be activated by collagen[49–53], aggrecan[54], and HA fragments[55–57], all of which are created as a result of the chondrocytes' upregulated catabolic activity. These pathways result in the nuclear localization of factors like NF-κB which upregulates genes relating to inflammation and catabolic activity[58–60]. In addition to upregulation of inflammatory markers, the nuclear localization of NF-κB can downregulate chondrogenic genes. This is done through destabilization of SOX9, a key component for the expression of chondrogenic markers including the production of collagen type II and aggrecan[61]. Finally, NF-κB nuclear localization can promote apoptosis of the chondrocytes through mitochondrial damage and disfunction[62,63]. As such, the progression of OA is caused by this cycle of inflammation, wherein the trigger of the inflammatory insult causes the production of additional inflammatory cytokines and catabolic enzymes. These catabolic enzymes produce ECM fragments which in turn promote inflammation, continuing the cycle until the eventual degradation of the articular cartilage. This is further exacerbated by the downregulation of anabolic activity and the promotion of apoptosis, preventing any repair to the degraded cartilage.

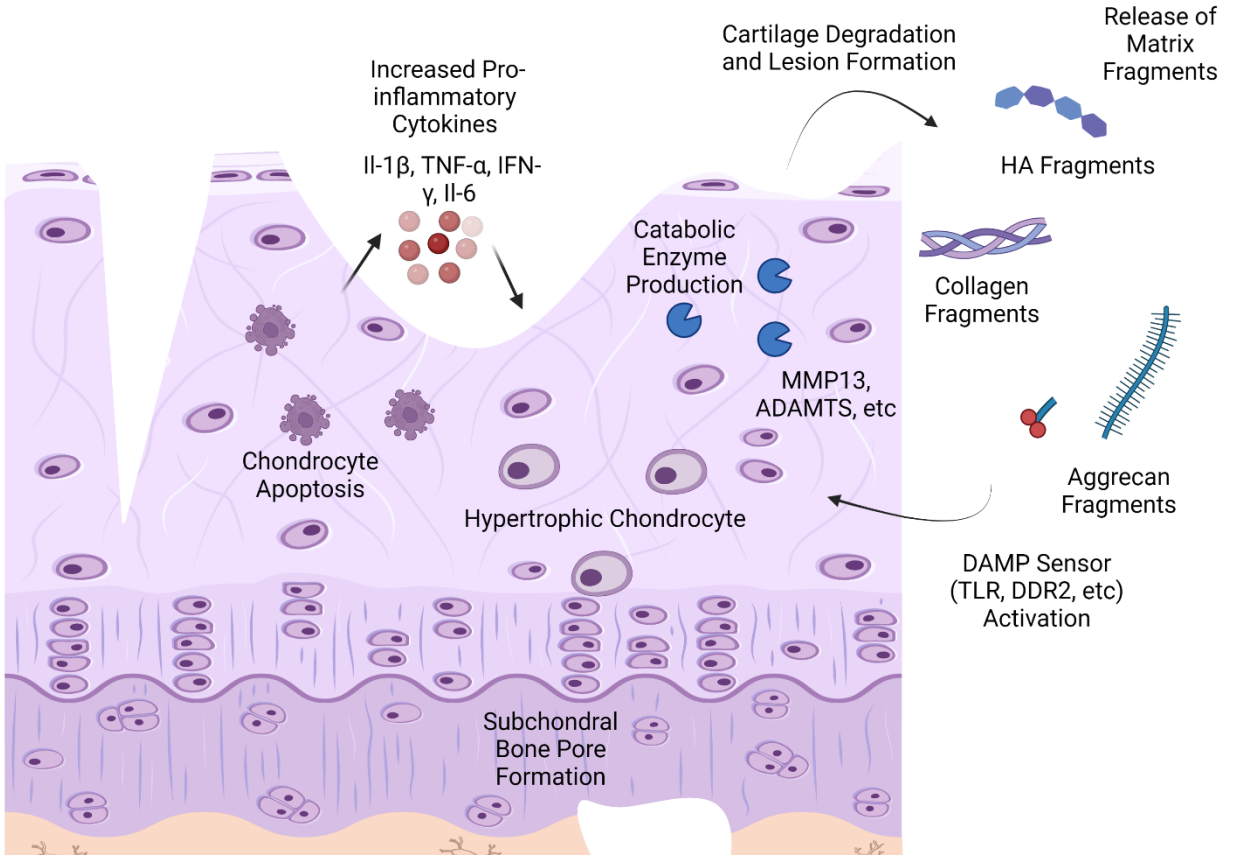


*Figure 1.4: Inflammatory positive feedback loops in osteoarthritis disease progression (created with Biorender.com)*

**1.2.1.2: Clinical Burden of Osteoarthritis**

OA is a widely prevalent disease, with an estimated 10% of men and 18% of women over the age of 60 having some form of OA[64,65]. Current treatments for OA range from pain management to total replacement of the joint. Pain management is done with small molecule drugs such as non-steroidal anti-inflammatory drugs, opioids, or HA intraarticular injections[66,67]. While these may relieve some of the pain, they do little to address the degeneration of the cartilage and will not prevent the progression of the disease. On the other hand, total joint replacement surgery replaces the entire joint with artificial components, often a metal base with ceramic or polymer joint components. While this can restore

movement, the surgery itself is invasive, costly, and opens the patient up to the possibility of complications such as bacterial infections[68] and wear debris poisoning[69].

Recent decades have seen the emergence of procedures to repair the damaged cartilage. This can be done through autologous chondrocyte implantation (ACI), where chondrocytes are isolated from healthy non-load bearing tissue and reintroduced into the defect site[70]. However, this procedure can lead to donor site morbidity[71,72] and it takes a considerable amount of time to expand the required number of cells[73,74]. Furthermore, this method does not shelter the implanted cells from the inflammatory cytokines present in the OA environment. Following the procedure, although improvements have been seen in many patients, graft failure, fibrosis, and hypertrophy were seen following the procedure in some patients[75]. It was found that increased production Il-1β was correlated with adverse effects following ACI, demonstrating a need to shield cells from inflammation following implantation[75–77].

**1.3: Proteoglycans and GAGs in Endothelial Tissue**

PGs and GAGs also play a major role in proper endothelial tissue function. The endothelium is comprised of a thin inner layer of endothelial cells supported by a bed of collagen fibers and smooth muscle cells. Above the layer of endothelial cells resides the glycocalyx, a mesh of proteoglycans, glycoproteins, and hyaluronic acid[18]. This layer provides separation between the components of the blood, including red blood cells, platelets, and neutrophils, regulating their interaction with the underlying endothelium[20]. In addition, the sulfated GAGs and protein cores of the PGs in the glycocalyx provide binding sites for circulating proteins, including antithrombin and thrombomodulin[78,79].

In the event that the glycocalyx and endothelial cell layer is damaged, the underlying collagen layer can be exposed to the circulating blood cells. This exposed collagen can activate circulating platelets and neutrophils, which while necessary for proper healing of the endothelium, can also lead to an inflammatory cascade that results in clot formation and neointimal hyperplasia[80]. When exposed to

collagen, platelets release their store of anabolic cytokines including transforming growth factor beta (TGF-β) and platelet derived growth factor (PDGF)[81]. PDGF in particular will act as a chemoattractant to the underlying smooth muscle cells, leading to their migration towards the intima in the interior of the blood vessel. This release of growth factors also shifts the phenotype of the underlying smooth muscle cells that results in rapid proliferation and the secretion of pro-inflammatory cytokines[80]. If left unchecked, rapid proliferation of intimal smooth muscle cells can result in the narrowing of the lumen and blockage of the blood vessel.

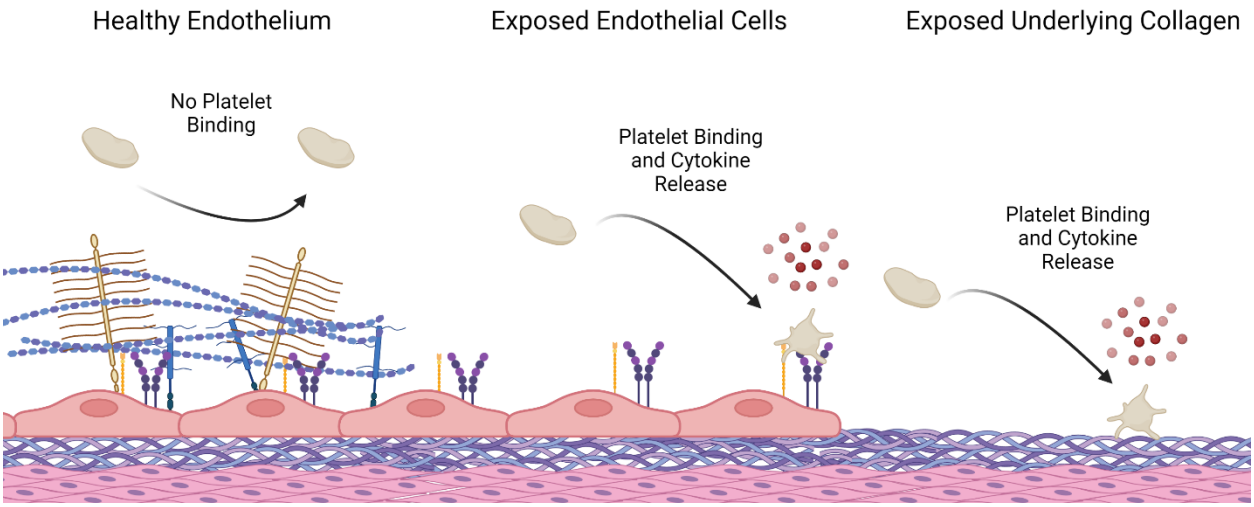


*Figure 1.5: Activation of platelets following injury to the endothelium (created with Biorender.com)*

For this reason, a stent will often be placed at the site of the balloon angioplasty to prevent closure of the blood vessel[82]. This treatment can be further augmented with a drug eluting stent, which will elute drugs to prevent the rapid proliferation of the platelet activated smooth muscle cells to further prevent vessel closure[82]. However, the drugs eluted from these stents are often non targeting and can lead to off target cell death, such as the surrounding endothelial cells. Furthermore, the underlying collagen remains exposed, leaving the possibility of further platelet activation and thrombosis formation[83,84]. As such, a

healthy glycocalyx is necessary for the proper function of the blood vessel endothelium since the lack of this vessel lining will lead to uncontrolled vessel closure.

### 1.4: Therapeutic Potential of Glycosaminoglycans

Given the prevalence of GAGs in the body and their importance to proper tissue function, many researchers have sought to use them for therapeutic purposes in a variety of applications. Of the different GAGs, the three most commonly studied have been heparin, HA, and CS, as these GAGs are readily commercially available. Heparin and CS can be isolated from animal tissues including porcine mucosa[85] and animal cartilage[86,87], respectively, while HA can be produced through *E. Coli* fermentation[88]. Other GAGs such as HS and DS can be isolated from tissues, but less research has been performed using them compared to the former GAGs due to them being relatively less abundant in tissues. Because the structures of these polymers are well preserved between species, GAGs isolated from other species can be used with little chance of a foreign body immune response[89]. While there are a myriad of possible therapeutic applications for GAGs, several specific applications relevant to the data presented in this thesis will be explored in more detailed below.

#### 1.4.1: Anti-Inflammatory Activity of Glycosaminoglycans

One notable bioactive property of GAGs is their ability to dampen inflammation, with this being most studied using the GAGs HA and CS. The anti-inflammatory activity of HA is correlated with its molecular weight, with high molecular weight HA eliciting an anti-inflammatory effect[90–92] but low molecular weight HA eliciting a pro-inflammatory effect on cells[56,57,93]. This is due to the differences in how low and high molecular weight HA bind with cell receptors. While both bind with the CD44 cell receptor, one of the prominent cell surface proteins responsible for interacting with HA, differences in the number of binding sites occupied by HA are responsible for either the suppressing or promoting the secretion of pro-inflammatory factors[94]. Furthermore, low molecular weight HA can also bind with the

TLR family of cell surface proteins as another start to the pro-inflammatory secretion cascade[57,t93]. In contrast, high molecular weight HA was found to inhibit TLR-2 signaling[95]. In the cases of both CD44 and TLR2/4, low molecular weight HA results in the nuclear localization of NF-κB, which in turn activates the synthesis of pro-inflammatory cytokines and catabolic factors, while high molecular weight HA inhibits NF-κB localization[96]. In the context of chondrocytes and osteoarthritis, this can result in either the upregulation[97] or downregulation[91] of the secretion of pro-inflammatory factors including Il-1β, Il-6, MMP13, and iNOS, depending on the size of the HA molecule.

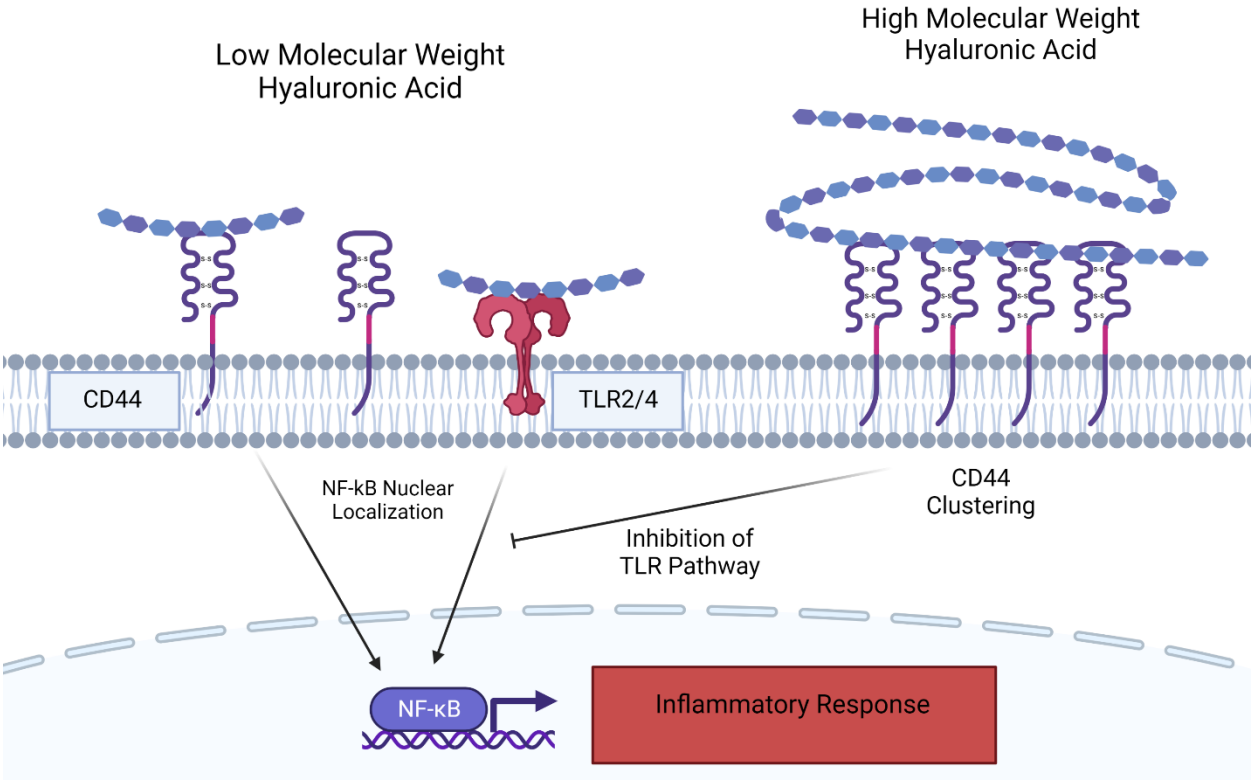


*Figure 1.6: Effect of HA molecular weight on inflammatory pathways (Created with Biorender.com)*

CS also elicits anti-inflammatory effects on cells through inhibition of NF-κB nuclear localization[98,99]. However, the mechanism of action of this anti-inflammatory is less well known compared to HA. Similar to high molecular weight HA, CS and other sulfated GAGs have been found to be TLR2/4 agonists, preventing the inflammation cascade from initiating through blocking this cell surface

receptor[100]. Other theories have suggested CS binds to HA related cell surface receptors including CD44 or the hyaluronan receptor for endocytosis (HARE), given the structural similarities to HA[101–104]. However, in contrast with HA, fragmented CS in the form of disaccharides have also been shown to have anti-inflammatory effects[105]. Similar anti-inflammatory effects to HA have been reported with CS, with reductions in secretions of cytokines such as Il-1β[106], TNF-α[107], and iNOS[108] found following treatment with soluble CS. To better understand the mechanism of action for the anti-inflammatory effects of CS, further research is required.

### 1.4.2: Chondrogenic Activity of Glycosaminoglycans

Another property of GAGs is their ability to direct cell fate and promote the expression of certain genes and proteins. This has been especially studied in the context of cartilage as a manner to treat osteoarthritis through the promotion of cartilage ECM production. In addition to preserving the phenotype of chondrocytes[109] and preventing cell dedifferentiation[110], the chondrogenic effects of GAGs has also been studied to differentiate mesenchymal stromal cells (MSCs), a multipotent mesenchymal progenitor cell type, toward a chondrogenic phenotype to replace chondrocytes[111]. In the case of HA, this is primarily mediated through binding with the CD44, where CD44 binding to high molecular weight HA leads to Sox9 phosphorylation which in turn results in the upregulation of chondrogenic behavior[112,113]. This leads to increased production of cartilage ECM components such as collagen type II and aggrecan[114] while preventing hypertrophic behavior including the secretion of collagen X[115] and alkaline phosphatase[116]. Similar effects have been seen with sGAGs, including CS and HS, where presenting these polymers to cells increases the production of cartilage ECM components[117–119]. Again, compared to HA, the exact mechanism for chondrogenic signaling through CS is less well known, but given the similar structure and upregulation of the intermediary protein Sox9 it is predicted that CS works in a similar manner to HA[120].

### 1.4.3 Antiplatelet activity

Heparin is the oldest GAG used for therapeutic purposes, with its discovery as an antithrombotic agent dating back to the early 20th century[121]. The primary mechanism of action for heparin is the activation of antithrombin by binding to its heparin-binding domain[122,123]. Following binding with antithrombin, the heparin-protein complex binds with thrombin, inactivating it. As such, heparin of sufficient length is required for thrombin inactivation in its free-floating form, as it requires around 18 saccharides to bind to both thrombin and antithrombin[124,125]. Inactivation of thrombin by heparin both reduces blood coagulation and thrombin induced platelet activation. In addition to antithrombin, heparin also binds to other coagulating factors like heparin cofactor II[126,127] and protein C inhibitor[128], both of which are activated through heparin binding and inactivate components of coagulation and thrombus formation. As such, heparin has been employed as a treatment when thrombus formation and clotting is a concern, such as coronary angioplasty procedures.

Although often used as a free-floating agent, recent decades have seen the development and use of heparin immobilized to surfaces[129]. For use cases where synthetic materials come into contact with blood, the complement system and coagulation cascade will be activated, leading to platelet activation and thrombus formation[130]. While this can be potentially treated with systemic delivery of heparin, off targets effects such as hemorrhages and poor clot formation are possible[129]. By immobilizing heparin to the biomaterial surface, these off target effects can be eliminated while achieving better biocompatibility and maintaining heparin's antithrombotic capabilities. To date, heparin has been immobilized to a variety of biomaterials, including polyurethane[131], poly(2-hydroxyethyl methacrylate) (pHEMA)[132], Teflon[133], Dacron[133], and polyethylene[134]. By covalently immobilizing heparin, groups have demonstrated decreased thrombin activation and platelet adherence, reducing the need for systemic heparin delivery through localization of heparin activity to the biomaterial surface.

### 1.5: Modification of Glycosaminoglycans for Therapeutic Uses

While potent on their own, researchers have sought to modify GAGs to better suit their needs. Given their many sites for modification as well as relatively simple structure and stability compared to other commonly studied biopolymers, many different modification strategies have been developed. These range from simple crosslinking of GAGs to increase molecular weight to the development of PG mimetic molecules to replace PG functionality. This section will overview several methods in which GAGs have been modified and engineered to fit biomedical needs.

#### 1.5.1: Chemical Modification of Glycosaminoglycans

Given their relatively simple structure compared to other biopolymers used for tissue engineering purposes, many strategies have been developed to chemically modify GAGs to better tune them to specific needs. GAGs contain many sites for chemical modification, with groups opting to target either the carboxylic acid group of the uronic acid residue or the hydroxyl groups of either sugar. Of all the GAGs, HA has seen the most work done with regards to chemical modification. This has ranged from benzyl esterification of HA to increase its hydrophobicity[135] to the sulfation of HA to modulate the GAG's negative charge[136]. Side chains such as cholesterol[137] and n-isopropylacrylamide[138] have also been grafted to HA to form physically formed hydrogels. However, one aspect of GAG modification that has seen much attention is the attachment of groups to facilitate covalent chemical crosslinking. This has been achieved with thiols[139], methacrylates[140], furans[141], tyramines[142], cyclodextrins[143], as well as many other species. CS and other GAGs have also seen some research regarding chemical modification, with similar strategies being employed[144–147]. Because of the hydrophilic functional groups on GAGs, GAGs are insoluble in most organic solvents and many modification strategies employ reactions done in aqueous conditions. However, an ion exchange can be performed with the sodium counter ions to allow for solubility in organic solvents[148].

#### 1.5.2: Proteoglycan Mimetic Molecules

To target pathologies that are a result of a loss of PGs, some groups have opted to chemically modify GAGs to make molecules that mimic the function of GAGs. To recapitulate the function of bottlebrush GAGs like aggrecan, a couple of groups created bottlebrush molecules using CS and a core polymer. For example, Prudnikova et al demonstrated the synthesis of a CS bottlebrush molecule by conjugating amine-terminated CS to a poly(acryloyl chloride) backbone[149,150]. Using this method, they synthesized a smaller molecule with a 10 kDa core and ~7-8 CS chains[150] and a large molecule with a 250 kDa core polymer with ~60 CS chains[149], demonstrating the flexibility with regard to size with this approach. This molecule demonstrated swelling comparable to aggrecan and unconjugated CS. Furthermore, the smaller molecule also demonstrated an ability to modulated collagen fibril formation through interactions with the attached GAG chains, as the core by itself had no effect. Another bottlebrush mimetic strategy was demonstrated by Pauly et al, who used hydrazide functionalized HA as their backbone, allowing them to conjugate CS through the carboxylic acid groups[151]. When added to an agarose hydrogel, this molecule increased the compressive strength of the hydrogel. This was hypothesized to be due to the molecule's significant negative charge, driving an increase in osmotic pressure. While molecules of these type can recapitulate the bottlebrush domains of PGs like aggrecan, they lack their binding domains and remain untethered within the area where they are delivered, possibly requiring multiple doses for effectiveness. However, the lack of a protein core results in resistance to proteolysis, possibly increasing their residence time following delivery.

Another PG mimetic strategy that has been studied is the use of peptide functionalized molecules, where substrate binding peptides are covalently conjugated to a polymer backbone. This is to recapitulate the matrix binding function of PGs, such as the collagen binding capabilities of SLRPs and the HA binding capability of hyalectans. This can be done using a GAG backbone, where multiple peptides are bound to the backbone to increase its binding affinity to its targeted substrate. For example, HA binding peptides were grafted to a CS backbone as an aggrecan mimetic, which demonstrated an ability to protect HA and

collagen from enzymatic degradation[152]. By adding a collagen type II binding peptide to the molecule, a lubricin mimetic was synthesized, which demonstrated an ability to lower the coefficient of friction of articular cartilage[153]. Using this strategy, endothelial PG mimetic molecules were also synthesized. A decorin mimetic molecule was synthesized by conjugating collagen binding peptides to a DS backbone and was shown to modulate collagen fibril formation and reduce smooth muscle cell proliferation to a greater degree compared to free floating DS[154]. Similarly, selectin binding peptides were conjugated to a DS backbone as a way to restore the glycocalyx following injury[155]. This allowed the molecule to localize to a damaged endothelial layer and prevent activation of circulating neutrophils and platelets. In addition to GAG backbones, peptides have also been conjugated to synthetic polymer backbones. Singh et al conjugated collagen type II and HA-binding peptides to a poly(ethylene glycol) (PEG) star polymer backbone, and following intra-articular delivery, demonstrated its use as a lubricin mimetic through decreases in joint friction and a dampening of OA progression[156].

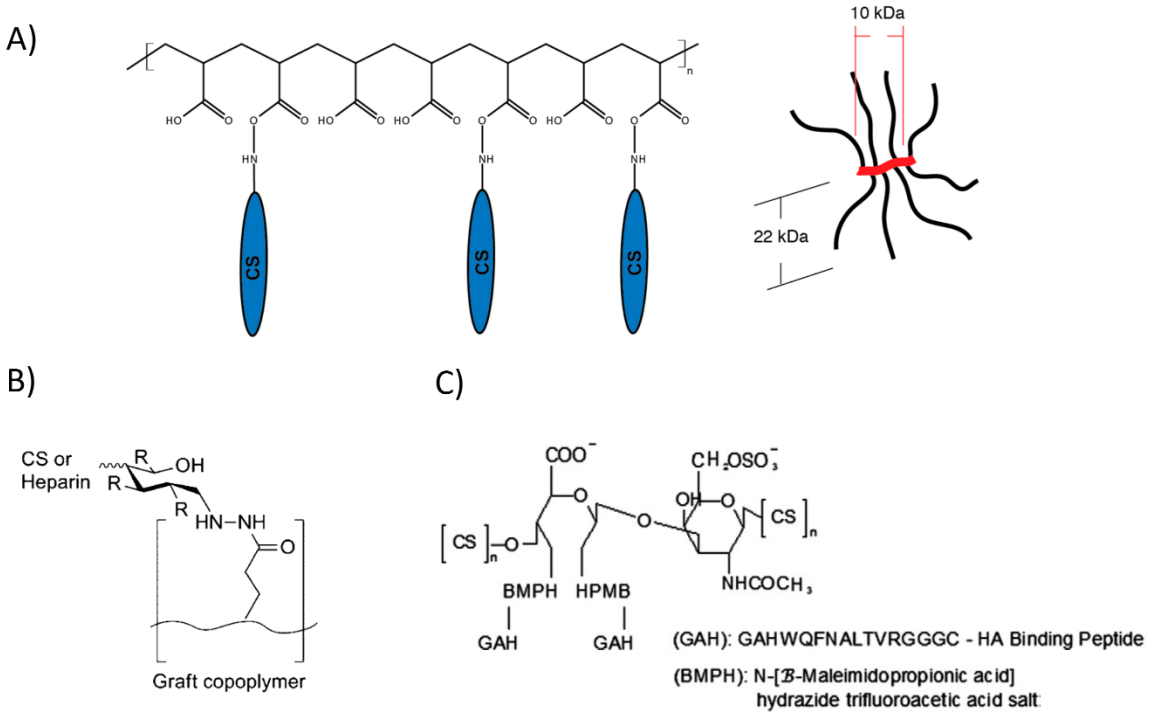

*Figure 1.7: Strategies for proteoglycan biomimetic molecules. A) Synthetic poly(acryloyl chloride) backbone grafted with CS. B) HA backbone grafted with CS or heparin. C) Oxidized CS with HA binding peptide grafted to opened rings.*

### 1.5.3: Glycosaminoglycan Biomaterials for Tissue Engineering

Using chemically modified GAGs, many researchers have developed biomaterials that incorporate GAGs to endow their material with desirable properties and enhance tissue engineering outcomes. Furthermore, since the structure of GAGs is well conserved between different species, minimal host-rejection response is often seen, compared to some protein-based biomaterial approaches. This approach has seen favorable results in a variety of tissue engineering fields, including skin[157], bone,[158] cartilage[159], and cardiac tissues[160]. For these applications, biomaterials have been made primarily of GAGs to leverage their biological properties or have been made in combination one or more other polymers to further tune the material properties.

#### 1.5.3.1: Biomaterials made primarily from GAGs

One of the simplest methods of fabricating a GAG biomaterial is using chemically modified GAGs to form hydrogels. This is most commonly done with HA, given its commercial availability and relevance to the ECM in many tissues, though some work has been done with other GAGs like CS[145] and heparin[161]. Using a catecholamine modified HA hydrogel, Shin et al demonstrated the survival of mouse hepatocytes and adipose derived mesenchymal stromal cells (ADSCs) to damaged liver and ischemic myocardial tissue, respectively, with the HA hydrogel showing favorable integration with the surrounding tissue[162]. The delivery of these cells to their respective locations improved tissue function while preserving the delivered cells. Using tetrazine/cyclooctene click-crosslinked HA hydrogels functionalized with a bone morphogenetic protein mimetic peptide, Park et al demonstrated their material's ability to encapsulate dental pulp stem cells and direct them toward an osteogenic lineage, as denoted by increased alkaline

phosphatase activity and upregulation of osteogenic markers[163]. Using methacrylated HA, Bian et al encapsulated a coculture of MSCs and chondrocytes, with the hydrogel supporting the survival and chondrogenic differentiation of these cells[164]. With regard to other GAGs, Conovaloff and Panitch used a thiolated CS hydrogel to support the growth of chick dorsal root ganglions, with the CS hydrogel supporting longer neurite growth compared to an HA hydrogel[145]. Similarly, Liu et al demonstrated the ability of a methacrylated CS hydrogel to maintain the phenotype of neuronal stem cells and prevent differentiation, demonstrating the biological activity of CS over a methacrylated gelatin hydrogel[165].

Beyond basic crosslinking, chemical modification of GAGs can allow for other desirable material properties. Although HA hydrogels are already biodegradable through cellular hyaluronidases, modifying HA with hydrolytically labile groups can result in hydrogels that degrade through another method. This was done by Sahoo et al, who used methacrylate lactic acid modified HA to increase the degradation rate of HA hydrogels, resulting in increased growth factor release[166]. Another aspect of GAG hydrogels is the delivery method of application. Although many of the GAG hydrogels are made through *in situ* gelation, HA modified specialized functional groups can allow for injectable hydrogels. This was done by Loebel et al, who created an injectable HA hydrogel using transient crosslinks[143]. This was done using an adamantane/β-cyclodextrin guest-host system, where HA modified with these groups created a shear thinning hydrogel. Using a material that thinned under shear, the group was able to 3D print the HA hydrogel, allowing them to form complex cell arrangements with multiple inks.

Finally, commercially available HA biomaterials have started to see adoption for several clinical applications. While many research groups have used HA in hydrogel form, many commercial HA products use a benzyl-esterified HA, sold under the name HYAFF[135]. This modification reduces the solubility of HA through the hydrophobic benzyl group while also providing a method for hydrolytic degradation through the esters, on top of the natural hyaluronidase activity. Using HYAFF fibers, woven materials like

HYALOFILL (Anika Therapeutics, USA) have been produced and used for wound dressings to allow for increase exudate absorption while also providing a biocompatible scaffold for wound healing[167].

In general, many groups have been able to leverage the biological properties of GAG biomaterials, with these materials supporting cell survival and promoting desirable tissue engineering outcomes. Most of these materials have been primarily made of HA, though some groups have used CS for certain applications. Heparin has also been used, though often used as a drug delivery vehicle due to its high negative charge[168,169]. However, by themselves, GAG hydrogels often lack tunability in certain aspects. For this reason, many groups have opted to use GAGs in combination with other polymers to further tune the material properties.

**1.5.3.2: Composite GAG Biomaterials**

By combining GAGs with other polymers, the properties of the biomaterial can be further modulated. For these composite materials, both synthetic polymers and biopolymers have been used. Synthetic polymers that have been used include PEG[117,170], poly(caprolactone)[120,171], NIPAAm[138,172], and poly(vinyl alcohol)[173]. A variety of biopolymers have also been used, with both biologically active polymers like collagen[174,175], silk fibroin[176], and gelatin[177] as well as bioinert polymers like alginate[178] and agarose[179] being combined with GAGs for biomaterials.

Many groups have opted to combine GAGs with synthetic polymers due to their well-defined mechanical properties and the ease of tunability. Strehin et al developed a CS-N-hydroxylsuccinimide/PEG -amine hydrogel for cartilage tissue engineering[180]. By varying different properties of the constituent polymers, such as the conditions of the synthesis, the pH of the PEG-amine, and the ratio of CS to PEG, they were able to control the mechanical properties of the bulk biomaterial through multiple mechanisms. Furthermore, since CS was a major component of the material, the hydrogel was still susceptible to enzymatic degradation, in contrast with a fully PEG material. To study the effects of GAGs on MSC

chondrogenesis, Wang and Yang used a PEG hydrogel combined with either CS or HS[119]. By using the PEG hydrogel as a base material, they were able to study the biological effects of CS and HS in a 3D environment while keeping properties including material stiffness constant, demonstrating the superiority of CS over HS for chondrogenic signals, despite GAG structural similarities. Aside from synthetic polymers, some bioinert biopolymers have also been combined with GAGs for tissue engineering purposes. Alginate, a polysaccharide derived from brown seaweed, can be crosslinked using divalent cations. Using alginate as a base hydrogel, Jeon et al used methacrylated heparin and a photomask to spatially pattern heparin within the hydrogel[181]. This allowed them to localized BMP to certain locations within the material, leading to osteogenic differentiation of MSCs primarily in these areas. Although these polymers can allow for biomaterials with tunable properties, their bioinert nature leaves the body unable to degrade them through natural methods. However, when co-crosslinked with GAGs, the materials can then be degraded through the body's hyaluronidases.

In contrast to bioinert polymers, many groups have combined GAGs with other biopolymers to leverage their bioactivity along with the signals from the GAGs. Kilmer et al fabricated a collagen hydrogel made from a blend of collagen type I and collagen type II and added CS conjugated with a collagen binding peptide[182]. They used this hydrogel to direct MSC towards a chondrogenic phenotype. While collagen type II itself can provide these chondrogenic signals, the addition of CS into the hydrogel further increasing the expression of chondrogenic markers such as the upregulation of cartilage matrix protein genes. Similarly, Levett et al combined methacrylated HA and CS with gelatin-methacrylamide for cartilage tissue engineering[183]. By combining CS and HA with their gelatin-based hydrogel, cartilage markers such as the production of aggrecan and collagen type II were upregulated over their gelatin only material. Ying et al combined HA and collagen to form biomimetic wound dressing hydrogel, as HA is a major component of the granulation tissue and wound healing process[174]. By combining these two polymers, the improved wound healing was seen compared to a collagen only gel due to the increased nutrient diffusion that

resulted from HA's negative charge. In these cases, the benefits of the base gel in the context of tissue engineering were augmented with the bioactivity of GAGs.

One consideration that must be made when combining GAGs with biopolymers is the effect on the microstructure of the material when the GAGs are added. Given the significant negative charge of GAGs, changes in structure can occur when the polymers interact. When combining CS with hydrogels made from a blend of collagen types I and III, Stuart and Panitch found decreases in collagen fibril diameter and increases in void space, compared to gels without the GAG[184]. Vázquez-Portalatín et al demonstrated increased protein incorporation when CS or HA were added to a blended collagen type I and type II hydrogel, again demonstrating the interactions of GAGs with collagen in the context of biomaterial fabrication[185].

**1.6: Thesis Outline and Contributions**

GAGs play a key role in almost all tissues and have been widely explored for their therapeutic potential in many roles. With this in mind, the work presented here documents my efforts to engineer GAGs through chemical modification to best suit clinical needs and maximize their bioactivity.

Chapter 2 focuses on understanding how the chemical modification of GAGs affects their bioactivity. This chapter describes how the degree of modification of thiolated CS and HA affects their recognition by hyaluronidase and GAG-binding peptides, analogues for how cells would interact with the GAGs following implantation. Furthermore, this chapter details how the blending off CS and HA into dual polymer network hydrogels (DPN) affects their mechanical and biological properties. This chapter consists of the manuscript published by Michael Nguyen, Julie C. Liu, and Alyssa Panitch published in Biomacromolecules, volume 22, issue 10, 2021. Michael Nguyen planned and conducted all experiments in this study.

Chapter 3 describes the use of these thiolated GAGs to form hydrogels that would shield articular chondrocytes from a pro-inflammatory environment. Fetal bovine articular chondrocytes were encapsulated in CS/HA DPN hydrogels with or without the addition of collagen and cultured in pro-inflammatory media. This chapter describes the effects of pro-inflammatory cytokines on these cells while inside the hydrogels. This chapter consists of a manuscript in progress by Michael Nguyen, Julie C. Liu, and Alyssa Panitch. Michael Nguyen planned and conducted all experiments in this study.

Chapter 4 describes the synthesis of a peptide-glycan molecule for the protection of exposed endothelial collagen and the inhibition of platelet activity. The spacer sequence and C-terminal modification of a collagen binding peptide was optimized for conjugation to a GAG backbone. The effects of peptide sequence and GAG backbone choice on peptide-GAG conjugation and collagen binding are detailed. Following molecule synthesis, the ability of the peptide-glycan to inhibit platelet activation and bind to exposed collagen are also demonstrated. This chapter consists of a manuscript submitted to Biomacromolecules by Michael Nguyen, Tanaya Walimbe, Andrew Woolley, John Paderi, and Alyssa Panitch. Michael Nguyen conducted the peptide-glycan synthesis experiments and wrote the associated sections. Tanaya Walimbe performed the circular dichroism experiments. Andrew Woolley and John Paderi performed the platelet inhibition and *in vivo* targeting experiments and wrote the methods and results for these sections, as well as the introduction.

Chapter 5 summarizes the data from the previous chapters and outlines possible avenues for future work based off these findings.

**1.7: References**


1. Schaefer, L. & Schaefer, R. M. Proteoglycans: from structural compounds to signaling molecules. *Cell Tissue Res* **339**, 237 (2009).
2. Iozzo, R. V. & Schaefer, L. Proteoglycan form and function: A comprehensive nomenclature of proteoglycans. *Matrix Biology* **42**, 11–55 (2015).
3. Kiani, C., Chen, L., Wu, Y. J., Yee, A. J. & Yang, B. B. Structure and function of aggrecan. *Cell Res* **12**, 19–32 (2002).
4. Knudson, C. B. & Knudson, W. Cartilage proteoglycans. *Seminars in Cell & Developmental Biology* **12**, 69–78 (2001).
5. Chen, S. & Birk, D. E. The regulatory roles of small leucine-rich proteoglycans in extracellular assembly. *FEBS J* **280**, 2120–2137 (2013).
6. Douglas, T., Heinemann, S., Bierbaum, S., Scharnweber, D. & Worch, H. Fibrillogenesis of Collagen Types I, II, and III with Small Leucine-Rich Proteoglycans Decorin and Biglycan. *Biomacromolecules* **7**, 2388–2393 (2006).
7. Geng, Y., McQuillan, D. & Roughley, P. J. SLRP interaction can protect collagen fibrils from cleavage by collagenases. *Matrix Biology* **25**, 484–491 (2006).
8. Henninger, H. B., Maas, S. A., Underwood, C. J., Whitaker, R. T. & Weiss, J. A. Spatial distribution and orientation of dermatan sulfate in human medial collateral ligament. *Journal of Structural Biology* **158**, 33–45 (2007).
9. Robinson, K. A. *et al.* Decorin and biglycan are necessary for maintaining collagen fibril structure, fiber realignment, and mechanical properties of mature tendons. *Matrix Biology* **64**, 81–93 (2017).
10. Robinson, P. S. *et al.* Influence of Decorin and Biglycan on Mechanical Properties of Multiple Tendons in Knockout Mice. *Journal of Biomechanical Engineering* **127**, 181–185 (2005).
11. Pratta, M. A. *et al.* Aggrecan Protects Cartilage Collagen from Proteolytic Cleavage *. *Journal of Biological Chemistry* **278**, 45539–45545 (2003).
12. Ni, G.-X., Li, Z. & Zhou, Y.-Z. The role of small leucine-rich proteoglycans in osteoarthritis pathogenesis. *Osteoarthritis and Cartilage* **22**, 896–903 (2014).
13. Pang, X., Dong, N. & Zheng, Z. Small Leucine-Rich Proteoglycans in Skin Wound Healing. *Frontiers in Pharmacology* **10**, 1649 (2020).
14. Whitelock, J. M., Melrose, J. & Iozzo, R. V. Diverse Cell Signaling Events Modulated by Perlecan. *Biochemistry* **47**, 11174–11183 (2008).
15. Zoeller, J. J., McQuillan, A., Whitelock, J., Ho, S.-Y. & Iozzo, R. V. A central function for perlecan in skeletal muscle and cardiovascular development. *J Cell Biol* **181**, 381–394 (2008).
16. Arikawa-Hirasawa, E., Watanabe, H., Takami, H., Hassell, J. R. & Yamada, Y. Perlecan is essential for cartilage and cephalic development. *Nat Genet* **23**, 354–358 (1999).
17. Costell, M. *et al.* Perlecan Maintains the Integrity of Cartilage and Some Basement Membranes. *J Cell Biol* **147**, 1109–1122 (1999).
18. Reitsma, S., Slaaf, D. W., Vink, H., van Zandvoort, M. A. M. J. & oude Egbrink, M. G. A. The endothelial glycocalyx: composition, functions, and visualization. *Pflugers Arch* **454**, 345–359 (2007).
19. Tarbell, J. M. & Cancel, L. M. The glycocalyx and its significance in human medicine. *Journal of Internal Medicine* **280**, 97–113 (2016).
20. Lipowsky, H. H. The Endothelial Glycocalyx as a Barrier to Leukocyte Adhesion and Its Mediation by Extracellular Proteases. *Ann Biomed Eng* **40**, 840–848 (2012).
21. Glyn-Jones, S. *et al.* Osteoarthritis. *The Lancet* **386**, 376–387 (2015).
22. Sophia Fox, A. J., Bedi, A. & Rodeo, S. A. The Basic Science of Articular Cartilage. *Sports Health* **1**, 461–468 (2009).

23. Hunziker, E. B., Quinn, T. M. & Häuselmann, H.-J. Quantitative structural organization of normal adult human articular cartilage. *Osteoarthritis and Cartilage* **10**, 564–572 (2002).
24. Hunziker, E. B. Articular cartilage repair: are the intrinsic biological constraints undermining this process insuperable? *Osteoarthritis Cartilage* **7**, 15–28 (1999).
25. Baugé, C. *et al.* Interleukin-1beta impairment of transforming growth factor beta1 signaling by down-regulation of transforming growth factor beta receptor type II and up-regulation of Smad7 in human articular chondrocytes. *Arthritis Rheum.* **56**, 3020–3032 (2007).
26. Shlopov, B. V. *et al.* Osteoarthritic lesions: involvement of three different collagenases. *Arthritis Rheum* **40**, 2065–2074 (1997).
27. Stanton, H. *et al.* ADAMTS5 is the major aggrecanase in mouse cartilage in vivo and in vitro. *Nature* **434**, 648–652 (2005).
28. Durigova, M., Troeberg, L., Nagase, H., Roughley, P. J. & Mort, J. S. INVOLVEMENT OF ADAMTS5 AND HYALURONIDASE IN AGGRECAN DEGRADATION AND RELEASE FROM OSM-STIMULATED CARTILAGE. *European cells & materials* **21**, 31.
29. Durigova, M., Roughley, P. J. & Mort, J. S. Mechanism of proteoglycan aggregate degradation in cartilage stimulated with oncostatin M. *Osteoarthritis and Cartilage* **16**, 98–104 (2008).
30. Yoshida, M. *et al.* Expression analysis of three isoforms of hyaluronan synthase and hyaluronidase in the synovium of knees in osteoarthritis and rheumatoid arthritis by quantitative real-time reverse transcriptase polymerase chain reaction. *Arthritis Res Ther* **6**, R514 (2004).
31. Shimizu, H. *et al.* Hyaluronan-Binding Protein Involved in Hyaluronan Depolymerization Is Up-Regulated and Involved in Hyaluronan Degradation in Human Osteoarthritic Cartilage. *The American Journal of Pathology* **188**, 2109–2119 (2018).
32. Knudson, W., Ishizuka, S., Terabe, K., Askew, E. B. & Knudson, C. B. The pericellular hyaluronan of articular chondrocytes. *Matrix Biology* **78–79**, 32–46 (2019).
33. Flannery, C. R., Little, C. B., Hughes, C. E. & Caterson, B. Expression and Activity of Articular Cartilage Hyaluronidases. *Biochemical and Biophysical Research Communications* **251**, 824–829 (1998).
34. Malemud, C. J., Islam, N. & Haqqi, T. M. Pathophysiological Mechanisms in Osteoarthritis Lead to Novel Therapeutic Strategies. *CTO* **174**, 34–48 (2003).
35. Saklatvala, J. Tumour necrosis factor α stimulates resorption and inhibits synthesis of proteoglycan in cartilage. *Nature* **322**, 547–549 (1986).
36. Garcia, J. P. *et al.* Association between Oncostatin M Expression and Inflammatory Phenotype in Experimental Arthritis Models and Osteoarthritis Patients. *Cells* **10**, 508 (2021).
37. Pap, T. & Korb-Pap, A. Cartilage damage in osteoarthritis and rheumatoid arthritis—two unequal siblings. *Nat Rev Rheumatol* **11**, 606–615 (2015).
38. Kaneko, S. *et al.* Interleukin–6 and interleukin–8 levels in serum and synovial fluid of patients with osteoarthritis. *Cytokines, Cellular & Molecular Therapy* **6**, 71–79 (2000).
39. Bondeson, J., Wainwright, S. D., Lauder, S., Amos, N. & Hughes, C. E. The role of synovial macrophages and macrophage-produced cytokines in driving aggrecanases, matrix metalloproteinases, and other destructive and inflammatory responses in osteoarthritis. *Arthritis Res Ther* **8**, R187 (2006).
40. Sutton, S. *et al.* The contribution of the synovium, synovial derived inflammatory cytokines and neuropeptides to the pathogenesis of osteoarthritis. *The Veterinary Journal* **179**, 10–24 (2009).
41. Sellam, J. & Berenbaum, F. The role of synovitis in pathophysiology and clinical symptoms of osteoarthritis. *Nature Reviews Rheumatology* **6**, 625–635 (2010).
42. Haywood, L. *et al.* Inflammation and angiogenesis in osteoarthritis. *Arthritis & Rheumatism* **48**, 2173–2177 (2003).

43. Tiku, K., Thakker-Varia, S., Ramachandrula, A. & Tiku, M. L. Articular chondrocytes secrete IL-1, express membrane IL-1, and have IL-1 inhibitory activity. *Cellular Immunology* **140**, 1–20 (1992).
44. Guerne, P. A., Carson, D. A. & Lotz, M. IL-6 production by human articular chondrocytes. Modulation of its synthesis by cytokines, growth factors, and hormones in vitro. *J Immunol* **144**, 499–505 (1990).
45. Martel-Pelletier, J., Mineau, F., Jovanovic, D., Di Battista, J. A. & Pelletier, J.-P. Mitogen-activated protein kinase and nuclear factor κB together regulate interleukin-17–induced nitric oxide production in human osteoarthritic chondrocytes: Possible role of transactivating factor mitogen–activated protein kinase–activated protein kinase (MAPKAPK). *Arthritis & Rheumatism* **42**, 2399–2409 (1999).
46. Olee, T., Hashimoto, S., Quach, J. & Lotz, M. IL-18 Is Produced by Articular Chondrocytes and Induces Proinflammatory and Catabolic Responses. *The Journal of Immunology* **162**, 1096–1100 (1999).
47. Afonso, V., Champy, R., Mitrovic, D., Collin, P. & Lomri, A. Reactive oxygen species and superoxide dismutases: Role in joint diseases. *Joint Bone Spine* **74**, 324–329 (2007).
48. Attur, M. *et al.* Prostaglandin E2 Exerts Catabolic Effects in Osteoarthritis Cartilage: Evidence for Signaling via the EP4 Receptor. *The Journal of Immunology* **181**, 5082–5088 (2008).
49. Ruettger, A., Schueler, S., Mollenhauer, J. A. & Wiederanders, B. Cathepsins B, K, and L Are Regulated by a Defined Collagen Type II Peptide via Activation of Classical Protein Kinase C and p38 MAP Kinase in Articular Chondrocytes *. *Journal of Biological Chemistry* **283**, 1043–1051 (2008).
50. Fichter, M. *et al.* Collagen degradation products modulate matrix metalloproteinase expression in cultured articular chondrocytes. *Journal of Orthopaedic Research* **24**, 63–70 (2006).
51. Tchetina, E. V. *et al.* Chondrocyte hypertrophy can be induced by a cryptic sequence of type II collagen and is accompanied by the induction of MMP-13 and collagenase activity: Implications for development and arthritis. *Matrix Biology* **26**, 247–258 (2007).
52. Yasuda, T. Type II collagen peptide stimulates Akt leading to nuclear factor-κB activation: Its inhibition by hyaluronan. *Biomedical Research* **35**, 193–199 (2014).
53. Zhang, Y. *et al.* An essential role of discoidin domain receptor 2 (DDR2) in osteoblast differentiation and chondrocyte maturation via modulation of Runx2 activation. *J Bone Miner Res* **26**, 604–617 (2011).
54. Lees, S. *et al.* Bioactivity in an Aggrecan 32-mer Fragment Is Mediated via Toll-like Receptor 2. *Arthritis & Rheumatology* **67**, 1240–1249 (2015).
55. Avenoso, A. *et al.* Hyaluronan in experimental injured/inflamed cartilage: In vivo studies. *Life Sciences* **193**, 132–140 (2018).
56. Campo, G. M. *et al.* Molecular size hyaluronan differently modulates toll-like receptor-4 in LPS-induced inflammation in mouse chondrocytes. *Biochimie* **92**, 204–215 (2010).
57. Termeer, C. *et al.* Oligosaccharides of Hyaluronan Activate Dendritic Cells via Toll-like Receptor 4. *Journal of Experimental Medicine* **195**, 99–111 (2002).
58. O'Neill, L. A. J., Golenbock, D. & Bowie, A. G. The history of Toll-like receptors — redefining innate immunity. *Nat Rev Immunol* **13**, 453–460 (2013).
59. Kim, H. A. *et al.* The catabolic pathway mediated by Toll-like receptors in human osteoarthritic chondrocytes. *Arthritis & Rheumatism* **54**, 2152–2163 (2006).
60. Gómez, R., Villalvilla, A., Largo, R., Gualillo, O. & Herrero-Beaumont, G. TLR4 signalling in osteoarthritis—finding targets for candidate DMOADs. *Nat Rev Rheumatol* **11**, 159–170 (2015).
61. Haag, J., Gebhard, P. M. & Aigner, T. SOX Gene Expression in Human Osteoarthritic Cartilage. *PAT* **75**, 195–199 (2008).
62. Blanco, F. J., Rego, I. & Ruiz-Romero, C. The role of mitochondria in osteoarthritis. *Nat Rev Rheumatol* **7**, 161–169 (2011).

63. Kim, J. *et al.* Mitochondrial DNA damage is involved in apoptosis caused by pro-inflammatory cytokines in human OA chondrocytes. *Osteoarthritis and Cartilage* **18**, 424–432 (2010).
64. Gage, B. E., McIlvain, N. M., Collins, C. L., Fields, S. K. & Comstock, R. D. Epidemiology of 6.6 million knee injuries presenting to United States emergency departments from 1999 through 2008. *Acad Emerg Med* **19**, 378–385 (2012).
65. Arthritis Foundation. Arthritis By The Numbers. *Book of trusted Facts & Figures* (2019).
66. Katz, J. N., Arant, K. R. & Loeser, R. F. Diagnosis and Treatment of Hip and Knee Osteoarthritis: A Review. *JAMA* **325**, 568–578 (2021).
67. Webb, D. & Naidoo, P. Viscosupplementation for knee osteoarthritis: a focus on Hylan G-F 20. *Orthop Res Rev* **10**, 73–81 (2018).
68. Gbejuade, H. O., Lovering, A. M. & Webb, J. C. The role of microbial biofilms in prosthetic joint infections. *Acta Orthop* **86**, 147–158 (2015).
69. Ingham, E. & Fisher, J. Biological reactions to wear debris in total joint replacement. *Proc Inst Mech Eng H* **214**, 21–37 (2000).
70. Huang, B. J., Hu, J. C. & Athanasiou, K. A. Cell-based tissue engineering strategies used in the clinical repair of articular cartilage. *Biomaterials* **98**, 1–22 (2016).
71. Bexkens, R. *et al.* Donor-site morbidity after osteochondral autologous transplantation for osteochondritis dissecans of the capitellum: a systematic review and meta-analysis. *Knee Surg Sports Traumatol Arthrosc* **25**, 2237–2246 (2017).
72. Andrade, R. *et al.* Knee donor-site morbidity after mosaicplasty – a systematic review. *J EXP ORTOP* **3**, 31 (2016).
73. Barlič, A., Drobnič, M., Maličev, E. & Kregar-Velikonja, N. Quantitative analysis of gene expression in human articular chondrocytes assigned for autologous implantation. *Journal of Orthopaedic Research* **26**, 847–853 (2008).
74. Duan, L. *et al.* Cytokine networking of chondrocyte dedifferentiation in vitro and its implications for cell-based cartilage therapy. *Am J Transl Res* **7**, 194–208 (2015).
75. Angele, P., Fritz, J., Albrecht, D., Koh, J. & Zellner, J. Defect type, localization and marker gene expression determines early adverse events of matrix-associated autologous chondrocyte implantation. *Injury* **46**, S2–S9 (2015).
76. Albrecht, C. *et al.* Influence of Cell Differentiation and IL-1β Expression on Clinical Outcomes After Matrix-Associated Chondrocyte Transplantation. *Am J Sports Med* **42**, 59–69 (2014).
77. Niemeyer, P., Pestka, J. M., Salzmann, G. M., Südkamp, N. P. & Schmal, H. Influence of Cell Quality on Clinical Outcome After Autologous Chondrocyte Implantation. *Am J Sports Med* **40**, 556–561 (2012).
78. Schött, U., Solomon, C., Fries, D. & Bentzer, P. The endothelial glycocalyx and its disruption, protection and regeneration: a narrative review. *Scandinavian Journal of Trauma, Resuscitation and Emergency Medicine* **24**, 48 (2016).
79. Ait-Oufella, H., Maury, E., Lehoux, S., Guidet, B. & Offenstadt, G. The endothelium: physiological functions and role in microcirculatory failure during severe sepsis. *Intensive Care Med* **36**, 1286–1298 (2010).
80. Newby, A. C. & Zaltsman, A. B. Molecular mechanisms in intimal hyperplasia. *The Journal of Pathology* **190**, 300–309 (2000).
81. Ip, J. H. *et al.* The role of platelets, thrombin and hyperplasia in restenosis after coronary angioplasty. *Journal of the American College of Cardiology* **17**, 77–88 (1991).
82. Htay, T. & Liu, M. W. Drug-Eluting Stent: A Review and Update. *Vasc Health Risk Manag* **1**, 263–276 (2005).
83. ten Berg, J. M., Plokker, H. T. & Verheugt, F. W. Antiplatelet and anticoagulant therapy in elective percutaneous coronary intervention. *Curr Control Trials Cardiovasc Med* **2**, 129–140 (2001).

84. Pfisterer Matthias E. Late Stent Thrombosis After Drug-Eluting Stent Implantation for Acute Myocardial Infarction. *Circulation* **118**, 1117–1119 (2008).
85. Van der Meer, J.-Y., Kellenbach, E. & Van den Bos, L. J. From Farm to Pharma: An Overview of Industrial Heparin Manufacturing Methods. *Molecules* **22**, 1025 (2017).
86. Garnjanagoonchorn, W., Wongekalak, L. & Engkagul, A. Determination of chondroitin sulfate from different sources of cartilage. *Chemical Engineering and Processing: Process Intensification* **46**, 465–471 (2007).
87. Schiraldi, C., Cimini, D. & De Rosa, M. Production of chondroitin sulfate and chondroitin. *Appl Microbiol Biotechnol* **87**, 1209–1220 (2010).
88. Woo, J. E., Seong, H. J., Lee, S. Y. & Jang, Y.-S. Metabolic Engineering of Escherichia coli for the Production of Hyaluronic Acid From Glucose and Galactose. *Frontiers in Bioengineering and Biotechnology* **7**, (2019).
89. Rice, K. G. The Chemistry, Biology, and Medical Applications of Hyaluronan and Its Derivatives Edited by T. C. Laurent. Portland Press, London, U.K. 1998. xvi + 341 pp. 17 × 25 cm. ISBN 1-85578-119-0. $127.50. *J. Med. Chem.* **41**, 5336–5336 (1998).
90. Ialenti, A. & Di Rosa, M. Hyaluronic acid modulates acute and chronic inflammation. *Agents Actions* **43**, 44–47 (1994).
91. Wang, C.-T., Lin, Y.-T., Chiang, B.-L., Lin, Y.-H. & Hou, S.-M. High molecular weight hyaluronic acid down-regulates the gene expression of osteoarthritis-associated cytokines and enzymes in fibroblast-like synoviocytes from patients with early osteoarthritis. *Osteoarthritis and Cartilage* **14**, 1237–1247 (2006).
92. Zhou, P.-H., Liu, S.-Q. & Peng, H. The effect of hyaluronic acid on IL-1β-induced chondrocyte apoptosis in a rat model of osteoarthritis. *Journal of Orthopaedic Research* **26**, 1643–1648 (2008).
93. Scheibner, K. A. *et al.* Hyaluronan Fragments Act as an Endogenous Danger Signal by Engaging TLR2. *The Journal of Immunology* **177**, 1272–1281 (2006).
94. Lesley, J., Hascall, V. C., Tammi, M. & Hyman, R. Hyaluronan Binding by Cell Surface CD44 *. *Journal of Biological Chemistry* **275**, 26967–26975 (2000).
95. Campo, G. M. *et al.* Hyaluronan reduces inflammation in experimental arthritis by modulating TLR-2 and TLR-4 cartilage expression. *Biochimica et Biophysica Acta (BBA) - Molecular Basis of Disease* **1812**, 1170–1181 (2011).
96. Noble, P. W., McKee, C. M., Cowman, M. & Shin, H. S. Hyaluronan fragments activate an NF-kappa B/I-kappa B alpha autoregulatory loop in murine macrophages. *Journal of Experimental Medicine* **183**, 2373–2378 (1996).
97. Campo, G. M. *et al.* Small hyaluronan oligosaccharides induce inflammation by engaging both toll-like-4 and CD44 receptors in human chondrocytes. *Biochemical Pharmacology* **80**, 480–490 (2010).
98. Iovu, M., Dumais, G. & du Souich, P. Anti-inflammatory activity of chondroitin sulfate. *Osteoarthritis and Cartilage* **16**, S14–S18 (2008).
99. Stabler, T. V., Huang, Z., Montell, E., Vergés, J. & Kraus, V. B. Chondroitin sulphate inhibits NF-κB activity induced by interaction of pathogenic and damage associated molecules. *Osteoarthritis and Cartilage* **25**, 166–174 (2017).
100. Pomin, V. H. Sulfated glycans in inflammation. *European Journal of Medicinal Chemistry* **92**, 353–369 (2015).
101. Kawashima, H. *et al.* Binding of a Large Chondroitin Sulfate/Dermatan Sulfate Proteoglycan, Versican, to L-selectin, P-selectin, and CD44 *. *Journal of Biological Chemistry* **275**, 35448–35456 (2000).
102. Suwan, K. *et al.* Versican/PG-M Assembles Hyaluronan into Extracellular Matrix and Inhibits CD44-mediated Signaling toward Premature Senescence in Embryonic Fibroblasts *. *Journal of Biological Chemistry* **284**, 8596–8604 (2009).

103. Fujimoto, T. *et al.* CD44 binds a chondroitin sulfate proteoglycan, aggrecan. *Int. Immunol.* **13**, 359–366 (2001).
104. Harris, E. N. & Weigel, P. H. The ligand-binding profile of HARE: hyaluronan and chondroitin sulfates A, C, and D bind to overlapping sites distinct from the sites for heparin, acetylated low-density lipoprotein, dermatan sulfate, and CS-E. *Glycobiology* **18**, 638–648 (2008).
105. Rolls, A. *et al.* A sulfated disaccharide derived from chondroitin sulfate proteoglycan protects against inflammation-associated neurodegeneration. *The FASEB Journal* **20**, 547–549 (2006).
106. Chou, M. M. *et al.* Effects of Chondroitin and Glucosamine Sulfate in a Dietary Bar Formulation on Inflammation, Interleukin-1β, Matrix Metalloprotease-9, and Cartilage Damage in Arthritis. *Exp Biol Med (Maywood)* **230**, 255–262 (2005).
107. Campo, G. M. *et al.* Efficacy of treatment with glycosaminoglycans on experimental collagen-induced arthritis in rats. *Arthritis Res Ther* **5**, R122 (2003).
108. Orth, M. W., Peters, T. L. & Hawkins, J. N. Inhibition of articular cartilage degradation by glucosamine-HCl and chondroitin sulphate. *Equine Veterinary Journal* **34**, 224–229 (2002).
109. Kawasaki, K., Ochi, M., Uchio, Y., Adachi, N. & Matsusaki, M. Hyaluronic acid enhances proliferation and chondroitin sulfate synthesis in cultured chondrocytes embedded in collagen gels. *Journal of Cellular Physiology* **179**, 142–148 (1999).
110. Peng, H. *et al.* Hyaluronic acid inhibits nitric oxide-induced apoptosis and dedifferentiation of articular chondrocytes in vitro. *Inflamm. Res.* **59**, 519–530 (2010).
111. Wu, S.-C. *et al.* Hyaluronan initiates chondrogenesis mainly via CD44 in human adipose-derived stem cells. *Journal of Applied Physiology* **114**, 1610–1618 (2013).
112. Wu, S.-C. *et al.* Hyaluronan size alters chondrogenesis of adipose-derived stem cells via the CD44/ERK/SOX-9 pathway. *Acta Biomaterialia* **66**, 224–237 (2018).
113. Xu, Y. *et al.* Effect of CD44 on differentiation of human amniotic mesenchymal stem cells into chondrocytes via Smad and ERK signaling pathways. *Molecular Medicine Reports* **21**, 2357–2366 (2020).
114. Chung, C. & Burdick, J. A. Influence of Three-Dimensional Hyaluronic Acid Microenvironments on Mesenchymal Stem Cell Chondrogenesis. *Tissue Engineering Part A* **15**, 243–254 (2009).
115. Skaalure, S. C., Dimson, S. O., Pennington, A. M. & Bryant, S. J. Semi-interpenetrating networks of hyaluronic acid in degradable PEG hydrogels for cartilage tissue engineering. *Acta Biomaterialia* **10**, 3409–3420 (2014).
116. Kudo, T. *et al.* Supplemented Chondroitin Sulfate and Hyaluronic Acid Suppress Mineralization of the Chondrogenic Cell Line, ATDC5, *via* Direct Inhibition of Alkaline Phosphatase. *Biological and Pharmaceutical Bulletin* **40**, 2075–2080 (2017).
117. Varghese, S. *et al.* Chondroitin sulfate based niches for chondrogenic differentiation of mesenchymal stem cells. *Matrix Biol.* **27**, 12–21 (2008).
118. Aisenbrey, E. A. & Bryant, S. J. The role of chondroitin sulfate in regulating hypertrophy during MSC chondrogenesis in a cartilage mimetic hydrogel under dynamic loading. *Biomaterials* **190–191**, 51–62 (2019).
119. Wang, T. & Yang, F. A comparative study of chondroitin sulfate and heparan sulfate for directing three-dimensional chondrogenesis of mesenchymal stem cells. *Stem Cell Research & Therapy* **8**, 284 (2017).
120. Meghdadi, M., Pezeshki-Modaress, M., Irani, S., Atyabi, S. M. & Zandi, M. Chondroitin sulfate immobilized PCL nanofibers enhance chondrogenic differentiation of mesenchymal stem cells. *International Journal of Biological Macromolecules* **136**, 616–624 (2019).
121. Brinkhous, K. M., Smith, H. P., Warner, E. D. & Seegers, W. H. THE INHIBITION OF BLOOD CLOTTING: AN UNIDENTIFIED SUBSTANCE WHICH ACTS IN CONJUNCTION WITH HEPARIN TO

PREVENT THE CONVERSION OF PROTHROMBIN INTO THROMBIN. *American Journal of Physiology-Legacy Content* **125**, 683–687 (1939).
122. Muñoz, E. M. & Linhardt, R. J. Heparin-Binding Domains in Vascular Biology. *ATVB* **24**, 1549–1557 (2004).
123. Al Dieri, R., Wagenvoord, R., Van Dedem, G. W. K., Béguin, S. & Hemker, H. C. The inhibition of blood coagulation by heparins of different molecular weight is caused by a common functional motif—the C-domain. *Journal of Thrombosis and Haemostasis* **1**, 907–914 (2003).
124. Gray, E., Hogwood, J. & Mulloy, B. The Anticoagulant and Antithrombotic Mechanisms of Heparin. in *Heparin - A Century of Progress* (eds. Lever, R., Mulloy, B. & Page, C. P.) 43–61 (Springer, 2012). doi:10.1007/978-3-642-23056-1_3.
125. Huntington, J. A., Read, R. J. & Carrell, R. W. Structure of a serpin–protease complex shows inhibition by deformation. *Nature* **407**, 923–926 (2000).
126. Griffith, M. J. Heparin-catalyzed inhibitor/protease reactions: kinetic evidence for a common mechanism of action of heparin. *Proceedings of the National Academy of Sciences* **80**, 5460–5464 (1983).
127. O'Keeffe, D. *et al.* The Heparin Binding Properties of Heparin Cofactor II Suggest an Antithrombin-like Activation Mechanism *. *Journal of Biological Chemistry* **279**, 50267–50273 (2004).
128. Van Walderveen, M. C., Berry, L. R. & Chan, A. K. C. Effect of covalent antithrombin-heparin on activated protein C inactivation by protein C inhibitor. *The Journal of Biochemistry* **148**, 255–260 (2010).
129. Linhardt, R. J., Murugesan, S. & Xie, J. Immobilization of Heparin: Approaches and Applications. *Current Topics in Medicinal Chemistry* **8**, 80–100 (2008).
130. Courtney, J. M., Lamba, N. M. K., Sundaram, S. & Forbes, C. D. Biomaterials for blood-contacting applications. *Biomaterials* **15**, 737–744 (1994).
131. Kang, I. K., Kwon, O. H., Lee, Y. M. & Sung, Y. K. Preparation and surface characterization of functional group-grafted and heparin-immobilized polyurethanes by plasma glow discharge. *Biomaterials* **17**, 841–847 (1996).
132. Duncan, A. C., Boughner, D., Campbell, G. & Wan, W. K. Preparation and characterization of a poly(2-hydroxyethyl methacrylate) biomedical hydrogel. *European Polymer Journal* **37**, 1821–1826 (2001).
133. Chandy, T., Das, G. S., Wilson, R. F. & Rao, G. H. R. Use of plasma glow for surface-engineering biomolecules to enhance bloodcompatibility of Dacron and PTFE vascular prosthesis. *Biomaterials* **21**, 699–712 (2000).
134. Favia, P. *et al.* Immobilization of Heparin and Highly-Sulphated Hyaluronic Acid onto Plasma-Treated Polyethylene. *Plasmas and Polymers* **3**, 77–96 (1998).
135. Turner, N. J., Kielty, C. M., Walker, M. G. & Canfield, A. E. A novel hyaluronan-based biomaterial (Hyaff-11®) as a scaffold for endothelial cells in tissue engineered vascular grafts. *Biomaterials* **25**, 5955–5964 (2004).
136. Rother, S. *et al.* Sulfated Hyaluronan Alters Endothelial Cell Activation in Vitro by Controlling the Biological Activity of the Angiogenic Factors Vascular Endothelial Growth Factor-A and Tissue Inhibitor of Metalloproteinase-3. *ACS Appl. Mater. Interfaces* **9**, 9539–9550 (2017).
137. Montanari, E. *et al.* Chasing bacteria within the cells using levofloxacin-loaded hyaluronic acid nanohydrogels. *European Journal of Pharmaceutics and Biopharmaceutics* **87**, 518–523 (2014).
138. Mazumder, M. A. J., Fitzpatrick, S. D., Muirhead, B. & Sheardown, H. Cell-adhesive thermogelling PNIPAAm/hyaluronic acid cell delivery hydrogels for potential application as minimally invasive retinal therapeutics. *J. Biomed. Mater. Res., Part A* **100A**, 1877–1887 (2012).
139. Shu, X. Z., Liu, Y., Luo, Y., Roberts, M. C. & Prestwich, G. D. Disulfide Cross-Linked Hyaluronan Hydrogels. *Biomacromolecules* **3**, 1304–1311 (2002).

140. Fenn, S. L. & Oldinski, R. A. Visible light crosslinking of methacrylated hyaluronan hydrogels for injectable tissue repair. *Journal of Biomedical Materials Research Part B: Applied Biomaterials* **104**, 1229–1236 (2016).
141. Owen, S. C., Fisher, S. A., Tam, R. Y., Nimmo, C. M. & Shoichet, M. S. Hyaluronic Acid Click Hydrogels Emulate the Extracellular Matrix. *Langmuir* **29**, 7393–7400 (2013).
142. Lee, F., Eun Chung, J. & Kurisawa, M. An injectable enzymatically crosslinked hyaluronic acid – tyramine hydrogel system with independent tuning of mechanical strength and gelation rate. *Soft Matter* **4**, 880–887 (2008).
143. Loebel, C., Rodell, C. B., Chen, M. H. & Burdick, J. A. Shear-thinning and self-healing hydrogels as injectable therapeutics and for 3D-printing. *Nature Protocols* **12**, 1521–1541 (2017).
144. Kim, H. D. *et al.* Chondroitin Sulfate-Based Biomineralizing Surface Hydrogels for Bone Tissue Engineering. *ACS Appl. Mater. Interfaces* **9**, 21639–21650 (2017).
145. Conovaloff, A. & Panitch, A. Characterization of a chondroitin sulfate hydrogel for nerve root regeneration. *J. Neural Eng.* **8**, 056003 (2011).
146. Butterfield, K. C., Conovaloff, A. W. & Panitch, A. Development of affinity-based delivery of NGF from a chondroitin sulfate biomaterial. *Biomatter* **1**, 174–181 (2011).
147. Varghese, J. M. *et al.* Thermoresponsive hydrogels based on poly(N-isopropylacrylamide)/chondroitin sulfate. *Sensors and Actuators B: Chemical* **135**, 336–341 (2008).
148. Feng, Q. *et al.* Sulfated hyaluronic acid hydrogels with retarded degradation and enhanced growth factor retention promote hMSC chondrogenesis and articular cartilage integrity with reduced hypertrophy. *Acta Biomaterialia* **53**, 329–342 (2017).
149. Prudnikova, K. *et al.* Aggrecan-like biomimetic proteoglycans (BPGs) composed of natural chondroitin sulfate bristles grafted onto a poly(acrylic acid) core for molecular engineering of the extracellular matrix. *Acta Biomater.* **75**, 93–104 (2018).
150. Prudnikova, K. *et al.* Biomimetic Proteoglycans Mimic Macromolecular Architecture and Water Uptake of Natural Proteoglycans. *Biomacromolecules* **18**, 1713–1723 (2017).
151. Pauly, H. M., Place, L. W., Haut Donahue, T. L. & Kipper, M. J. Mechanical Properties and Cell Compatibility of Agarose Hydrogels Containing Proteoglycan Mimetic Graft Copolymers. *Biomacromolecules* **18**, 2220–2229 (2017).
152. Bernhard, J. C. & Panitch, A. Synthesis and characterization of an aggrecan mimic. *Acta Biomater.* **8**, 1543–1550 (2012).
153. Lawrence, A. *et al.* Synthesis and characterization of a lubricin mimic (mLub) to reduce friction and adhesion on the articular cartilage surface. *Biomaterials* **73**, 42–50 (2015).
154. Scott, R. A., Paderi, J. E., Sturek, M. & Panitch, A. Decorin Mimic Inhibits Vascular Smooth Muscle Proliferation and Migration. *PLOS ONE* **8**, e82456 (2013).
155. Dehghani, T. *et al.* Selectin-targeting glycosaminoglycan-peptide conjugate limits neutrophil-mediated cardiac reperfusion injury. *Cardiovascular Research* (2020) doi:10.1093/cvr/cvaa312.
156. Singh, A. *et al.* Enhanced lubrication on tissue and biomaterial surfaces through peptide-mediated binding of hyaluronic acid. *Nature Mater* **13**, 988–995 (2014).
157. Hu, M., Sabelman, E. E., Cao, Y., Chang, J. & Hentz, V. R. Three-dimensional hyaluronic acid grafts promote healing and reduce scar formation in skin incision wounds. *J. Biomed. Mater. Res., Part B* **67B**, 586–592 (2003).
158. Patterson, J. *et al.* Hyaluronic acid hydrogels with controlled degradation properties for oriented bone regeneration. *Biomaterials* **31**, 6772–6781 (2010).
159. Bian, L. *et al.* The influence of hyaluronic acid hydrogel crosslinking density and macromolecular diffusivity on human MSC chondrogenesis and hypertrophy. *Biomaterials* **34**, 413–421 (2013).
160. Yoon, S. J. *et al.* Regeneration of ischemic heart using hyaluronic acid-based injectable hydrogel. *Journal of Biomedical Materials Research Part B: Applied Biomaterials* **91B**, 163–171 (2009).

161. Kim, M., Lee, J. Y., Jones, C. N., Revzin, A. & Tae, G. Heparin-based hydrogel as a matrix for encapsulation and cultivation of primary hepatocytes. *Biomaterials* **31**, 3596–3603 (2010).
162. Shin, J. *et al.* Tissue Adhesive Catechol-Modified Hyaluronic Acid Hydrogel for Effective, Minimally Invasive Cell Therapy. *Advanced Functional Materials* **25**, 3814–3824 (2015).
163. Park, S. H. *et al.* An injectable click-crosslinked hyaluronic acid hydrogel modified with a BMP-2 mimetic peptide as a bone tissue engineering scaffold. *Acta Biomaterialia* **117**, 108–120 (2020).
164. Bian, L., Zhai, D. Y., Mauck, R. L. & Burdick, J. A. Coculture of Human Mesenchymal Stem Cells and Articular Chondrocytes Reduces Hypertrophy and Enhances Functional Properties of Engineered Cartilage. *Tissue Eng., Part A* **17**, 1137–1145 (2010).
165. Liu, C. *et al.* Inhibition of astrocytic differentiation of transplanted neural stem cells by chondroitin sulfate methacrylate hydrogels for the repair of injured spinal cord. *Biomater. Sci.* **7**, 1995–2008 (2019).
166. Sahoo, S., Chung, C., Khetan, S. & Burdick, J. A. Hydrolytically Degradable Hyaluronic Acid Hydrogels with Controlled Temporal Structures. *Biomacromolecules* **9**, 1088–1092 (2008).
167. Colletta, V., Dioguardi, D., Di Lonardo, A., Maggio, G. & Torasso, F. A trial to assess the efficacy and tolerability of Hyalofill-F in non-healing venous leg ulcers. *J Wound Care* **12**, 357–361 (2003).
168. Hettiaratchi, M. H. *et al.* Heparin-mediated delivery of bone morphogenetic protein-2 improves spatial localization of bone regeneration. *Science Advances* **6**, eaay1240.
169. Wang, P. *et al.* Controlled Growth Factor Release in 3D-Printed Hydrogels. *Advanced Healthcare Materials* **9**, 1900977 (2020).
170. Jin, R. *et al.* Synthesis and characterization of hyaluronic acid–poly(ethylene glycol) hydrogels via Michael addition: An injectable biomaterial for cartilage repair. *Acta Biomaterialia* **6**, 1968–1977 (2010).
171. Chang, K.-Y., Hung, L.-H., Chu, I.-M., Ko, C.-S. & Lee, Y.-D. The application of type II collagen and chondroitin sulfate grafted PCL porous scaffold in cartilage tissue engineering. *J. Biomed. Mater. Res., Part A* **92A**, 712–723 (2010).
172. Tan, H. *et al.* Thermosensitive injectable hyaluronic acid hydrogel for adipose tissue engineering. *Biomaterials* **30**, 6844–6853 (2009).
173. Oh, S. H., An, D. B., Kim, T. H. & Lee, J. H. Wide-range stiffness gradient PVA/HA hydrogel to investigate stem cell differentiation behavior. *Acta Biomaterialia* **35**, 23–31 (2016).
174. Ying, H. *et al.* In situ formed collagen-hyaluronic acid hydrogel as biomimetic dressing for promoting spontaneous wound healing. *Materials Science and Engineering: C* **101**, 487–498 (2019).
175. Guo, Y. *et al.* Hydrogels of collagen/chondroitin sulfate/hyaluronan interpenetrating polymer network for cartilage tissue engineering. *J Mater Sci: Mater Med* **23**, 2267–2279 (2012).
176. Sawatjui, N. *et al.* Silk fibroin/gelatin–chondroitin sulfate–hyaluronic acid effectively enhances in vitro chondrogenesis of bone marrow mesenchymal stem cells. *Materials Science and Engineering: C* **52**, 90–96 (2015).
177. Hu, X., Li, D., Zhou, F. & Gao, C. Biological hydrogel synthesized from hyaluronic acid, gelatin and chondroitin sulfate by click chemistry. *Acta Biomater.* **7**, 1618–1626 (2011).
178. Little, C. J., Kulyk, W. M. & Chen, X. The Effect of Chondroitin Sulphate and Hyaluronic Acid on Chondrocytes Cultured within a Fibrin-Alginate Hydrogel. *Journal of Functional Biomaterials* **5**, 197–210 (2014).
179. Bahcecioglu, G., Hasirci, N., Bilgen, B. & Hasirci, V. Hydrogels of agarose, and methacrylated gelatin and hyaluronic acid are more supportive for in vitro meniscus regeneration than three dimensional printed polycaprolactone scaffolds. *Int. J. Biol. Macromol.* **122**, 1152–1162 (2019).
180. Strehin, I., Nahas, Z., Arora, K., Nguyen, T. & Elisseeff, J. A versatile pH sensitive chondroitin sulfate–PEG tissue adhesive and hydrogel. *Biomaterials* **31**, 2788–2797 (2010).

181. Jeon, O., Lee, K. & Alsberg, E. Spatial Micropatterning of Growth Factors in 3D Hydrogels for Location-Specific Regulation of Cellular Behaviors. *Small* **14**, 1800579 (2018).
182. Kilmer, C. E., Walimbe, T., Panitch, A. & Liu, J. C. Incorporation of a Collagen-Binding Chondroitin Sulfate Molecule to a Collagen Type I and II Blend Hydrogel for Cartilage Tissue Engineering. *ACS Biomater. Sci. Eng.* **8**, 1247–1257 (2022).
183. Levett, P. A. *et al.* A biomimetic extracellular matrix for cartilage tissue engineering centered on photocurable gelatin, hyaluronic acid and chondroitin sulfate. *Acta Biomater.* **10**, 214–223 (2014).
184. Stuart, K. & Panitch, A. Characterization of Gels Composed of Blends of Collagen I, Collagen III, and Chondroitin Sulfate. *Biomacromolecules* **10**, 25–31 (2009).
185. Vázquez-Portalatín, N., Kilmer, C. E., Panitch, A. & Liu, J. C. Characterization of Collagen Type I and II Blended Hydrogels for Articular Cartilage Tissue Engineering. *Biomacromolecules* **17**, 3145–3152 (2016).

# 2. Physical and Bioactive Properties of Glycosaminoglycan Hydrogels Modulated by Polymer Design Parameters and Polymer Ratio

This chapter consists of the manuscript published by Michael Nguyen, Julie C. Liu, and Alyssa Panitch published in Biomacromolecules, volume 22, issue 10, 2021.

**Abstract:**

Glycosaminoglycans (GAGs), such as hyaluronic acid (HA) and chondroitin sulfate (CS), have seen widespread adoptions as components of tissue engineering scaffolds due to their potent bioactive properties and ease of chemical modification. However, modification of the biopolymers will impair biological recognition of the GAG and reduce the bioactive properties of the material. In this work, we studied how the degree of thiolation of HA and CS, along with other key hydrogel design parameters, affected the physical and bioactive properties of the bulk hydrogel. Although properties, such as the HA molecular weight, did not have a major effect, increasing the degree of thiolation of both HA and CS decreased their biorecognition in experimental analogues for cell/matrix remodeling and binding. Furthermore, combining HA and CS into dual polymer network hydrogels also modulated the physical and bioactive properties, as seen with differences in gel stiffness, degradation rate, and encapsulated cell viability.

## 2.1. Introduction:

While the human body possesses natural healing capacity, situations can arise where the body is incapable of repairing the damaged tissue, such as in the case of critically sized tissue defects or

disfunction of the natural repair pathways[1,2]. To address these medical needs, the field of tissue engineering has been developing methods to engineer replacement tissue. Tissue engineering approaches often employ cells seeded in a scaffold, such as a hydrogel, where the cells generate new tissue while the gel serves as a support structure. Synthetic polymers, such as poly(ethylene glycol) or poly(lactic acid), can provide scaffolds with very well-defined properties and characteristics; however, they lack the biological signals present in natural extracellular matrix[3–6]. On the other hand, natural polymers such as collagen and fibrin have also been used, but they lack the degree of chemical and mechanical tunability present in synthetic polymers[3,7–11].

Over the past two decades, glycosaminoglycans (GAGs), including hyaluronic acid (HA) and chondroitin sulfate (CS), have seen increased use as components of tissue engineering scaffolds in a variety of fields, including bone[12,13], cartilage[14,15], skin[16,17], vocal fold[18], and nerve tissue regeneration[19]. HA and CS are naturally produced polymers, widely distributed within the extracellular matrix, and important for bodily function and cellular processes[20,21]. These GAGs possess potent bioactive properties including cell-directive signals[22–24] and anti-inflammatory properties[25], and they possess many chemically reactive hydroxyl and carboxylic acid groups. While these reactive moieties can exist as part of the bioactive motifs, they can also support chemical functionalization to allow for crosslinking and hydrogel formation. A wide variety of modifying agents including methacrylates[26], thiols[27], furans[28], tyramines[29], and various other species[30] have been conjugated to HA and CS for gel formation. Although the addition of these groups can allow for increases in stiffness and compressive strength of the gel through increased crosslink density as well as provide handles for chemical addition of other bioactive factors, modification of the natural polymer structure may inhibit the ability of the cell to recognize and interact with native chemical moieties and thus reduce the number and potency of bioactive signals presented to the cells[31,32]. Among the previously reported studies, there is little consensus regarding the optimal degree of modification for HA and CS, and the degree of modification of these GAGs varies widely between papers.

In this study, we focused on designing CS and HA hydrogels that maximize the bioactive properties of the GAGs while maintaining the ability to crosslink the polymers into hydrogels and encapsulate cells. To do so, we synthesized and characterized hydrogels using thiolated HA and CS with increasing degrees of thiolation (DOT) and tested their biorecognition with two *in vitro* analogues of in vivo bioactivity. These tests included a hyaluronidase digestion assay, which represented how well encapsulated cells would be able to remodel their environment, and a GAG binding assay, which represented how well proteins, including receptors and growth factors, would be able to interact with the modified GAGs. Next, we examined the effect of HA molecular weight ranging from 40 kDa[33] to 1.5 MDa[19,34] and evaluated the viscoelastic properties of the resultant gels and effects of molecular weight on bioactivity. Finally, we fabricated and tested dual polymer network (DPN) hydrogels with the two GAGs to combine the chemical and biological signals of CS and HA. The ratio of CS to HA was tested to determine how it affected physical and bioactive properties of the hydrogel. Specifically, we fabricated CS/HA DPN hydrogels utilizing DOT and molecular weight that retained maximum biological activity, as determined using the hyaluronidase and peptide binding assays, to investigate how the combination of these two polymers affected hydrogel properties and cell survival.

## 2.2. Materials and Methods:

### 2.2.1: Preparation and Characterization of Thiolated Hyaluronic Acid and Chondroitin Sulfate

Thiolated HA (HA-SH) was prepared using a modified version of a previously reported protocol[18]. Hyaluronic acid (molecular weight ($M_w$): 10 kDa, 60 kDa, 100 kDa, 200 kDa, 500 kDa, Lifecore Biomedical) was first dissolved in 0.1 M 2-(N-morpholino)ethanesulfonic acid (MES) buffer with 0.2 wt% NaCl at a concentration of 2 mg/mL. To attach free thiol groups, dithio-bis(propionohydrazide) (DTP) and 1-ethyl-3-(3-dimethylaminopropyl)carbodiimide (EDC) were dissolved in the HA solution. The degree of thiolation was controlled through the amount of DTP added, and a 1:1 molar ratio of DTP to the desired percentage

of modified HA carboxylic acid groups was used. EDC was added in a 2:1 molar ratio with respect to DTP. The reaction solution was titrated to a pH of 4.5 and was reacted overnight at room temperature. To cleave the disulfide bond of DTP, the HA solution was titrated to a pH of 8 and dithiothreitol (DTT) was added in 3:1 molar excess of the DTP. The DTT was allowed to react for 3 hours at room temperature before the solution was titrated to pH 4.5 to prevent the reformation of disulfide bonds. The polymer was then purified using a KrosFlo KR2i tangential flow filtration (TFF) unit (Repligen) using a 5 kDa molecular weight cut off column and a transmembrane pressure of 18 PSI. The solution was purified until a permeate volume of three times the reaction volume had been reached. After purification, the polymer was frozen and lyophilized until further use. Thiolated CS (CS-SH) ($M_w$: 40 kDa, Seikigaku Corporation) was synthesized using the same methods. Free thiol content of HA-SH and CS-SH were quantified using an Ellman's assay, and cysteine was used to construct a standard curve. Degree of thiolation (DOT) was defined as the percentage of GAG carboxylic acid groups converted to free thiols. To validate the results from the Ellman's assay, the DOT of low and high DOT HA-SH and CS-SH was determined using $^1$H nuclear magnetic resonance (NMR) spectroscopy. Samples were dissolved in $D_2O$ and run on a Bruker 800 MHz Avance III. DOT was determined by integrating the beta methylene peak on the thiol side chain and dividing by the integral of the of the *N*-acetyl methyl group of the *N*-acetylglucosamine monomer on both HA and CS[27]. DOT determined through NMR were within ± 5% of the Ellman's assay (Figure 2.1, 2.2).

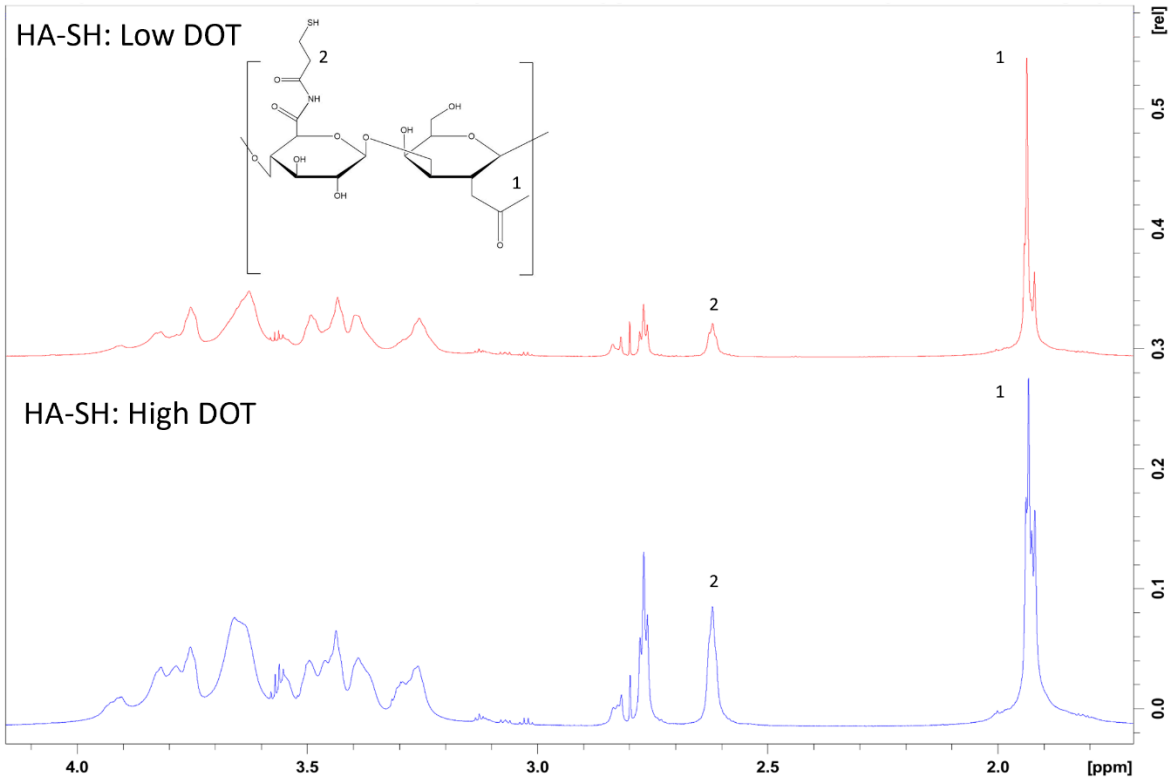


*Figure 2.1: $^{1}H$ NMR (800 MHz, $D_2O$) Spectra of HA-SH with High (30.4%) and Low (17.8%) DOT. (1) N-acetyl methyl, δ 1.93 (m, 3H, $CH_2$-C(O)-$CH_3$). (2) Thiol side chain methylene, δ 2.62 (s, 2H, N-C(O)-$CH_2$-C).*

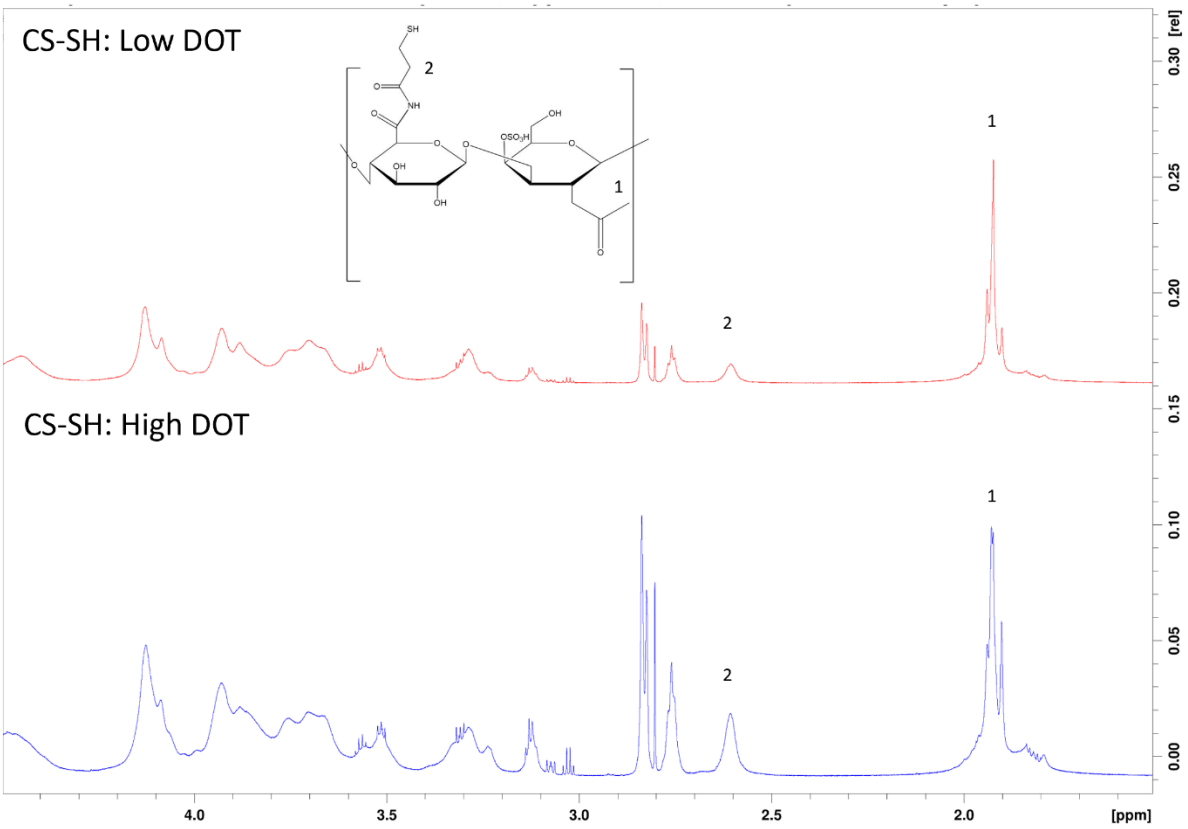


*Figure 2.2: $^{1}H$ NMR (800 MHz, $D_2O$) Spectra of CS-SH with High (34.8%) and Low (17.6%) DOT. (1) N-acetyl methyl, δ 1.93 (m, 3H, $CH_2$-C(O)-$CH_3$). (2) Thiol side chain methylene, δ 2.61 (s, 2H, N-C(O)-$CH_2$-C).*

### 2.2.2: Fabrication of HA-SH and CS-SH Hydrogels

Hydrogels composed of 1.5 w/v% HA-SH and CS-SH were formed by crosslinking the polymer chains with poly(ethylene glycol) diacrylate (PEGDA) ($M_w$: 3.4 kDa, Alfa Aesar). HA-SH and CS-SH were dissolved at a concentration of 3 w/v% in 360 µL of phosphate buffered saline (PBS). For CS/HA DPN hydrogels, weight/ weight ratios of 10:0, 7:3, 5:5, 3:7, and 0:10 CS to HA were used with the total GAG content being kept at 1.5 w/v% (Table 1). For determination of the minimum DOT for gel formation, a stoichiometric quantity of PEGDA to fully react with all available free thiols was added. For experiments

comparing properties of HA-SH and CS-SH with low and high thiolation degrees, the lower mass of PEGDA was used to crosslink both low and high DOT gels. To prevent spontaneous disulfide bridge formation in the high thiolation gels, N-ethyl maleimide (NEM) was added to the PEGDA fraction to cap free thiols in a 1:1 molar ratio of NEM to remaining free thiols after PEGDA crosslinking. For experiments involving CS/HA DPN gels, PEGDA content was held constant between all groups to maintain a constant crosslink density between groups, using the PEGDA required to fully crosslink the 10:0 group. For all experiments, PEGDA was dissolved in PBS and mixed with the HA-SH or CS-SH solution. To form the gels, the prepolymer solutions were titrated to pH 7.8, after which sufficient PBS was added to bring the concentration of the GAG to 1.5 w/v%. The hydrogels were then incubated overnight at 37 ºC in a humidified environment.

**Table 2.1:** Concentrations of CS and HA used for CS/HA DPN hydrogels

| **Ratio of CS/HA** | **10:0** | **7:3** | **5:5** | **3:7** | **0:10** |
|---|---|---|---|---|---|
| **Concentration of CS (mg/mL)** | 15 | 10.5 | 7.5 | 4.5 | 0 |
| **Concentration of HA (mg/mL)** | 0 | 4.5 | 7.5 | 10.5 | 15 |

### 2.2.3: Mechanical Testing of GAG Hydrogels

To determine the stiffness of the HA-SH and CS-SH hydrogels, 150 µL hydrogels were polymerized directly onto Teflon coated microscope slides (Tekdon), with a hydrophilic area of 20 mm. After overnight incubation, stiffness of the hydrogels was determined using a Discovery Hybrid Rheometer (TA Instruments). An oscillation frequency sweep from 0.1 to 100 rad/s was performed using a 20 mm head with a constant stress of 1 Pa. Storage modulus and tan(δ) of the hydrogels were determined from the

linear region of the sweep, if available. For determination of the minimum DOT for gel formation, 100 kDa HA-SH was used based off HA molecular weight experiments.

### 2.2.4: Enzymatic Degradation of GAG Hydrogels

For all degradation experiments, enzymatic degradation was conducted using a 50 U/mL solution of bovine testes hyaluronidase type I-S (Sigma Aldrich) in PBS. Degradation of hydrogels was conducted at 37 $^{o}$C with the gels continuously agitated on a plate shaker.

#### *2.2.4.1: Degradation of GAG homopolymer hydrogels*

To determine the degradation rate of HA-SH of varying molecular weights, as well as HA-SH and CS-SH of low and high DOTs, 100 µL gels were made directly in 96-well plates and left to incubate overnight at 37 $^{o}$C. At the start of the experiment, 100 µL fresh hyaluronidase solution was pipetted on top of the hydrogels then immediately removed to obtain a zero-hour time point. Fresh hyaluronidase solution was pipetted on top, with the supernatant removed and replaced with fresh hyaluronidase solution every two hours for a total of ten hours. To assess degradation of HA, a carbazole assay was performed to determine the concentration of free HA in the collected supernatants. To assess degradation of CS, a dimethylmethylene blue (DMMB) assay was performed to determine the concentration of free CS in the collected supernatants.

#### *2.2.4.2: Degradation of CS/HA DPN hydrogels*

To determine the degradation rate of CS/HA DPN hydrogels, 100 µL gels were made directly in the bottom of 0.5 mL microcentrifuge tubes, with the initial masses of the tubes recorded to calculate gel masses. After polymerization, hydrogels were first allowed to swell overnight with PBS. After overnight swelling, 300 µL of fresh hyaluronidase solution was added atop the gels and incubated for 24 hours at 37

°C. After 24 hours, the supernatant was discarded, the gels were blotted dry, and the mass of the gel was recorded. A total of seven time points were taken, and the hyaluronidase solution was replaced and the gel masses were recorded every 24 hours. After seven days, the gels were dialyzed against ultrapure water to remove salt at 4 °C overnight. Gels were then frozen and lyophilized, and the dry masses of the gels were recorded.

### 2.2.5: Peptide-Glycan Binding to GAG Hydrogels

#### *2.2.5.1: Peptide-Glycan synthesis and characterization*

The HA-binding peptide GAH (GAHWQFNALTVGSG) was synthesized with a C-terminal hydrazide for coupling to CS and was obtained from Chinese Peptide Company. The CS-binding peptide YKT (YKTNFRRYYRFGSG) was also synthesized with a C-terminal hydrazide for coupling to HA and was produced using a Liberty Blue peptide synthesizer with standard Fmoc solid phase peptide synthesis techniques. After synthesis, YKT was purified using reverse phase fast protein liquid chromatography, and the collected fractions were verified using matrix assisted time of flight mass spectrometry.

Synthesis of peptide-glycan conjugates was performed using a modified version of a previously reported method[35]. To synthesize GAH coupled to CS (CS-GAH) and YKT coupled to 100 kDa HA (HA-YKT), the GAGs were dissolved at 10 mg/mL in 0.1 M MES buffer with 8 M urea. One hundred molar excess of 4-(4,6-dimethoxy-1,3,5-triazin-2-yl)-4-methyl-morpholinium chloride (DMTMM) was added with respect to the GAG. GAH was added in a 10:1 molar ratio of peptide to CS and YKT was added in a 30:1 ratio of peptide to HA. The solution was titrated to a pH of 4.5 and allowed to react for three days at room temperature. At the end of the reaction, the solutions were diluted 5X to stop the reaction and purified using TFF using the same parameters as the HA-SH and CS-SH synthesis. Peptide attachment was

quantified by measuring the 280 nm absorbance of the peptide-glycan and comparing the results to a standard curve made of the free peptide.

*2.2.5.2: Peptide-Glycan binding assay*

To determine the binding ability of CS-GAH and HA-YKT to HA-SH and CS-SH, respectively, of low and high DOTs, 40 µL gels were made directly in a black opaque 96-well plate. After gelation, 10 µM solutions of CS-GAH and HA-YKT were pipetted atop the gels and left to incubate for thirty minutes at room temperature. After this time, the supernatant was removed, and the gels were washed three times with PBS to remove non adherent peptide-glycans. After washing, peptide-glycan attachment was quantified by measuring the intrinsic fluorescence of tryptophan and tyrosine residues of the gels to determine CS-GAH and HA-YKT binding, respectively. Intrinsic fluorescence of tryptophan was measured at an excitation of 295 nm and emission of 350, and the intrinsic fluorescence of tyrosine was measured at an excitation of 280 nm and emission of 305 nm.

**2.2.6: MSC Viability in CS/HA DPN Hydrogels**

*2.2.6.1: Rabbit MSC isolation and culture*

Rabbit MSCs were isolated from the bone marrow from the femurs of 6-month old New Zealand white rabbits. After euthanasia following an unrelated procedure, the discarded femurs were isolated. The neck of the femur was clipped off, and the bone marrow was rinsed out using warmed Dulbecco's Modified Eagle Medium (DMEM) (Gibco) into 50 mL conical tubes. Erythrocytes were lysed through the addition of sterile deionized water into the tube, and the tubes were centrifuged to remove the dead cells. The resulting pellet was broken up and cells were plated on polystyrene tissue culture plates and incubated overnight in a humidified environment at 37 $^{o}$C. The next day, the non-adherent cell population was aspirated, and the adherent MSC population was subsequently cultured using a medium consisting

of low glucose DMEM with Glutamax supplement (Gibco), 10% fetal bovine serum (Gibco), 5% penicillin/streptomycin (Gibco), and 10 µg/ml basic fibroblast growth factor (Lonza). Cells were passaged at 70-80% confluence and used at passage two.

*2.2.6.2: MSC Viability in CS/HA DPN Hydrogels*

To assess cell viability as a function of CS/HA ratio on DPN hydrogels, MSCs were encapsulated in CS/HA DPN hydrogels at a cell concentration of $10^6$ cells/mL. Ten µL gels were pipetted directly onto Ibidi µ-Slides and allowed to gel for one hour at 37 $^oC$ in a humidified environment. After polymerization, fresh cell medium was pipetted atop the gels, and the medium was changed every day. At time points of one and six days, the cell medium was aspirated and replaced with 4 µM of Calcein AM (Invitrogen) and 6 µM of ethidium homodimer (Invitrogen) in PBS to stain for live and dead cells, respectively. The cells were incubated for thirty minutes, after which the staining solution was removed and replaced with PBS. To image the cells, fluorescent images were taken using a Keyence BZ-X700 fluorescent microscope at a magnification of 10X. A Z-stack image of the gels was taken with a depth of 500 µm, and Z-stack images were combined using the full focus algorithm in the accompanying Keyence image analysis software. Each Z-stack image had a cross sectional area of 1.6 $mm^2$, corresponding to 13% of the total hydrogel area. One image from the center of each biological replicate was taken. Live/dead counts were determined using the find maxima algorithm in ImageJ.

**2.2.7: Statistics**

Data are represented as means, and error bars correspond to standard deviation. For the comparison of two groups, statistical significance was determined using a T-Test. For comparing more than two groups, statistical significance was determined with single factor equal variance ANOVA, and differences between groups were determined using Tukey's post hoc tests. Statistical analysis was

performed using Graphpad Prism, and a probability value of 95% ($P < 0.05$) was used to determine statistical significance.

**2.3. Results and Discussion:**

**2.3.1: Minimum Thiolation for Hydrogel Formation**

To examine how degree of thiolation affected bioactivity of HA and CS, GAGs with varying percentages of thiolation, as determined by the percentages of available carboxylate groups that were converted to thiols, were synthesized. However, prior to bioactivity assays, the minimum DOT required for gelation had to be determined. Following reaction with DTP and EDC, HA with DOTs of 2.3%, 5.3%, 9.9%, 13.7%, 17.8%, and 24.0% were obtained (Table 2.2). Results from rheological testing showed that HA-SH with a DOT of 5.3% thiolation formed a gel (Figure2. 3) whereas, at a DOT of 2.3%, the HA-SH did not gel as denoted by a tan(δ) value greater than 1 (Figure 2.3c). Furthermore, at 5.3% thiolation, the gel exhibited an average G' value of 16.5 Pa, which would not be robust enough for most tissue engineering applications. As expected, G' values increased with increasing degrees of thiolation. The 17.8% DOT HA-SH produced robust gels with a modest DOT. This result, coupled with the data presented below showing a similar degree of thiolation (17.6%) was required for robust CS gelation, led to 17.8% DOT HA-SH being chosen for experiments investigating the impact of HA molecular weight on gel stability and as the low DOT for experiments investigating the impact of DOT on HA biological activity.

**Table 2.2: Free Thiol Quantification for HA-SH Batches**

| HA MW | Average 412 nm Abs | Average mM -SH | Average DOT |
|---|---|---|---|
| 100 kDa | 0.037 | 0.061 | 2.3% |
| 100 kDa | 0.086 | 0.138 | 5.2% |
| 100 kDa | 0.164 | 0.262 | 9.9% |
| 100 kDa | 0.227 | 0.361 | 13.7% |
| 100 kDa | 0.295 | 0.468 | 17.8% |
| 100 kDa | 0.344 | 0.545 | 20.7% |
| 100 kDa | 0.400 | 0.633 | 24.0% |
| 10 kDa | 0.275 | 0.437 | 16.6% |
| 60 kDa | 0.285 | 0.453 | 17.2% |
| 100 kDa | 0.285 | 0.452 | 17.1% |
| 200 kDa | 0.288 | 0.456 | 17.3% |
| 500 kDa | 0.281 | 0.446 | 16.9% |
| 100 kDa | 0.515 | 0.801 | 30.4% |

For CS-SH, it was found that a DOT higher than that required for HA-SH was needed to form a robust gel. Following reactions with DTP and EDC, CS with DOTs of 4.2%, 8.2%, 15.1%, 17.6%, 25.5%, 28.8%, and 35.1% were obtained (Table 2.3). Below 15.1%, CS-SH gels did not form, and 15.1% thiolated CS-SH formed a weak gel with a G' of 43.2 Pa (Figure 2.3). To maintain parity with HA-SH in terms DOT, a CS-SH thiolation degree of 17.6% was chosen for future experiments. Given similar DOT levels, it was found that CS-SH hydrogels were weaker than HA-SH hydrogels (697.9 Pa for HA-SH and 304.4 Pa for CS-SH at a DOT of ~17.7%). The chosen DOT for HA-SH and CS-SH falls on the lower end of previously reported degrees of modification for both polymers, and other groups reported degrees of modification between 7[36,37] and 71%[26,38]. While other groups achieved hydrogel formation at degrees of modification lower than 17%, other factors such as reacting the GAG chains directly with one another[36], the addition of other polymers[39,40], or differences in the concentration of polymer used[41] may account for the need for a DOT of ~17% to support gel formation in the study reported here. In this regard, the minimum DOT for gel formation is specific to a chosen crosslinking method and polymer concentration.

**Table 2.3: Free Thiol Quantification for CS-SH Batches**

| CS MW | Average 412 nm Abs | Average mM -SH | Average DOT |
|---|---|---|---|
| 40 kDa | 0.054 | 0.088 | 4.2% |
| 40 kDa | 0.108 | 0.173 | 8.2% |
| 40 kDa | 0.199 | 0.317 | 15.1% |
| 40 kDa | 0.233 | 0.370 | 17.6% |
| 40 kDa | 0.338 | 0.536 | 25.5% |
| 40 kDa | 0.382 | 0.605 | 28.8% |
| 40 kDa | 0.465 | 0.737 | 35.1% |
| 40 kDa | 0.462 | 0.731 | 34.8% |

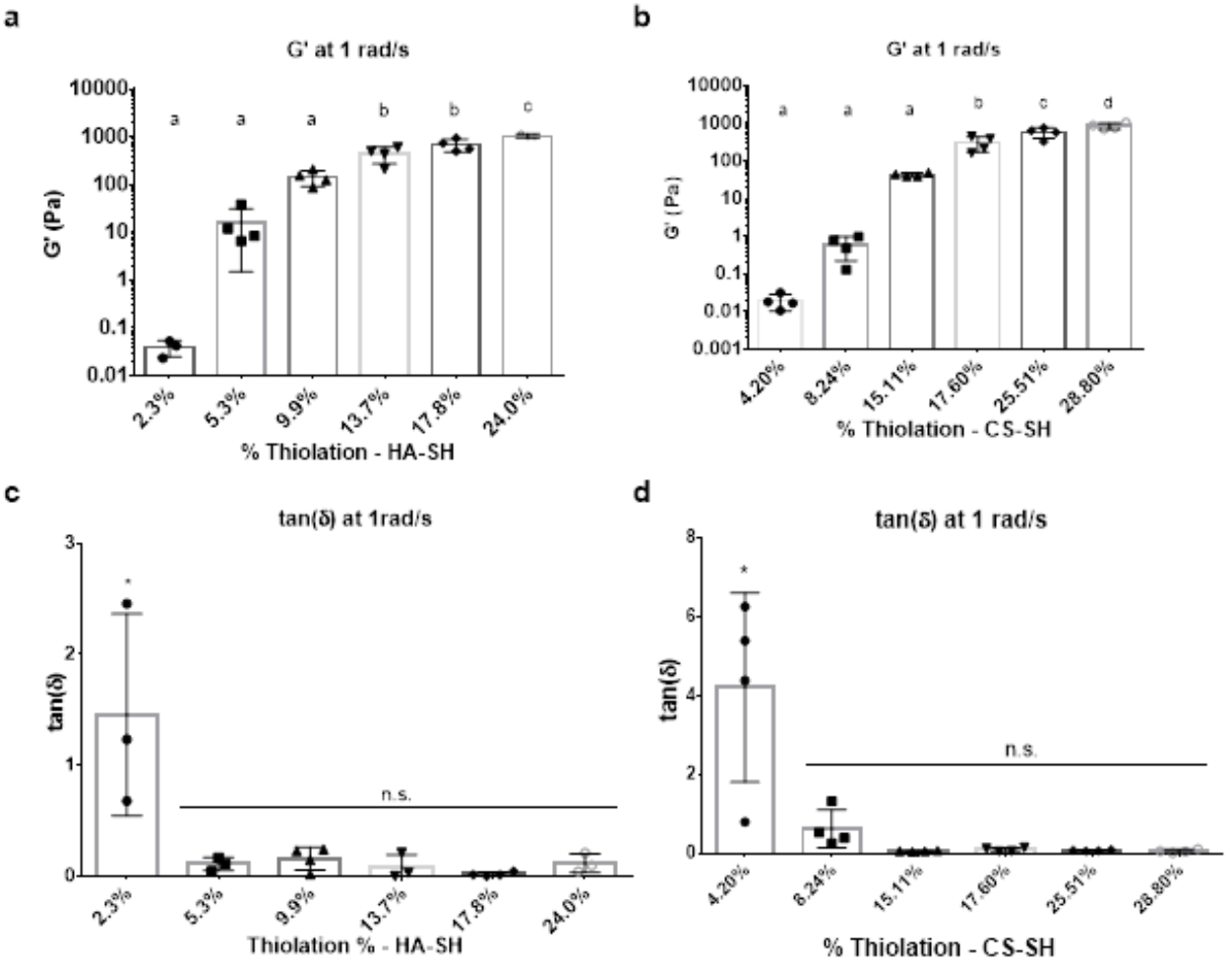


*Figure 2.3: Mechanical properties of HA-SH (MW: 100 kDa, 1.5 w/v%) and CS-SH (MW: 40 kDa, 1.5 w/v%) hydrogels increase as a function of DOT. (a) Storage modulus of HA-SH gels as a function of DOT. (b)*

*Storage modulus of CS-SH gels as a function of DOT. (c) tan(δ) of HA-SH gels. (d) tan(δ) of CS-SH gels. * denotes statistical significance (P < 0.05) from all other groups. n.s. denotes no significance between groups (P > 0.05)*

### 2.3.2: Effects of GAG DOT on Bioactivity

#### 2.3.2.1: Effect of GAG DOT on Hyaluronidase Activity

To assess bioactivity of HA-SH hydrogels, one chosen metric was to measure hydrogel susceptibility to hyaluronidases as a measure of hyaluronidase recognition and degradation of HA as a function of DOT. This assay assessed the effect of thiolation on enzymatic recognition sites within the HA chain since fewer recognition sites would lead to decreased degradation. Hyaluronidase degradation was chosen as a proxy to understand how the degree of modification of the GAGs would affect the encapsulated cells' ability to remodel the environment via secretion of hyaluronidase or how durable the material would be in a pro-inflammatory environment characterized by an increased level of hyaluronidases. To maintain consistent crosslink density, low DOT HA-SH (17.8%) and high DOT HA-SH (30.2%) were both crosslinked with the same amount of PEGDA needed to fully crosslink the 17.8% DOT HA-SH. Free thiols in the high DOT gels were capped with NEM to prevent disulfide bridge formation (Figure 2.4a). It has been previously demonstrated that maleimide groups react with thiols at a faster rate than acrylates; therefore, it is believed that the amount of free thiols available for crosslinking with PEGDA between the high and low DOT groups is roughly equivalent[42]. As such, any inefficiencies in crosslinking should be seen in both groups. This was further confirmed through rheological analysis of gels with high (with NEM) and low DOT, with the stiffness of the two groups being statistically equivalent (Figure 2.5).

Following 10 hours of hyaluronidase degradation, it was found that the 30.2% DOT HA-SH degraded significantly less than the 17.8% DOT HA-SH, and these results suggest that fewer hyaluronidase recognition sites exist at a higher DOT (Figure 2.4b, c).

Similarly, the bioactivity of CS-SH with respect to DOT was tested through hyaluronidase digestion since CS is also cleavable by hyaluronidase. Low DOT CS-SH (17.6%) and high DOT CS-SH (35.1%) were gelled with consistent crosslink density using the same methods as described for HA-SH. As expected, CS-SH generally degraded less than HA-SH due to the molecular differences between the two GAGs. Furthermore, similar to HA-SH, high DOT CS-SH also degraded less than low DOT CS-SH, and these results also suggest limited hyaluronidase recognition of CS due to increased modification (Figure 2.4b, c).

For both CS and HA, decreasing DOT resulted in increased susceptibility to hyaluronidase degradation. Increased susceptibility would not only allow encapsulated cells to more easily remodel their environment but also make the hydrogels more susceptible to degradation in the presence of increased concentrations of hyaluronidase, such as those found in pro-inflammatory environments[43]. As such, the optimal DOT of CS-SH and HA-SH will depend on the intended application and target environment of the hydrogel. While others have detailed how crosslink density affected the degradation rate of HA hydrogels, changes in degradation rate depended on both the degree of modification and the diffusivity of species within the hydrogel[44,45]. By capping free thiols, we were able keep crosslink density constant, removing a confounding factor with regard to hyaluronidase degradation.

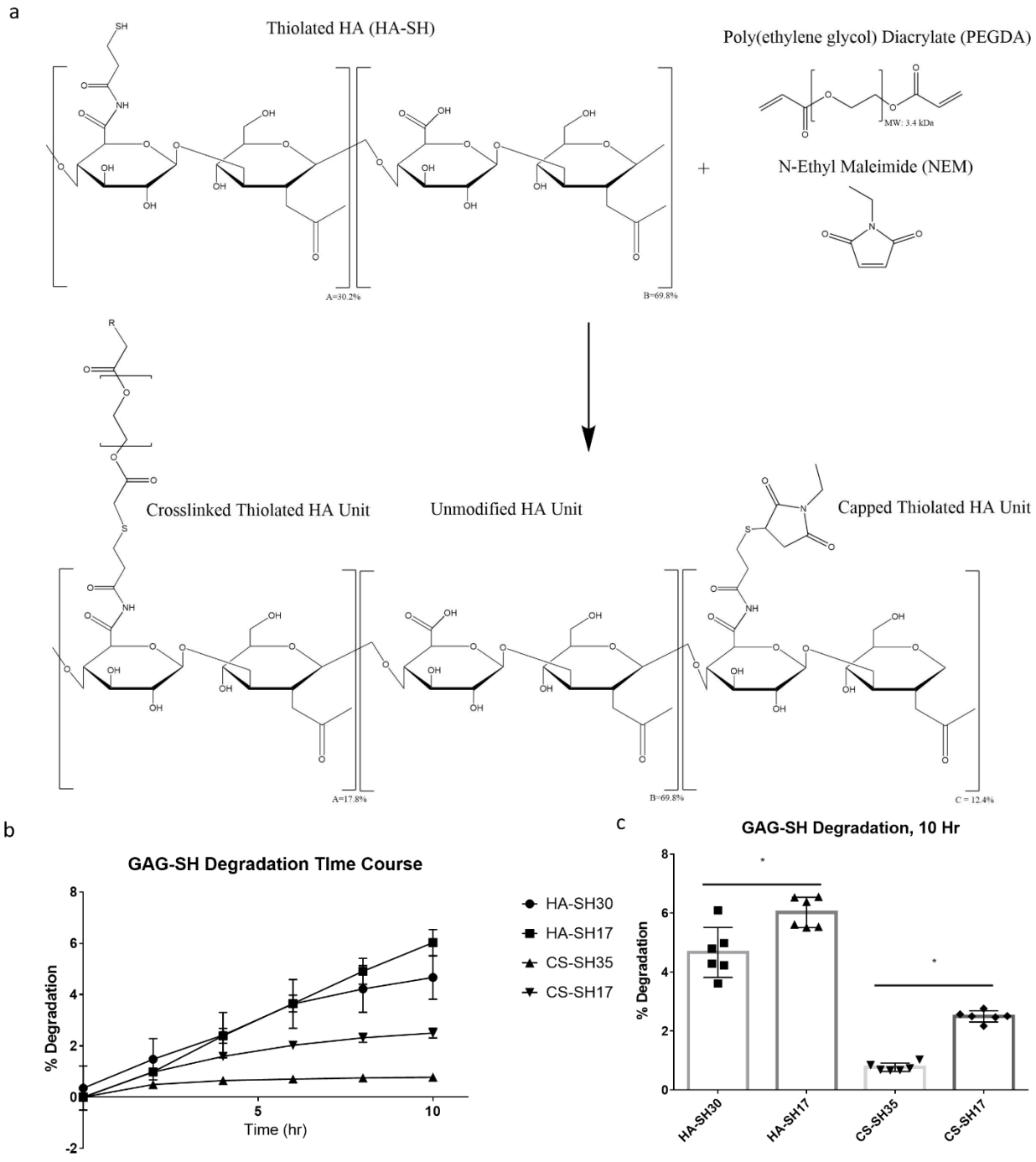


*Figure 2.4: Degradation of HA-SH (MW: 100 kDa, 1.5 w/v%) and CS-SH (MW: 40 kDa, 1.5 w/v%) hydrogels as a function of GAG DOT. (a) Schematic of NEM mediated capping of free thiols on HA-SH. (b) Degradation of HA-SH and CS-SH over time. (c) Cumulative Degradation of HA-SH and CS-SH at 10 hours. * denotes statistical significance (P < 0.05) between groups*

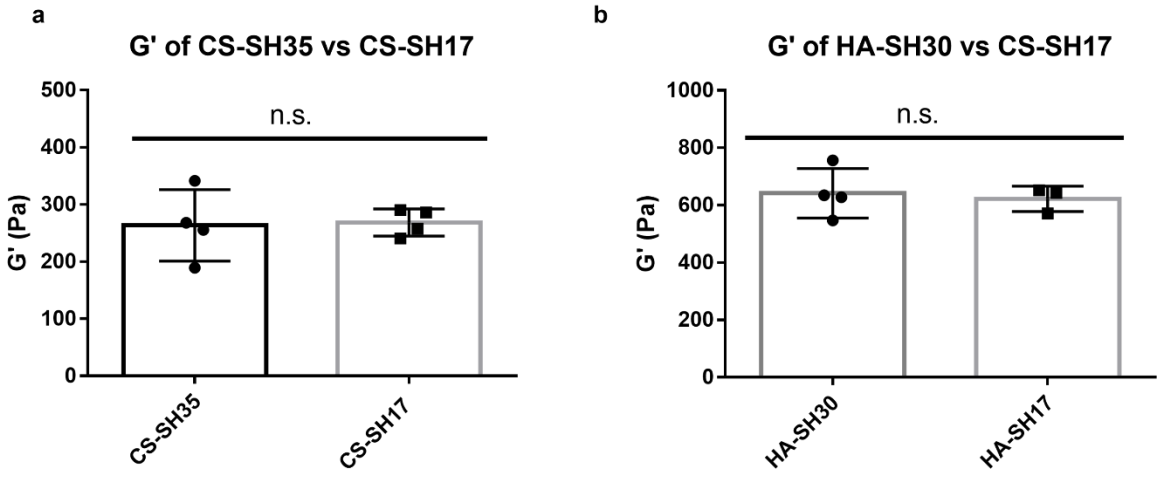


*Figure 2.5: G' of GAG-SH at high and low DOT. (a) G' of CS-SH at high (34.8%) and low (17.6%) DOT. (b) G' of HA-SH at high (30.4%) and low (17.8%) DOT. n.s. denotes no significance between groups (p > 0.05)*

**2.3.2.2: Peptide-Glycan Interaction with Thiolated GAG Hydrogels**

Another selected measure of bioactivity with regard to the DOT of the GAGs was the ability for biomolecules to interact with or bind to the thiolated GAGs, as occurs between proteins, such as growth factors, and GAGs within the extracellular matrix (ECM). As biomolecule analogs, the peptide-glycans CS-GAH and HA-YKT, which bind to HA and CS, respectively, served as proxies for protein and proteoglycans that interact with GAGs. These molecules were chosen as biomolecule analogs due to our previous experience developing and characterizing peptide-glycan constructs, with CS-GAH in particular previously described as an aggrecan mimetic that binds to HA[35,46]. Both GAH and YKT peptides were originally discovered from peptide arrays with the intention of maximizing interaction with HA and CS, respectively[47,48]. Following incubation with solubilized CS-GAH, which had an average of ten peptides bound to one CS molecule, it was found that significantly less CS-GAH bound to HA-SH of higher DOT compared to that of the lower DOT (Figure 2.6). Similarly, significantly less HA-YKT, which had an average

30 peptides bound to one HA molecule, bound to the high thiolation CS-SH compared to the lower thiolation CS-SH (Figure 2.6). These results are consistent with other previously reported protein binding studies. Kwon et al demonstrated decreased CD44 binding to HA as the HA was increasingly modified[31]. Although the HA and CS binding peptides are not derived from a specific protein, cationic charge motifs similar to those found in GAH and YKT peptides have been documented in the heparin binding domains of several proteins[49]. Because of these similarities in amino acid sequence and charge, the ability of these peptide-glycans to bind to HA-SH and CS-SH provides insight as to how heparin binding proteins might interact with the GAGs as a function of DOT. After six days of culture in HA-SH and CS-SH gels of high and low DOT, a small increase in MSC viability was found in the low DOT CS-SH gel compared to the high DOT gel, but no difference was found between the HA-SH gels of low and high DOT (figure 2.7). This difference in viability may be explained through differences in protein binding, as seen in the peptide-glycan binding assay. A decrease in cell viability was seen in all groups over the culture period, though this may have been due to the slow diffusion of cellular DNA from the hydrogel.

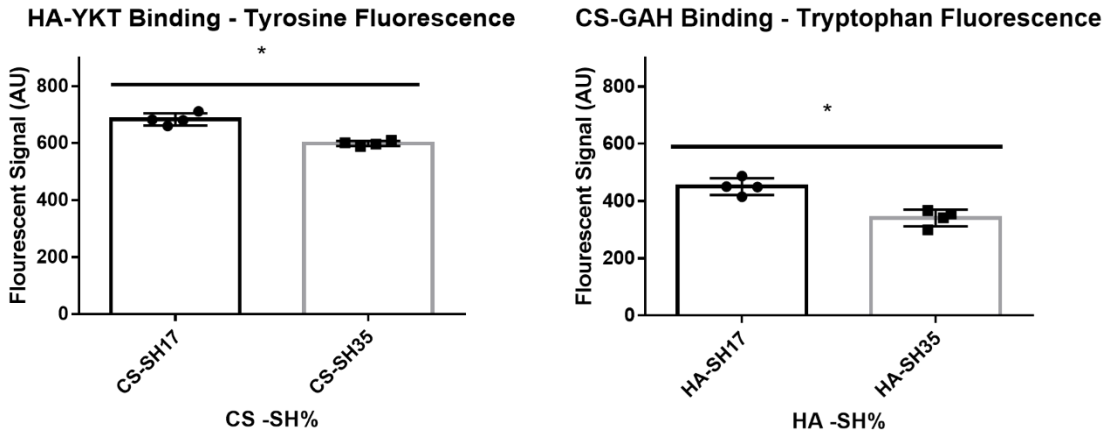


*Figure 2.6: HA-YKT Binding to CS-SH (MW: 40 kDa) and CS-GAH binding to HA-SH (MW: 100 kDa) as measured by intrinsic fluorescence of tyrosine and tryptophan Residues. * denotes statistical significance ($P < 0.05$) between groups*

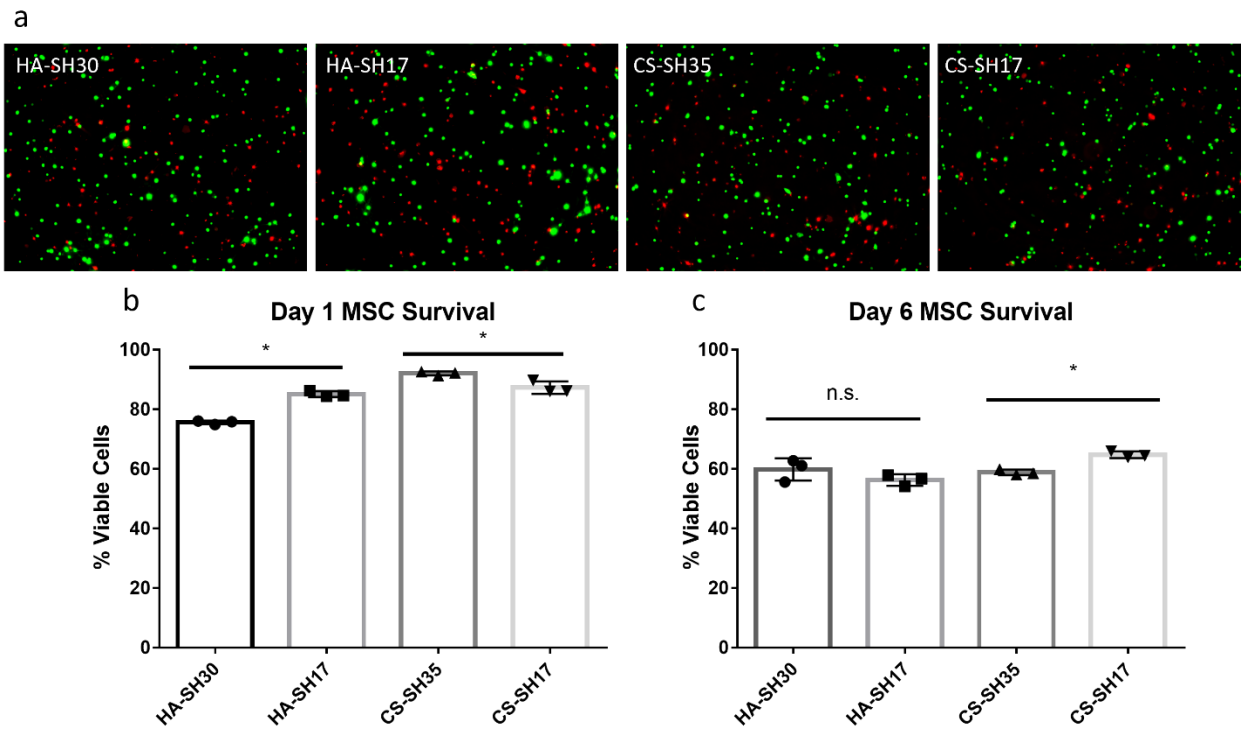


*Figure 2.7: Live/dead assay of MSCs encapsulated in HA-SH (MW: 100 kDa, High DOT 30.4%, low DOT: 17.8%, 1.5 w/v%) and CS-SH (MW: 100 kDa, High DOT 34.8 %, low DOT: 17.6%, 1.5 w/v%) gels at high and low DOT. (a) MSCs in HA-SH or CS-SH Hydrogels stained with Calcein AM (green) and Ethidium homodimer (red) at day six. Scale bar represents 100 µm (b) MSC viability at day one, n = 3. (c) MSC viability at day six, n = 3. * denotes statistical significance (P < 0.05) from all other groups. n.s. denotes no significance between groups (P > 0.05)*

### 2.3.3: Effect of HA Molecular Weight on Hydrogel Stiffness and Hyaluronidase Activity

To determine the effect of HA molecular weight on the enzymatic degradation of the resulting hydrogel, 10 kDa, 60 kDa, 100 kDa, 200 kDa, and 500 kDa HA-SH were synthesized with an approximate DOT of 17±0.4%. For this experiment, we hypothesized that hydrogels formed with higher molecular weight HA would be more resistant to degradation due to the increased number of crosslinks per polymer

chain and reduced number of chain ends. As such, once one glycosidic bond was hydrolyzed by hyaluronidase, the probability of the cleaved chain remaining connected to the polymer network would be higher for polymers of higher molecular weight. To keep crosslink density consistent between all groups, the same amount of PEGDA was used to crosslink all HA-SH groups. Following 8 hours of enzymatic degradation with hyaluronidase, it was found that between 60 kDa and 500 kDa, there was little difference in the rate of enzymatic degradation, contrary to our initial hypothesis. In contrast the 10 kDa HA-SH did show significantly greater degradation than did the HA-SH of higher molecular weights (Figure 2.8a,b). To contextualize this difference in degradation between the different molecular weights of HA-SH, the stiffness of the intact gels was determined. It was found that between 60 kDa and 500 kDa, there was no significant difference in stiffness, but the gels made with 10 kDa HA-SH were significantly weaker than the other groups (Figure 2.8c). The similar rates of degradation is probably due to the diffusivity of these hydrogels being similar, with this being inferred from the similar storage moduli between these groups. As such, the diffusivity of hyaluronidase could be the rate limiting factor for hydrogel degradation and why these hydrogels had similar degradation rates. In contrast, the weaker 10 kDa HA hydrogel may have allowed for increased hyaluronidase diffusion, resulting in quicker degradation. Thus, at an HA MW $\geq$60 kDA and a DOT of ~17%, the number of end groups does not significantly alter the stiffness of gels or the susceptibility to enzymatic degradation.

Although the molecular weights of HA used in other reported hydrogel systems have varied between studies and ranged from 40 kDa[50] to 1.5 MDa[36], the results reported here suggest that this inconsistency between MW of HA studied should not have a large effect on the enzymatic degradation rates nor on the stiffness of HA gels. Therefore, when fabricating HA only or DPN hydrogels, molecular weights above 60 kDa may not be one of the governing factors in polymer design with regard to degradation or stiffness. Going forward, 100 kDa HA-SH was chosen for CS/HA DPN experiments as it readily dissolved at the high concentrations required for hydrogel synthesis compared to the 200 kDa and

500 kDa variants, which exhibited lower solubility and are challenging to work with due to higher solution viscosity.

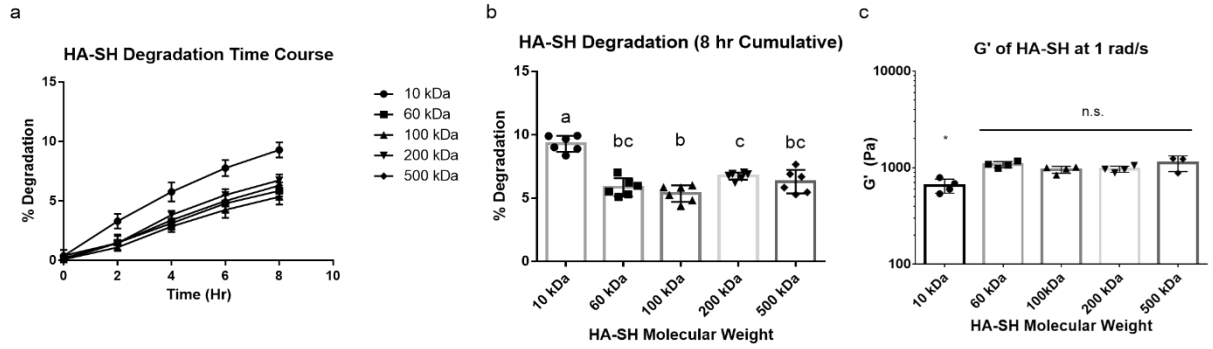


*Figure 2.8: Enzymatic Degradation of HA-SH Hydrogels (DOT: ~17±0.4%) with Respect to HA Molecular Weight. (a) Degradation of HA-SH gels of multiple molecular weights over time. (b) Cumulative degradation of HA-SH gels at eight hours. (c) Storage modulus of HA-SH with respect to HA molecular weight. Groups sharing letters are not statistically different (P > 0.05). * denotes statistical significance (P < 0.05) from all other groups. n.s. denotes no significance between groups ( P > 0.05).*

### 2.3.4: Mechanical Properties of CS/HA DPN Hydrogels

After determining the effects of DOT on degradation and peptide-glycan binding, we sought to characterize hydrogels fabricated with a CS/HA DPN network. The goal of this study was to develop an understanding of how the combination of CS and HA, specifically the ratio in which the two GAGs were incorporated, affected the properties of the hydrogel. Two main considerations regarding the GAGs were taken into account. First, the molecular weight of the HA was more than double that of the CS, and therefore crosslinking the two polymers together at different ratios may affect the stiffness and degradation of the materials. Second, due to the sulfate groups present on CS but not HA, modulating the

CS to HA ratio of the CS/HA DPN hydrogels would affect the internal charge of the hydrogels and could in turn affect swelling, stiffness, and degradation.

To test the mechanical properties of the CS/HA DPN hydrogels, gels with CS to HA w/w ratios of 10:0, 7:3, 5:5, 3:7, and 0:10 were fabricated with the same amount of PEGDA crosslinker to ensure that the crosslink density was consistent between groups. All groups containing any amount of CS had shear moduli that were not significantly different from one another (Figure 2.9). However, the group containing only HA had a significantly higher G' than all groups containing CS, including the DPN group that was predominantly HA (Figure 2.9). These results suggest that inclusion of CS into the DPN reduces the modulus of the gel, but this reduction did not depend on CS concentration. Although it has been shown that inclusion of CS into collagen hydrogels can decrease gel stiffness through interactions with the protein, it has not been shown previously that CS has a similar effect on HA gels[51]. This observation warrants further future study to determine whether CS-HA interactions, or perhaps the presence of increased negative charge, are responsible for altering gel polymer structure and therefore the stiffness of these gels.

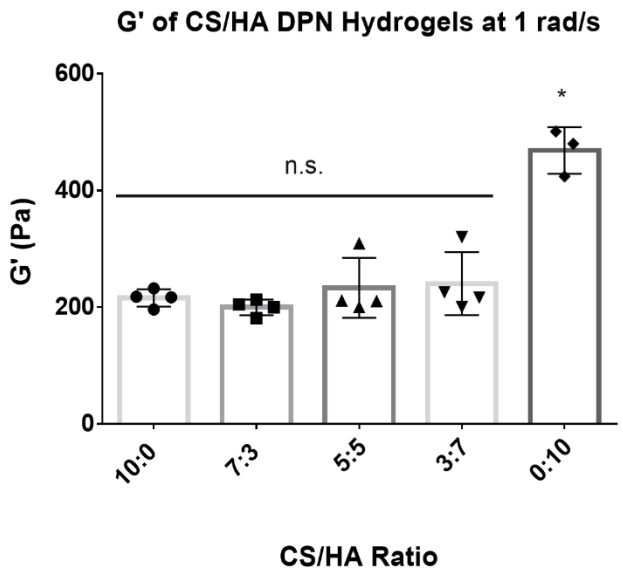


*Figure 2.9: Storage Modulus of CS/HA (CS MW: 40kDa, CS DOT: 17.6%; HA MW: 100 kDa, HA DOT: 17.8%; 1.5 w/v% GAG) DPN hydrogels at 1 rad/s. * denotes statistical significance (P < 0.05) from all other groups. n.s. denotes no significance between groups (P > 0.05)*

**2.3.5: CS/HA DPN Hydrogels Resist Enzymatic Degradation**

The enzymatic degradation of CS/HA DPNs was tested to determine the effect of blending the two polymers on the degradation of the bulk hydrogel, given the differences in enzymatic degradation between CS-SH and HA-SH. Chemical analysis of the hydrogel supernatant could not be performed due to a lack of HA-specific assays. For example, the carbazole assay measures the presence of glucuronic acid from HA and CS indiscriminately, whereas HA enzyme-linked immunosorbent assays (ELISAs) are limited because of decreased recognition of the modified, short fragments of HA that are released upon degradation[52]. As a result, bulk degradation of the DPN hydrogels was assessed through recording the total mass of the swollen gels daily and measuring the change in mass of the polymer content within the gel at the end of seven days. As the gels degraded over the course of seven days, most gels experienced an initial increase in mass likely caused by decreased crosslink density and increased swelling capacity

(Figure 2.10a,c). At longer times, a decrease in mass was observed likely coincident with sufficient polymer degradation to release free polymer fragments from the gels (Figure 2.10a,d). Although all groups reached a similar maximum increase in mass (~14-18%), the time point at which they did so roughly corresponded to their relative CS content. Groups with increased relative CS content reached their maximum mass earlier, and groups with increased relative HA content reached their peak later (Figure 2.10a).

Based upon findings regarding the degradation of the CS-SH and HA-SH homopolymer gels, we expected the CS only gel to have the slowest degradation rate and that increased CS content in the DPN groups would result in slower degradation. However, after seven days, the percentage of the polymer degradation of the DPN hydrogels was significantly lower than both the CS and HA homopolymer gels (Figure 2.10b). Over the same period, there was no significant difference in polymer content loss between the DPN groups. Although initial homopolymer tests did show resistance to hyaluronidase by CS, that previous experiment did not explore the long-term degradation mechanics of the gels. As such, our initial hypothesis did not consider the swelling mechanics of DPN hydrogels as they degraded over a longer period of time. The CS hydrogel swelled to a greater degree and at a faster rate than all of the other groups, likely due to the high density of the negatively-charged sulfate groups on the CS backbone, and this swelling may have allowed for increased hyaluronidase infiltration and more rapid degradation. On the other hand, although the HA did not swell to the same degree as the CS gel, HA is more susceptible to hyaluronidase degradation and thus the HA gel degraded at a faster rate than the CS gel. Based on the observed degradation of the HA-only and CS-only gels, it is believed that DPN hydrogels degraded less due to a balance of decreased hyaluronidase-susceptibility of CS and the lower swelling capacity of HA. As such, given the multifaceted nature of exogenous enzyme degradation involving both enzyme substrate recognition and enzyme infiltration, DPN hydrogels demonstrated reduced polymer degradation over time.

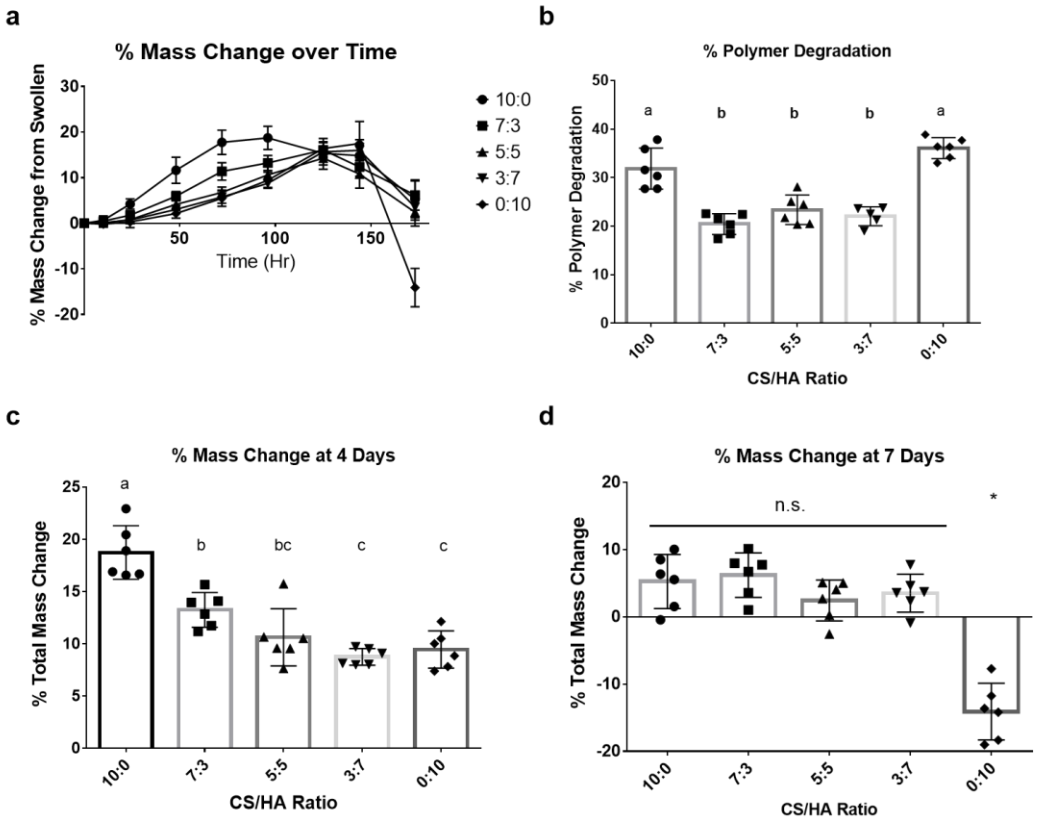


*Figure 2.10: Swelling and Degradation Mechanics of CS/HA (CS MW: 40kDa, CS DOT: 17.6%; HA MW: 100 kDa, HA DOT: 17.8%; 1.5 w/v% GAG) DPN Hydrogels in the Presence of Hyaluronidase. (a) Change in total mass of gels over time. (b) Percent polymer degradation after seven days. (c) Percent change in total gel mass after four days of hyaluronidase treatment. (d) Percent change in total gel mass after seven days hyaluronidase treatment. Groups sharing letters are not statistically different (P > 0.05). * denotes statistical significance (P < 0.05) from all other groups. n.s. denotes no significance between groups (P > 0.05)*

**2.3.6: CS/HA DPN Hydrogels Promote MSC Viability**

Although it is known that MSCs are able to interact with HA through the CD44 receptor, it has not been shown directly that MSCs use CD44 to interact with CS. However, CD44 is able to interact with CS in a cell-free system, and these results suggest that MSCs can bind to CS through CD44[53]. To evaluate the ability of the CS/HA DPN hydrogels to support cell survival, rabbit MSCs were encapsulated and cultured in gels for periods of one and six days. At the end of these time points, live and dead cells were stained and counted to determine average cell viability with respect to the hydrogel formulation. After one day of culture, no significant difference was found in cell viability, and average cell viability of the MSCs ranged from 83% to 87% (Figure 2.11). After culturing for six days, it was found that the cell populations in the HA homopolymer gel decreased and exhibited an average viability of 60% (Figure 2.11). In contrast, cell populations cultured in groups containing any amount of CS showed significantly higher viability at six days, ranging from 76% to 83%, and no significant difference was found between groups incorporating CS (Figure 2.7).

Although the MSCs should be able to bind and interact with the HA only gel via CD44, this formulation showed decreased cell viability compared to all CS groups. This finding suggests that the biological signals, in addition to CD44 interactions, provided by CS promote cell viability, but this signal does not promote cell viability in a dose-dependent manner. An alternative explanation to increased biological signaling coming directly from CS is that swelling due to increased CS content may have allowed enhanced nutrient diffusion and thus increased cell viability. Furthermore, the HA only gel was found to be significantly stiffer than all CS containing gels, with this increase in stiffness also possibly contributing to decreases in cell viability. Of note, all groups showed significant decreases in the percentage of viable cells between one day and six days of culture. This decrease may have been due to the lack of other supporting biological polymers, such as collagen, as similar decreases in cell viability over time in GAG-only gels have been reported elsewhere[18,54]. In those cases, cell viability increased following the inclusion

of collagen into the polymer network. To promote cell viability in future studies, collagen or other ECM proteins can be included to provide support for encapsulated cells.

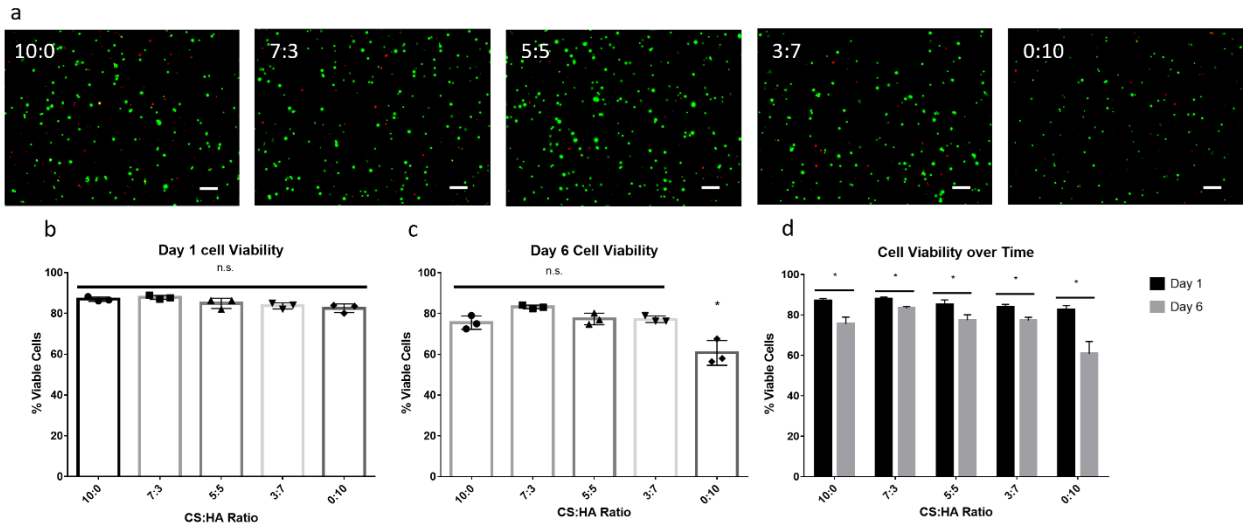


*Figure 2.11: Live/dead assay of MSCs encapsulated in CS/HA (CS MW: 40kDa, CS DOT: 17.6%; HA MW: 100 kDa, HA DOT: 17.8%; 1.5 w/v% GAG) DPN Hydrogels. (a) MSCs in CS/HA DPN Hydrogels stained with Calcein AM (green) and Ethidium homodimer (red) at day six. Scale bar represents 100 µm (b) MSC viability at day one, n = 3. (c) MSC viability at day six, n = 3. (d) Change in MSC viability between day one and day six. * denotes statistical significance (P < 0.05) from all other groups. n.s. denotes no significance between groups (P > 0.05)*

**2.4. Conclusion**

In this study we demonstrated the effects of CS-SH and HA-SH polymer design on the physical and bioactive properties of hydrogels. The minimum DOT was determined for the formation of robust hydrogels. HA molecular weight $\geq$60 kDa was not found to be a large factor impacting the enzymatic degradation and hydrogel stiffness. Increasing the DOT of both HA-SH and CS-SH was found to decrease their bioactivity as determined by both their ability to be degraded by hyaluronidase and their ability to

interact with HA and CS-binding peptides. These assays were performed as analogues for cellular interactions with their environment. CS-SH and HA-SH were incorporated together into DPN hydrogels with the eventual goal of stimulating encapsulated cells with the combined biological signals of the GAGs. DPN hydrogels resisted degradation by hyaluronidase to a greater degree than CS and HA homopolymer gels. Finally, the incorporation of CS in any amount into the DPN hydrogels demonstrated an increased ability to promote cell viability over the HA homopolymer gel.

**2.5. References:**


(1) Roddy, E.; DeBaun, M. R.; Daoud-Gray, A.; Yang, Y. P.; Gardner, M. J. Treatment of Critical-Sized Bone Defects: Clinical and Tissue Engineering Perspectives. *Eur J Orthop Surg Traumatol* **2018**, *28* (3), 351–362. https://doi.org/10.1007/s00590-017-2063-0.

(2) Groeber, F.; Holeiter, M.; Hampel, M.; Hinderer, S.; Schenke-Layland, K. Skin Tissue Engineering — In Vivo and in Vitro Applications. *Adv. Drug Delivery Rev.* **2011**, *63* (4), 352–366. https://doi.org/10.1016/j.addr.2011.01.005.

(3) Spicer, C. D. Hydrogel Scaffolds for Tissue Engineering: The Importance of Polymer Choice. *Polym. Chem.* **2020**, *11* (2), 184–219. https://doi.org/10.1039/C9PY01021A.

(4) Lin, L.; Zhu, J.; Kottke-Marchant, K.; Marchant, R. E. Biomimetic-Engineered Poly (Ethylene Glycol) Hydrogel for Smooth Muscle Cell Migration. *Tissue Eng., Part A* **2013**, *20* (3–4), 864–873. https://doi.org/10.1089/ten.tea.2013.0050.

(5) Zustiak, S. P.; Durbal, R.; Leach, J. B. Influence of Cell-Adhesive Peptide Ligands on Poly(Ethylene Glycol) Hydrogel Physical, Mechanical and Transport Properties. *Acta Biomater.* **2010**, *6* (9), 3404–3414. https://doi.org/10.1016/j.actbio.2010.03.040.

(6) Flaig, F.; Ragot, H.; Simon, A.; Revet, G.; Kitsara, M.; Kitasato, L.; Hébraud, A.; Agbulut, O.; Schlatter, G. Design of Functional Electrospun Scaffolds Based on Poly(Glycerol Sebacate) Elastomer and Poly(Lactic Acid) for Cardiac Tissue Engineering. *ACS Biomater. Sci. Eng.* **2020**, *6* (4), 2388–2400. https://doi.org/10.1021/acsbiomaterials.0c00243.

(7) Bidault, L.; Deneufchatel, M.; Hindié, M.; Vancaeyzeele, C.; Fichet, O.; Larreta-Garde, V. Fibrin-Based Interpenetrating Polymer Network Biomaterials with Tunable Biodegradability. *Polymer* **2015**, *62*, 19–27. https://doi.org/10.1016/j.polymer.2015.02.014.

(8) Ahmed, T. A. E.; Dare, E. V.; Hincke, M. Fibrin: A Versatile Scaffold for Tissue Engineering Applications. *Tissue Eng., Part B* **2008**, *14* (2), 199–215. https://doi.org/10.1089/ten.teb.2007.0435.

(9) Ma, K.; Titan, A. L.; Stafford, M.; Zheng, C. hua; Levenston, M. E. Variations in Chondrogenesis of Human Bone Marrow-Derived Mesenchymal Stem Cells in Fibrin/Alginate Blended Hydrogels. *Acta Biomater.* **2012**, *8* (10), 3754–3764. https://doi.org/10.1016/j.actbio.2012.06.028.

(10) Lotz, C.; Schmid, F. F.; Oechsle, E.; Monaghan, M. G.; Walles, H.; Groeber-Becker, F. Cross-Linked Collagen Hydrogel Matrix Resisting Contraction To Facilitate Full-Thickness Skin Equivalents. *ACS Appl. Mater. Interfaces* **2017**, *9* (24), 20417–20425. https://doi.org/10.1021/acsami.7b04017.

(11) Buitrago, J. O.; Patel, K. D.; El-Fiqi, A.; Lee, J.-H.; Kundu, B.; Lee, H.-H.; Kim, H.-W. Silk Fibroin/Collagen Protein Hybrid Cell-Encapsulating Hydrogels with Tunable Gelation and Improved

Physical and Biological Properties. *Acta Biomater.* **2018**, *69*, 218–233. https://doi.org/10.1016/j.actbio.2017.12.026.
(12) Patterson, J.; Siew, R.; Herring, S. W.; Lin, A. S. P.; Guldberg, R.; Stayton, P. S. Hyaluronic Acid Hydrogels with Controlled Degradation Properties for Oriented Bone Regeneration. *Biomaterials* **2010**, *31* (26), 6772–6781. https://doi.org/10.1016/j.biomaterials.2010.05.047.
(13) Zhai, P.; Peng, X.; Li, B.; Liu, Y.; Sun, H.; Li, X. The Application of Hyaluronic Acid in Bone Regeneration. *Int. J. Biol. Macromol.* **2020**, *151*, 1224–1239. https://doi.org/10.1016/j.ijbiomac.2019.10.169.
(14) Zhu, M.; Feng, Q.; Sun, Y.; Li, G.; Bian, L. Effect of Cartilaginous Matrix Components on the Chondrogenesis and Hypertrophy of Mesenchymal Stem Cells in Hyaluronic Acid Hydrogels: Effect of Cartilaginous Matrix Components on Chondrogenesis and Hypertrophy of Human MSCs. *J. Biomed. Mater. Res.* **2017**, *105* (8), 2292–2300. https://doi.org/10.1002/jbm.b.33760.
(15) Li, H.; Qi, Z.; Zheng, S.; Chang, Y.; Kong, W.; Fu, C.; Yu, Z.; Yang, X.; Pan, S. The Application of Hyaluronic Acid-Based Hydrogels in Bone and Cartilage Tissue Engineering. *Adv. Mater. Sci. Eng.* **2019**, *2019*, e3027303. https://doi.org/10.1155/2019/3027303.
(16) Hu, M.; Sabelman, E. E.; Cao, Y.; Chang, J.; Hentz, V. R. Three-Dimensional Hyaluronic Acid Grafts Promote Healing and Reduce Scar Formation in Skin Incision Wounds. *J. Biomed. Mater. Res., Part B* **2003**, *67B* (1), 586–592. https://doi.org/10.1002/jbm.b.20001.
(17) Mahapatra, C.; Jin, G.-Z.; Kim, H.-W. Alginate-Hyaluronic Acid-Collagen Composite Hydrogel Favorable for the Culture of Chondrocytes and Their Phenotype Maintenance. *Tissue Eng. Regen. Med.* **2016**, *13* (5), 538–546. https://doi.org/10.1007/s13770-016-0059-1.
(18) Walimbe, T.; Calve, S.; Panitch, A.; Sivasankar, M. P. Incorporation of Types I and III Collagen in Tunable Hyaluronan Hydrogels for Vocal Fold Tissue Engineering. *Acta Biomater.* **2019**, *87*, 97–107. https://doi.org/10.1016/j.actbio.2019.01.058.
(19) Suri, S.; Schmidt, C. E. Cell-Laden Hydrogel Constructs of Hyaluronic Acid, Collagen, and Laminin for Neural Tissue Engineering. *Tissue Eng., Part A* **2010**, *16* (5), 1703–1716. https://doi.org/10.1089/ten.tea.2009.0381.
(20) Fraser, J. R. E.; Laurent, T. C.; Laurent, U. B. G. Hyaluronan: Its Nature, Distribution, Functions and Turnover. *J. Intern. Med.* **1997**, *242* (1), 27–33. https://doi.org/10.1046/j.1365-2796.1997.00170.x.
(21) Mourão, P. A. S. Distribution of Chondroitin 4–Sulfate and Chondroitin 6–Sulfate in Human Articular and Growth Cartilage. *Arthritis Rheum.* **1988**, *31* (8), 1028–1033. https://doi.org/10.1002/art.1780310814.
(22) Ishida, O.; Tanaka, Y.; Morimoto, I.; Takigawa, M.; Eto, S. Chondrocytes Are Regulated by Cellular Adhesion Through CD44 and Hyaluronic Acid Pathway. *J. Bone Miner. Res.* **1997**, *12* (10), 1657–1663. https://doi.org/10.1359/jbmr.1997.12.10.1657.
(23) Hamann, K. J.; Dowling, T. L.; Neeley, S. P.; Grant, J. A.; Leff, A. R. Hyaluronic Acid Enhances Cell Proliferation during Eosinopoiesis through the CD44 Surface Antigen. *J. Immunol.* **1995**, *154* (8), 4073–4080.
(24) Varghese, S.; Hwang, N. S.; Canver, A. C.; Theprungsirikul, P.; Lin, D. W.; Elisseeff, J. Chondroitin Sulfate Based Niches for Chondrogenic Differentiation of Mesenchymal Stem Cells. *Matrix Biol.* **2008**, *27* (1), 12–21. https://doi.org/10.1016/j.matbio.2007.07.002.
(25) Ialenti, A.; Di Rosa, M. Hyaluronic Acid Modulates Acute and Chronic Inflammation. *Agents Actions* **1994**, *43* (1), 44–47. https://doi.org/10.1007/BF02005763.
(26) Fenn, S. L.; Oldinski, R. A. Visible Light Crosslinking of Methacrylated Hyaluronan Hydrogels for Injectable Tissue Repair. *J. Biomed. Mater. Res. Part B Appl. Biomater.* **2016**, *104* (6), 1229–1236. https://doi.org/10.1002/jbm.b.33476.
(27) Shu, X. Z.; Liu, Y.; Luo, Y.; Roberts, M. C.; Prestwich, G. D. Disulfide Cross-Linked Hyaluronan Hydrogels. *Biomacromolecules* **2002**, *3* (6), 1304–1311. https://doi.org/10.1021/bm025603c.

(28) Owen, S. C.; Fisher, S. A.; Tam, R. Y.; Nimmo, C. M.; Shoichet, M. S. Hyaluronic Acid Click Hydrogels Emulate the Extracellular Matrix. *Langmuir* **2013**, *29* (24), 7393–7400. https://doi.org/10.1021/la305000w.
(29) Lee, F.; Eun Chung, J.; Kurisawa, M. An Injectable Enzymatically Crosslinked Hyaluronic Acid – Tyramine Hydrogel System with Independent Tuning of Mechanical Strength and Gelation Rate. *Soft Matter* **2008**, *4* (4), 880–887. https://doi.org/10.1039/B719557E.
(30) Mazumder, M. A. J.; Fitzpatrick, S. D.; Muirhead, B.; Sheardown, H. Cell-Adhesive Thermogelling PNIPAAm/Hyaluronic Acid Cell Delivery Hydrogels for Potential Application as Minimally Invasive Retinal Therapeutics. *J. Biomed. Mater. Res., Part A* **2012**, *100A* (7), 1877–1887. https://doi.org/10.1002/jbm.a.34021.
(31) Kwon, M. Y.; Wang, C.; Galarraga, J. H.; Puré, E.; Han, L.; Burdick, J. A. Influence of Hyaluronic Acid Modification on CD44 Binding towards the Design of Hydrogel Biomaterials. *Biomaterials* **2019**, *222*, 119451. https://doi.org/10.1016/j.biomaterials.2019.119451.
(32) Eng, D.; Caplan, M.; Preul, M.; Panitch, A. Hyaluronan Scaffolds: A Balance between Backbone Functionalization and Bioactivity. *Acta Biomater.* **2010**, *6* (7), 2407–2414. https://doi.org/10.1016/j.actbio.2009.12.049.
(33) Erickson, I. E.; Huang, A. H.; Sengupta, S.; Kestle, S.; Burdick, J. A.; Mauck, R. L. Macromer Density Influences Mesenchymal Stem Cell Chondrogenesis and Maturation in Photocrosslinked Hyaluronic Acid Hydrogels. *Osteoarthritis and Cartilage* **2009**, *17* (12), 1639–1648. https://doi.org/10.1016/j.joca.2009.07.003.
(34) Yu, F.; Cao, X.; Zeng, L.; Zhang, Q.; Chen, X. An Interpenetrating HA/G/CS Biomimic Hydrogel via Diels–Alder Click Chemistry for Cartilage Tissue Engineering. *Carbohydrate Polymers* **2013**, *97* (1), 188–195. https://doi.org/10.1016/j.carbpol.2013.04.046.
(35) Bernhard, J. C.; Panitch, A. Synthesis and Characterization of an Aggrecan Mimic. *Acta Biomater.* **2012**, *8* (4), 1543–1550. https://doi.org/10.1016/j.actbio.2011.12.029.
(36) Poldervaart, M. T.; Goversen, B.; de Ruijter, M.; Abbadessa, A.; Melchels, F. P. W.; Öner, F. C.; Dhert, W. J. A.; Vermonden, T.; Alblas, J. 3D Bioprinting of Methacrylated Hyaluronic Acid (MeHA) Hydrogel with Intrinsic Osteogenicity. *PLoS One* **2017**, *12* (6), e0177628. https://doi.org/10.1371/journal.pone.0177628.
(37) Fajardo, A. R.; Fávaro, S. L.; Rubira, A. F.; Muniz, E. C. Dual-Network Hydrogels Based on Chemically and Physically Crosslinked Chitosan/Chondroitin Sulfate. *React. Funct. Polym.* **2013**, *73* (12), 1662–1671. https://doi.org/10.1016/j.reactfunctpolym.2013.10.003.
(38) Gao, Y.; Li, B.; Kong, W.; Yuan, L.; Guo, L.; Li, C.; Fan, H.; Fan, Y.; Zhang, X. Injectable and Self-Crosslinkable Hydrogels Based on Collagen Type II and Activated Chondroitin Sulfate for Cell Delivery. *Int. J. Biol. Macromol.* **2018**, *118*, 2014–2020. https://doi.org/10.1016/j.ijbiomac.2018.07.079.
(39) Möller, L.; Krause, A.; Dahlmann, J.; Gruh, I.; Kirschning, A.; Dräger, G. Preparation and Evaluation of Hydrogel-Composites from Methacrylated Hyaluronic Acid, Alginate, and Gelatin for Tissue Engineering. *Int J Artif Organs* **2011**, *34* (2), 93–102. https://doi.org/10.5301/IJAO.2011.6397.
(40) Hozumi, T.; Kageyama, T.; Ohta, S.; Fukuda, J.; Ito, T. Injectable Hydrogel with Slow Degradability Composed of Gelatin and Hyaluronic Acid Cross-Linked by Schiff's Base Formation. *Biomacromolecules* **2018**, *19* (2), 288–297. https://doi.org/10.1021/acs.biomac.7b01133.
(41) Tous, E.; Ifkovits, J. L.; Koomalsingh, K. J.; Shuto, T.; Soeda, T.; Kondo, N.; Gorman, J. H.; Gorman, R. C.; Burdick, J. A. Influence of Injectable Hyaluronic Acid Hydrogel Degradation Behavior on Infarction-Induced Ventricular Remodeling. *Biomacromolecules* **2011**, *12* (11), 4127–4135. https://doi.org/10.1021/bm201198x.

(42) Gennari, A.; Wedgwood, J.; Lallana, E.; Francini, N.; Tirelli, N. Thiol-Based Michael-Type Addition. A Systematic Evaluation of Its Controlling Factors. *Tetrahedron* **2020**, *76* (47), 131637. https://doi.org/10.1016/j.tet.2020.131637.
(43) Yoshida, M.; Sai, S.; Marumo, K.; Tanaka, T.; Itano, N.; Kimata, K.; Fujii, K. Expression Analysis of Three Isoforms of Hyaluronan Synthase and Hyaluronidase in the Synovium of Knees in Osteoarthritis and Rheumatoid Arthritis by Quantitative Real-Time Reverse Transcriptase Polymerase Chain Reaction. *Arthritis Res Ther* **2004**, *6* (6), R514. https://doi.org/10.1186/ar1223.
(44) Jeon, O.; Song, S. J.; Lee, K.-J.; Park, M. H.; Lee, S.-H.; Hahn, S. K.; Kim, S.; Kim, B.-S. Mechanical Properties and Degradation Behaviors of Hyaluronic Acid Hydrogels Cross-Linked at Various Cross-Linking Densities. *Carbohydr. Polym.* **2007**, *70* (3), 251–257. https://doi.org/10.1016/j.carbpol.2007.04.002.
(45) Nimmo, C. M.; Owen, S. C.; Shoichet, M. S. Diels−Alder Click Cross-Linked Hyaluronic Acid Hydrogels for Tissue Engineering. *Biomacromolecules* **2011**, *12* (3), 824–830. https://doi.org/10.1021/bm101446k.
(46) Sharma, S.; Panitch, A.; Neu, C. P. Incorporation of an Aggrecan Mimic Prevents Proteolytic Degradation of Anisotropic Cartilage Analogs. *Acta Biomater.* **2013**, *9* (1), 4618–4625. https://doi.org/10.1016/j.actbio.2012.08.041.
(47) Mummert, M. E.; Mohamadzadeh, M.; Mummert, D. I.; Mizumoto, N.; Takashima, A. Development of a Peptide Inhibitor of Hyaluronan-Mediated Leukocyte Trafficking. *J Exp Med* **2000**, *192* (6), 769–780.
(48) Butterfield, K. C.; Caplan, M.; Panitch, A. Identification and Sequence Composition Characterization of Chondroitin Sulfate-Binding Peptides through Peptide Array Screening. *Biochemistry* **2010**, *49* (7), 1549–1555. https://doi.org/10.1021/bi9021044.
(49) Heparin-Binding Domains in Vascular Biology | Arteriosclerosis, Thrombosis, and Vascular Biology https://www.ahajournals.org/doi/full/10.1161/01.ATV.0000137189.22999.3f (accessed 2021 -08 -19).
(50) Gwon, K.; Kim, E.; Tae, G. Heparin-Hyaluronic Acid Hydrogel in Support of Cellular Activities of 3D Encapsulated Adipose Derived Stem Cells. *Acta Biomater.* **2017**, *49*, 284–295. https://doi.org/10.1016/j.actbio.2016.12.001.
(51) Stuart, K.; Panitch, A. Influence of Chondroitin Sulfate on Collagen Gel Structure and Mechanical Properties at Physiologically Relevant Levels. *Biopolymers* **2008**, *89* (10), 841–851. https://doi.org/10.1002/bip.21024.
(52) Yuan, H.; Tank, M.; Alsofyani, A.; Shah, N.; Talati, N.; LoBello, J. C.; Kim, J. R.; Oonuki, Y.; de la Motte, C. A.; Cowman, M. K. Molecular Mass Dependence of Hyaluronan Detection by Sandwich ELISA-like Assay and Membrane Blotting Using Biotinylated Hyaluronan Binding Protein. *Glycobiology* **2013**, *23* (11), 1270–1280. https://doi.org/10.1093/glycob/cwt064.
(53) Fujimoto, T.; Kawashima, H.; Tanaka, T.; Hirose, M.; Toyama-Sorimachi, N.; Matsuzawa, Y.; Miyasaka, M. CD44 Binds a Chondroitin Sulfate Proteoglycan, Aggrecan. *Int. Immunol.* **2001**, *13* (3), 359–366. https://doi.org/10.1093/intimm/13.3.359.
(54) Spearman, B. S.; Agrawal, N. K.; Rubiano, A.; Simmons, C. S.; Mobini, S.; Schmidt, C. E. Tunable Methacrylated Hyaluronic Acid-Based Hydrogels as Scaffolds for Soft Tissue Engineering Applications. *J. Biomed. Mater. Res. Part A* **2020**, *108* (2), 279–291. https://doi.org/10.1002/jbm.a.36814.

# 3. Glycosaminoglycan Blend Hydrogels Suppress Inflammation from Pro-inflammatory Cytokines in Encapsulated Chondrocytes

This chapter consists of a manuscript in progress by Michael Nguyen, Julie C. Liu, and Alyssa Panitch

**Abstract:**

Osteoarthritis is characterized by the enzymatic breakdown of the articular cartilage through a disruption of chondrocyte homeostasis, ultimately resulting in the destruction of the articular surface and reduced limb movement. Although several methods have been employed to attempt to reconstruct the damaged cartilage, recent decades of research have highlighted the importance of inflammation in the progression of osteoarthritis. Inflammatory cytokines including interleukin 1-beta and tumor necrosis factor alpha shift resident chondrocytes into a pro-catabolic state, resulting in poor outcomes following cell implantation. As such, a method to both promote the growth of new cartilage and to protect the implanted cells from the pro-inflammatory cytokines found in the joint space is required. In this study, we fabricated dual polymer network hydrogels out of chondroitin sulfate and hyaluronic acid, glycosaminoglycans known for their anti-inflammatory and pro-chondrogenic biological signals, as well as interpenetrating network hydrogels through the addition of collagen type I to modulate hydrogel mechanical properties. When stimulated with pro-inflammatory cytokines, glycosaminoglycan hydrogels showed no significant degradation compared to their unstimulated controls. Mild inflammation was detected through changes in metabolism, DNA production, interleukin 6 production, and gene expression of catabolic and anabolic markers, though this inflammation was less than that seen in a collagen type I

only hydrogel. Overall, glycosaminoglycan hydrogels can suppress inflammation in the encapsulated cells, laying the groundwork for future anti-inflammatory materials.

### 3.1. Introduction

Osteoarthritis (OA) is one of the most common and significant joint diseases in the world, with factors such as age, obesity, and genetics contributing to its prevalence[1,2]. OA is a degenerative disease of the joint, characterized by a disruption in the homeostasis of the articular cartilage, breakdown of the extracellular matrix and the malfunction of the resident chondrocytes[3]. While it was previously thought that much of the degradation of cartilage in OA was due to mechanical wear, research in the recent decades have highlighted the importance of pro-inflammatory cues such as Interleukin 1β (Il-1β)[4] and tumor necrosis factor alpha (TNF-α)[5] in the context of total joint inflammation[6–9]. Although not as inflamed as joints in rheumatoid arthritis, pro-inflammatory cues have been found in the synovial fluid of OA affected joints, with these cytokines now believed to play a significant role in the progression of OA[10,11].

In late-stage OA, excessive degradation of the articular cartilage can lead to the formation of significantly sized cartilage defects, leading to pain and loss of limb movement[12]. Due to the avascular nature of cartilage, as well as the low resident cell population, cartilage has limited healing capability[13,14]. Treatments like autologous chondrocyte implantation (ACI), where the cartilage defect is repopulated with the patient's own chondrocytes to repair the defect, have seen some clinical success, though the quality of the new cartilage is still inferior to that of the original[15]. Furthermore, adverse effects such as graft failure, fibrosis, and hypertrophy have been observed following the ACI procedure[16]. These adverse effects have been correlated with increased levels of Il-1β, suggesting that inflammatory activity may be the cause of the procedure failure[16–18].

To address the issue of cartilage defects, the field of tissue engineering has sought to develop methods to engineer cartilage to repair the defect[19–22]. Although many solutions using a diverse set of

materials have been developed, many of these studies were performed in the absence of pro-inflammatory cytokines. As such, while many of these studies have produced robust cartilage replacements, few studies have looked at the potential effects of pro-inflammatory cytokines on the outcomes of the engineered cartilage. This is an important consideration to make, as exposure to these pro-inflammatory cytokines can significantly affect the chondrocytes' ability to produce new matrix components and can shift them into a catabolic state. Stimulation with pro-inflammatory cytokines can lead to increased secretion of collagenases like matrix metalloproteinase 13 (MMP13)[23], aggrecanases like a disintegrin and metalloproteinase with thrombospondin motifs 4 and 5 (ADAMTS4, ADAMTS5)[24], and hyaluronidases. Conversely, many studies have looked to dampen the effects of inflammation on chondrocytes through methods such as soluble factors and cell cocultures, but many of these studies have been focused on the inflammatory response of the chondrocytes, rather than their anabolic capability[25–30]. As such, although both aspects of OA treatment, the repair of defects and the dampening of inflammation, have been well studied, there are few studies that have looked at the overlap of tissue engineering and the pro-inflammatory environment.

To fill this knowledge gap, we sought to study the engineering of a cartilage replacement using chondrocytes encapsulated in a hydrogel scaffold while also protecting the cells from a pro-inflammatory environment. To accomplish this, we opted to employ the glycosaminoglycans (GAGs) chondroitin sulfate (CS) and hyaluronic acid (HA) as the polymers for our hydrogel. The use of these GAGs for a cell scaffold provides two main benefits: promotion of chondrogenic activity[25,31–34] and anti-inflammatory effects[35–39]. For one, HA and CS are native components of cartilage, as a free-floating GAG in the case of HA[40] and as part of the proteoglycan aggrecan in the case of CS[41]. Many studies have demonstrated that the incorporation of these GAGs, either as scaffold components[32,42] or in their soluble form[43], leads to better outcomes with regard to cartilage tissue engineering. Similarly, many studies have demonstrated the anti-inflammatory effects of HA and CS in their soluble form against many different pro-inflammatory

agents[26,27,38]. For our study, to maximize the signals of the GAGs, we opted to use minimally modified HA and CS to prevent loss of biological activity. Furthermore, we used a blend of CS and HA at two ratios of CS to HA, as our previous work demonstrated the superiority of a blended GAG hydrogel over a homopolymer hydrogel of either CS or HA[44]. This was also done to probe for any differences in outcomes with regard to CS and HA ratio, as it is possible these two GAGs have different effects on encapsulated cells. Finally, to add a tensile force to oppose the swelling force of the GAG hydrogel, reducing fluid infiltration and volumetric expansion, as well as add additional binding sites for the cells, we made some hydrogel groups into GAG/collagen type I interpenetrating network (IPN) hydrogels[45]. Altogether, we used our GAG hydrogels, at different GAG blends and collagen contents, to study the interplay between the cells and a bioactive material in the context of tissue engineering in a pro-inflammatory environment.

### 3.2. Materials and Methods

#### *3.2.1: Synthesis and Characterization of Thiolated Hyaluronic Acid and Chondroitin Sulfate*

Thiolated GAGs were synthesized using a previously reported method[44]. GAGs HA (molecular weight 100 kDa, Lifecore Biomedical) and CS (molecular weight 40 kDa, Seikigaku Corporation) were first dissolved in 0.1 M 2-(N-morpholino)ethanesulfonic acid (MES) buffer with 0.2 wt% NaCl at a concentration of 5 mg/mL. To convert GAG carboxylic acid groups to thiols, dithio-bis(propionohydrazide) (DTP) was added in sufficient quantity to convert eighteen percent of GAG carboxylic acid groups. Conjugation was performed using 1-ethyl-3-(3-dimethylaminopropyl)carbodiimide (EDC), which was added in a 2:1 ratio of EDC to DTP. The solutions were titrated to pH 4.5 and reacted overnight. The disulfide bonds of DTP were cleaved through titrating the solutions to pH 8.5 and the addition of dithiothreitol (DTT), which was added in 3:1 molar excess of DTP. After three hours at room temperature, the solutions were then titrated back down to pH 4.5 to prevent the reformation of disulfide bonds. Polymer solutions were then purified using a KrossFlo KR2i tangential flow filtration (TFF) unite (Repligen) using a 10 kDa molecular weight cut off

column and a transmembrane pressure of 18 PSI. Polymer solutions were purified until a permeate volume of three times the reaction volume had been reached. Following purification, polymer solutions were filtered through a 0.2 µm filter, frozen, and lyophilized. Free thiol content of thiolated GAGs was determined using an Ellman's assay, with degree of thiolation defined as the percentage of GAG carboxylic acid groups converted to free thiols.

*3.2.2: Fabrication of Blended GAG Hydrogels and GAG/Collagen IPNs*

Dry polymer was first sterilized through immersion in absolute ethanol. Excess ethanol was removed and the polymer was dried in a laminar flow hood. Stock solutions of HA-SH and CS-SH were prepared by dissolving the GAGs in phosphate buffered saline (PBS) at a concentration of 80.8 mg/ml. To prepare blended GAG hydrogels, stock GAG solutions were made of either 7:3 CS-SH to HA-SH, or 3:7 CS-SH to HA-SH to study any differences in anti-inflammatory activity arising from differences in GAG structure and sulfate content. 3 wt% GAG hydrogels were prepared by combining 150 µL 20 mM acetic acid, 35 µL PBS, 25 µL 260 mg/ml poly(ethylene glycol) diacrylate (PEGDA), and 130 µL of the blended GAG solutions. Polymerization was done by titrating the pre-gel solutions to pH 7.8. For GAG/collagen IPNs, the 20 mM acetic acid solution was substituted for a 9.33 mg/mL solution of rat tail collagen type 1 (Corning), leading to a final collagen concentration of 0.4 wt%. Following titration, 90 µL gels were made by placing the solution into 8 mm silicone molds and incubating them at $37^{O}$ C for one hour in a humidified environment. Collagen only gels were made by mixing 265 uL of 9.33 mg/mL collagen type I solution with 35 uL 10X PBS, titrating to pH 7.8, and then mixing in 35 uL of the cell suspension at the same cell concentration. Collagen gels were pipetted into the 8 mm silicone molds and incubated at $37^{o}$ C for two hours.

*3.2.3: Mechanical Testing of Hydrogels*

Compressive mechanical testing was performed using a Discovery Hybrid Rheometer (TA Instruments). Prior to compressive testing, hydrogels were allowed to swell in PBS overnight. Hydrogels were placed on the stage under an 8 mm head and compressed until 50% strain at a constant rate of 5 μm/s. Compressive modulus was then calculated from the linear portion of the stress/strain curve.

*3.2.4: Characterization of Hydrogel Swelling and Diffusive Properties*

For the characterization of hydrogel swelling as a function of composition, gels were made directly in 0.5 mL centrifuge tubes. Following gelation, PBS was pipetted atop and the tubes were allowed to equilibrate. After swelling, the new mass of the hydrogels was taken and the hydrogels were washed three times with deionized water. Hydrogels were then lyophilized, with the swelling ratio being calculated as the ratio between the swollen and dry masses.

To characterize the diffusivity of the hydrogels, hydrogels were loaded with rhodamine isothiocyanate labeled 70 kDa dextran (dextran-RITC) prior to gelation. Following gelation, gels were submersed in PBS, with the mass of dextran-RITC being determined from the fluorescence of the supernatant. Dextran-RITC release from the hydrogels was monitored over the course of one week.

*3.2.5: Primary Animal Chondrocyte Isolation and Culture*

Primary fetal bovine articular chondrocytes (fbACs) were isolated from the cartilage of hind knees of fetal bovines (Animal Technologies). Cartilage slices were shaved off of the medial condyle and digested in a solution of 0.2 w/v% collagenase P (Millipore Sigma), 0.1 w/v% bovine serum albumin (Millipore Sigma), 3% fetal bovine serum (FBS) (Gibco) for two hours. Following digestion, cells were strained out of undigested cartilage through a 70 μm cell strainer. Collected cells were either cryopreserved in Cryo-SFM (Promocell) until needed or expanded in Dulbecco's Modified Eagle Medium (DMEM) (Gibco) supplemented with 10% FBS and 1% penicillin/streptomycin/amphotericin (Gibco). Cells were used between passage 2-5.

Primary rabbit chondrocytes (rACs) were isolated from the cartilage of the hind limbs of skeletally mature New Zealand White rabbits. Chondrocytes were isolated using the same method and were used between passages 1-3.

### 3.2.6: Chondrocyte Culture in Pro-inflammatory Conditions

#### *3.2.6.1: Effect of Pro-inflammatory Conditions on Hydrogels*

Cell laden hydrogels were either cultured in pro-inflammatory media consisting of the cell expansion media supplemented with 50 µg/mL ascorbic acid (Millipore Sigma) and 20 ng/mL recombinant human IL-1β (Peprotech) for fbACs and 10 ng/mL for rACs to simulate the osteoarthritic environment, or in non-inflammatory media consisting of the cell expansion media supplemented with 50 µg/mL ascorbic acid and 40 ng/mL Dexamethasone (Millipore Sigma). Hydrogels were cultured in 48-well plates with media exchanged and collected every two days. fbACs were encapsulated at a final cell concentration of 2 million cells/mL and rACs were encapsulated at a final cell concentration of 0.5 million cells/mL. fBACs were used for the majority of studies to study the anti-inflammatory effects of the hydrogels, with rACs from mature rabbits as a secondary cell type for proliferation studies due to differences in proliferative behavior seen in juvenile cells. A lower cell seeding density was used for rACs due to difficulties in chondrocyte expansion.

#### *3.2.6.2: Analysis of Cell Proliferation in Response to Pro-inflammatory Conditions*

Cell proliferation and metabolic assays were studied with both fbACs and rACs. Changes in cell proliferation as a result of culture in pro-inflammatory conditions was determined through differences in total cell metabolism at the beginning and end of a fourteen-day period. Cell metabolism was determined by immersing the hydrogels in 10% AlamarBlue (Invitrogen) in culture media for four hours, then measuring the fluorescence of the media. Prior to the assay, hydrogels were allowed to swell overnight to ensure equal diffusion of AlamarBlue into the hydrogel.

To measure changes in hydrogel DNA content following pro-inflammatory culture, hydrogels were placed in 400 µL 1 mg/mL hyaluronidase type I-S (Millipore Sigma) and 1X proteinase inhibitor (ThermoFisher), mechanically homogenized with a rotary tissue homogenizer, and digested overnight. 50 µL gel digest was combined with 50 µL PicoGreen reagent (ThermoFisher), with DNA concentration determined through the fluorescent signal at excitation 485 nm and emission 535 nm. A DNA calibration curve was constructed using lambda phage DNA (Thermofisher).

*3.2.6.3: Effect of Pro-inflammatory Conditions on Hydrogel Integrity*

To assess how the pro-inflammatory conditions changed the physical properties of the material through stimulation of the fbACs, the changes in wet and dry mass, as well as changes compressive strength were measured. At time points of seven and fourteen days, the hydrogels were harvested and weighed in pre weighed centrifuge tubes. The compressive strength was then tested using the methods previously described. Finally, the hydrogels were frozen, lyophilized, and weighed again to determine the dry mass. For further testing of changes in hydrogel mass, the amount of CS released into the media during culture was determined using a dimethylmethylene blue (DMMB) assay.

*3.2.6.4: Analysis of Secreted Cytokines in Response to Pro-inflammatory Conditions*

To determine ability of Il-1β to induce inflammation in the embedded chondrocytes, the secretion of Il-6 as a marker of inflammation was analyzed. The collected media for each replicate from the fbAC culture was pooled together and then analyzed for Il-6 content through a sandwich enzyme linked immunosorbent assay (R&D Systems) targeting bovine Il-6. Media collected between 2-6 days and 8-14 days were pooled together to study changes in Il-6 production overtime. As controls, collagen type one hydrogels were also seeded with fbACs and analyzed for Il-6 production over time.

*3.2.6.5: Analysis of Gene Expression in Response to Pro-inflammatory Conditions*

To determine the effects on Il-1β on the expression of anabolic and catabolic chondrocyte genes, the mRNA of the embedded fbACs was analyzed using quantitative polymerase chain reaction (qPCR) following fourteen days of either pro or non-inflammatory culture. Following culture, hydrogels were immersed in TRIzol LS according to manufacturer directions, then homogenized using a Tissue Tearor rotor homogenizer. Samples were centrifuged to remove the solid components, with the mRNA extracted from the supernatant according to manufacturer's instructions. Following mRNA extraction, cDNA was synthesized using a High-Capacity cDNA Reverse Transcription kit (Invitrogen) according to manufacturer instructions.

qPCR was performed using Taqman probes (Thermofisher) targeting collagen II and aggrecan as markers for chondrogenic anabolic activity, collagen I and collagen X as markers for hypertrophy, and MMP13 and ADAMTS5 as markers for inflammation induced catabolic activity. Regulation of gene expression was analyzed using the ΔΔCt method, with expression of genes of interest first normalized to expression of GAPDH and then to either the Il-1β stimulated collagen only hydrogel control or to each group's respective unstimulated control.

*3.2.7 Statistical Analysis*

All experiments were conducted in at least triplicate. Statistical significance between two groups was determined using a Student's T-Test. Statistical significance between three or more groups was determined using a one-way ANOVA, with significance between groups being determined using a Tukey post hoc test. Statistical analysis was done with GraphPad Prism software. A probability value of 95% ($P < 0.05$) was used to determine statistical significance.

**3. Results**

*3.3.1: Effect of GAG ratio and the Inclusion of Collagen on Hydrogel Physical Properties*

One consequence of modulating the ratio of CS to HA in the blended GAG hydrogels was changes in the charge density of the hydrogel due to the difference in charge between the sulfated CS and the unsulfated HA. As a result, the 7:3 CS/HA hydrogel exhibited increased swelling compared to the 3:7 CS/HA hydrogel, likely due to an increased negative charge (figure 3.1c). However, the inclusion of collagen in the 7:3 hydrogel reduced hydrogel swelling, making it equal to the 3:7 hydrogel with and without collagen. This is likely due to the tension of collagen network resisting the swelling in 7:3 formulation. Despite this difference in swelling, the initial compressive moduli of all hydrogel formulations, with and without collagen, in their swollen state were equivalent (figure 3.1a). However, after one week of incubation in cell media, acellular hydrogels had reduced compressive strength (figure 3.1b). This was the most apparent in the 7:3 with no collagen hydrogel, which lost a quarter of its initial compressive modulus. The inclusion of collagen in both GAG blend formulations reduced the loss of compressive strength, possibly through the restriction of further swelling and through preventing further loss of material.

To characterize how the hydrogel formulation affects its diffusivity, hydrogels were loaded with dextran-RITC, with the rate of dextran-RITC release monitored over the course of a week (figure 3.1d). The inclusion of collagen appeared to stabilize the release of dextran-RITC, with the 7:3 and 3:7 formulations with collagen releasing equivalent amounts of dextran-RITC over the course of a week. In contrast, the 3:7 without collagen hydrogel released the most dextran-RITC, with the 7:3 without collagen formulation releasing the least dextran-RITC. However, this difference in release can be attributed to the difference in burst release in the first day. Since the 7:3 without collagen hydrogel demonstrated significant swelling, it is theorized that the influx of water reduced the release of dextran-RITC. Following the burst release of dextran-RITC, the rate of release was more consistent between groups, implying similar hydrogel diffusivities across all formulations.

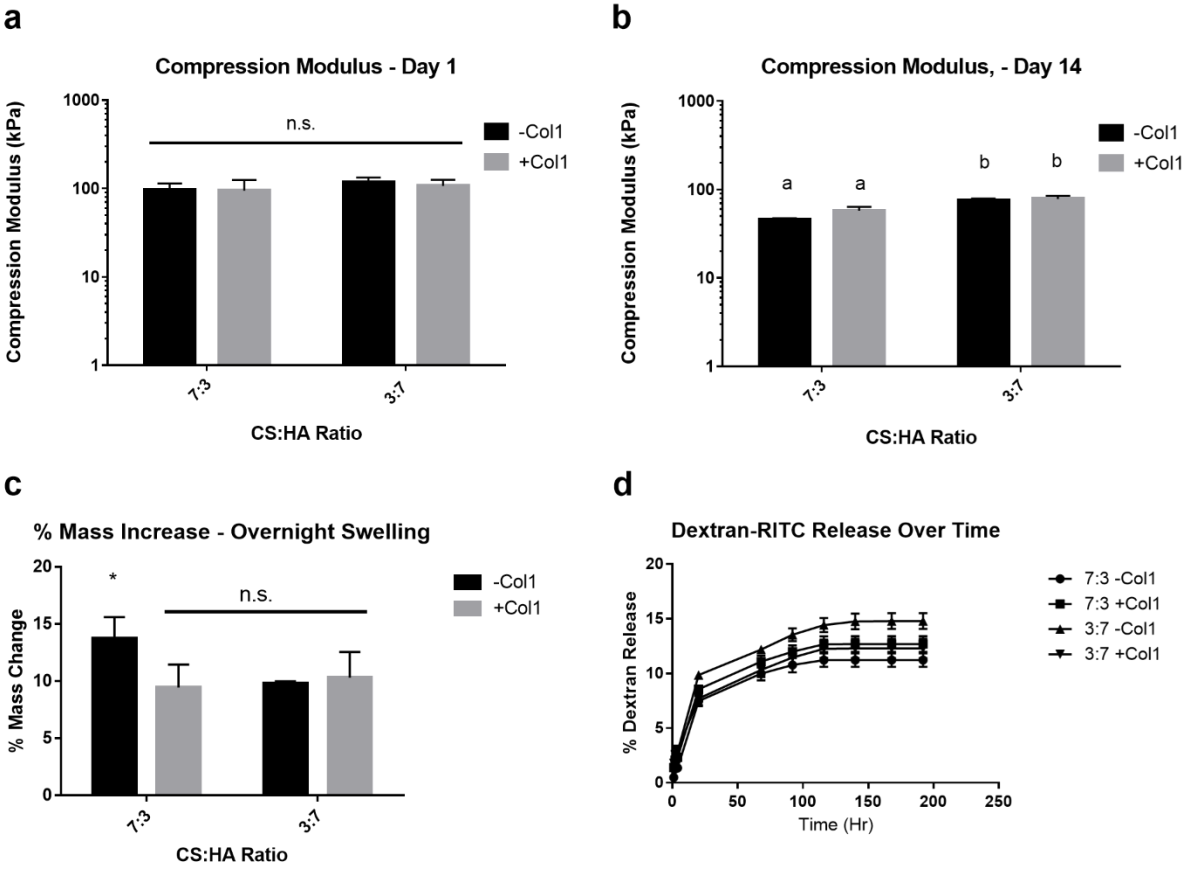


*Figure 3.1: Physical properties of GAG hydrogels with differing GAG blends and collagen contents. A) Initial compression modulus of swollen hydrogels. B) Compression modulus after fourteen days of acellular culture. C) Change in mass of hydrogels (%) following overnight swelling in PBS. D) Release profiles of dextran-RITC over 196 hours. Groups denoted by * are statistically significant from other groups ($P < 0.05$). Groups sharing the same letter are not statistically significant from one another ($P > 0.05$). Groups denoted by n.s. are not statistically significant from one another.*

### *3.3.2: Changes in Hydrogel Integrity Following Culture in Pro-inflammatory Conditions*

To understand the changes in encapsulated cell behavior with regard to their environment when cultured in pro-inflammatory conditions, changes in hydrogel mass and compressive strength were tested.

During the fourteen days of culture, all cell laden hydrogels exhibited a decrease in compressive strength over time, with the degree of loss of compressive strength correlating with the formulation of the hydrogel (figure 3.2a). As with the acellular hydrogels, the formulations that lost the most strength were the 7:3 groups, with the addition of collagen in both GAG blends reducing the loss of stiffness. Furthermore, all groups exhibited lower compressive strength than their acellular counterparts, indicating that this change was due in part to cell activity. However, there were no significant differences in compressive strength between the hydrogels cultured in the pro-inflammatory media and the non-inflammatory media, meaning this behavior was due to normal cell remodeling behavior and not due to inflammatory stimulation. Further measurements of the wet and dry masses of the hydrogels, as well as the CS released into the media, showed no significant differences between hydrogels cultured in pro and non-inflammatory conditions, with the exception of the 3:7 CS/HA -Col1 group, which showed a difference in final dry mass between the groups stimulated with and without Il-1β (figure 3.2b,c). Overall, stimulating the hydrogels with 20 ng/mL Il-1β showed no large effects on hydrogel integrity, indicating that the encapsulated cells are not significantly degrading the scaffold as a result of pro-inflammatory conditions.

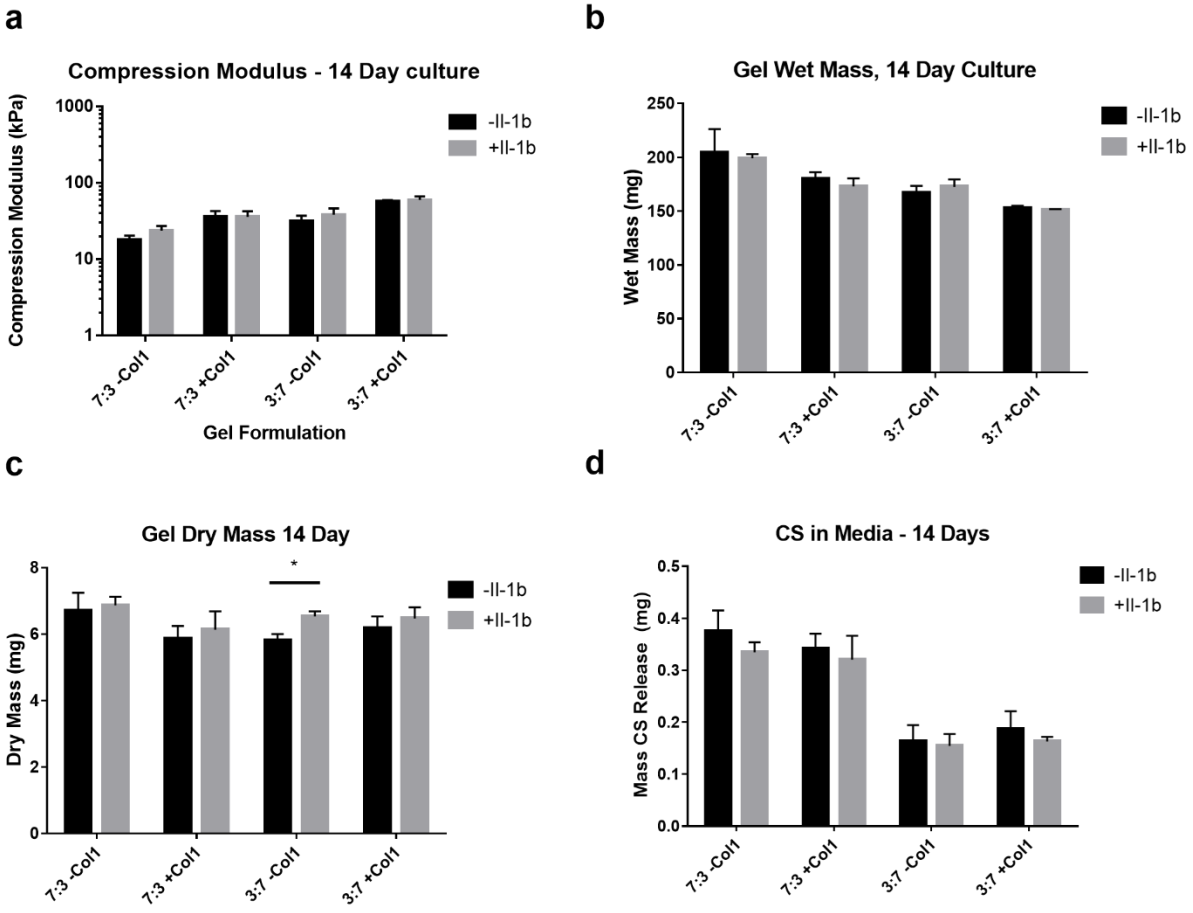


*Figure 3.2: Changes in fbAC laden GAG hydrogel integrity over fourteen days of Il-1β stimulated and unstimulated culture. A) Compression Modulus of GAG gels after fourteen days of culture. B) Gel wet mass after fourteen days of culture. C) Gel dry mass after fourteen days of culture. D) Cumulative CS release into media over fourteen days of culture. Multiple T-tests were run between stimulated and unstimulated groups. Groups marked with * show significant differences between groups ($p < 0.05$)*

*3.3.3: Changes in Cell Viability and Proliferation Under Pro-Inflammatory Conditions*

To study the effects of Il-1β stimulated culture on the encapsulated cells, an Alamar blue assay was performed to analyze changes in metabolic rate over the fourteen-day culture period as an analogue for cell viability. In the 7:3 CS/HA groups, along with the 3:7 CS/HA without collagen group, there was a

significant increase in metabolic rate in the groups stimulated with Il-1β compared to the unstimulated control. (Figure 3.3a). For the 3:7 CS/HA with collagen and collagen only gels, there was no significant difference in metabolic rate between the stimulated and unstimulated groups. (Figure 3.3a).

To further understand the effects of pro-inflammatory cytokines on cell proliferation, the DNA content was measured from the digested hydrogels. In all GAG groups, there was no significant difference in DNA content between the groups cultured in pro-inflammatory and control conditions (Figure 3b). However, the DNA content of GAG gels that were stimulated with Il-1β trended upward, with the smallest increase in average DNA content being found in the 3:7 + collagen gel. In contrast, when stimulated with Il-1β, there was a significant increase in DNA content in the collagen only gels (Figure 3.3b). Taken together with the data from the metabolic assays, these experiments suggest that culture in Il-1β caused the encapsulated cells to proliferate, with small increases seen in the GAG containing gels and a larger increase in the collagen only gel.

Given the patterns seen with cell metabolism and proliferation with the fbACs, changes in proliferation and metabolic rate were also studied with rACs from skeletally mature rabbits over the course of one week. In this case, the opposite trend was observed with the collagen only gel, where stimulation with Il-1β resulted in the significant decrease in metabolic rate and cellular DNA (figure 3.4). No significant differences in metabolic rate or DNA content were observed with the rACs in the GAG hydrogels, with no clear trend seen, unlike the fbACs (figure 3.4). This better aligns with the current understanding of how Il-1β interacts with the proliferation of chondrocytes. While increases in proliferation were seen with the juvenile fbACs, decreases in proliferation were seen with the adult rACs.

*3.3.4: Changes in Cell Inflammation and Secretion of Il-6*

As a marker of inflammation in response to stimulation by Il-1β, production of Il-6 was measured over the course of the fourteen-day culture period (figure 3.3c). As expected, no inflammation was

detected in the cells not stimulated by Il-1β, as indicated by no Il-6 produced. All groups stimulated with Il-1β produced some level of Il-6, indicating that Il-1β was able to penetrate the scaffolds and stimulate the cells. However, the cells in collagen only gels produced ten times the amount of Il-6 compared to the cells in the GAG gels, demonstrating that the cells in the collagen gels were more susceptible to becoming inflamed in the presence of Il-1β. Furthermore, although the cells in the GAG gels produced significantly less Il-6 than those in the collagen gels, there were no differences in Il-6 production among the GAG gels. In this case, neither the ratio of CS to HA nor the presence of collagen had an effect on Il-6 production when stimulated with Il-1β, despite the differences in presented biomolecules and hydrogel physical properties over time. In this case, it appears that culturing in a GAG based gel alone was sufficient to dampen the pro-inflammatory effect of Il-1β compared to the collagen only gel control.

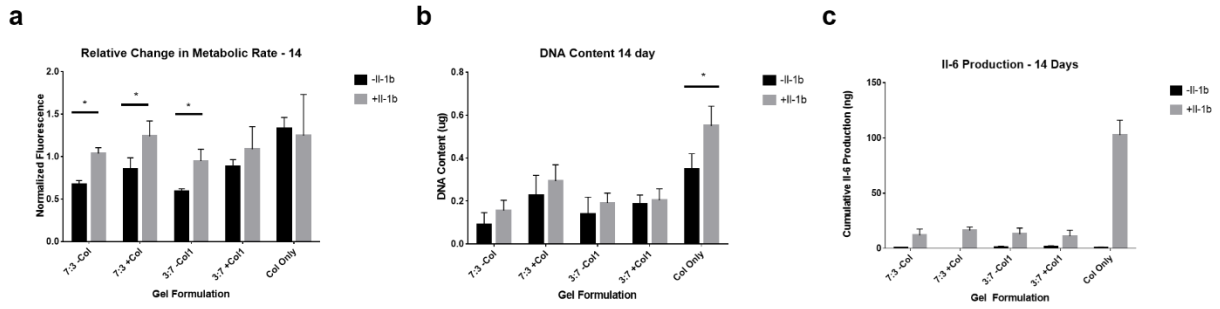


*Figure 3.3: Changes in fbAC behavior due to Il-1β stimulation. A) Relative change in metabolic activity after fourteen days of culture. B) Total DNA content after fourteen days of culture. C) Cumulative Il-6 production after fourteen days of culture. Multiple T-tests were run between stimulated and unstimulated groups. * denotes statistical significance between two groups (P < 0.05).*

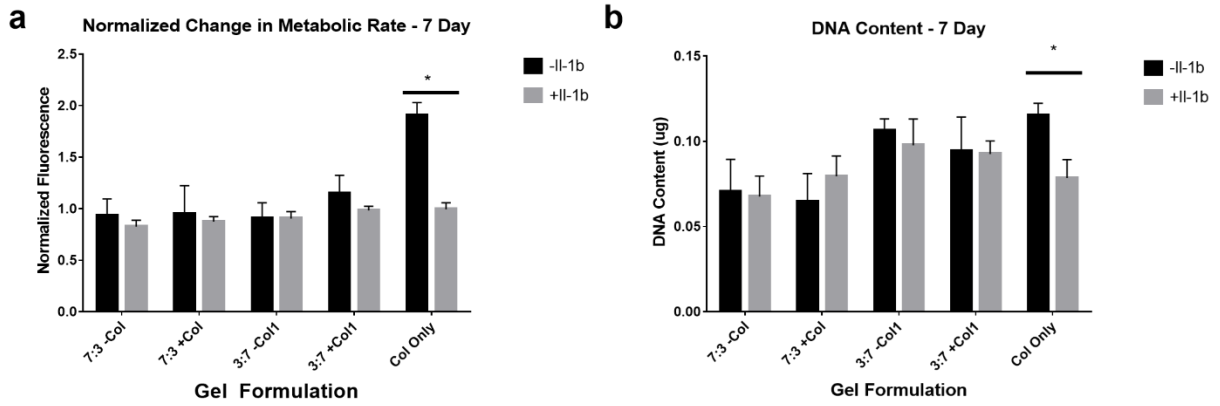


*Figure 3.4: Changes in rAC behavior in response to Il-1β stimulation. A) Relative change in metabolic activity after seven days of culture. B) Total DNA content after seven days of culture. * denotes statistical significance between two groups (P > 0.05).*

*3.3.5: Changes in Expression of Chondrogenic Genes*

To further quantify the effect of culture in pro-inflammatory conditions on the encapsulated fbACs, isolated mRNA was analyzed using qPCR to look at changes in gene expression. Changes in gene expression in gel groups stimulated with Il-1β were normalized to the collagen only gel stimulated with Il-1β to assess how culture in GAG blend gels under pro-inflammatory conditions differed from a collagen gel control and to their respective unstimulated control to assess the effect on Il-1β on the encapsulated cells given a certain scaffold formulation.

In general, all cartilage matrix related genes were downregulated and MMP13 was upregulated when all hydrogel groups were stimulated with Il-1β (figure 3.5c,d). There were no large changes in expression of Collagen type I and ADAMTS5 with regard to Il-1β stimulation, with the expression of collagen type X not detected in any of the groups regardless of Il-1β stimulation. While downregulation of chondrogenic genes suggests the cells of all groups are still being affected by Il-1β, a lack of change in

collagen type I and X indicate that Il-1β is not contributing to any hypertrophic differentiation of the chondrocytes.

When normalized to the collagen only gel control stimulated with IL-1β, all groups showed a decrease in MMP13 expression and most groups demonstrated an increase in collagen type II and aggrecan, with the exception of the 3:7 without collagen gel (figure 3.5a,b). No significant trends were found with the expression of COMP. While collagen type I and ADAMTS5 showed increased expression compared to the collagen only gel, the lack of change compared to the unstimulated controls suggest that this increase in expression may be due to the gel composition rather than due to the inflammatory effects of Il-1β. Furthermore, although expression of collagen type X was probed, there was no detectable expression of collagen type X, suggesting no hypertrophic differentiation due to cytokine stimulation or culture conditions. Overall, culture in the GAG gels under pro-inflammatory conditions promoted the expression of certain chondrogenic genes, though the expression of these genes was still lower than their respective unstimulated controls.

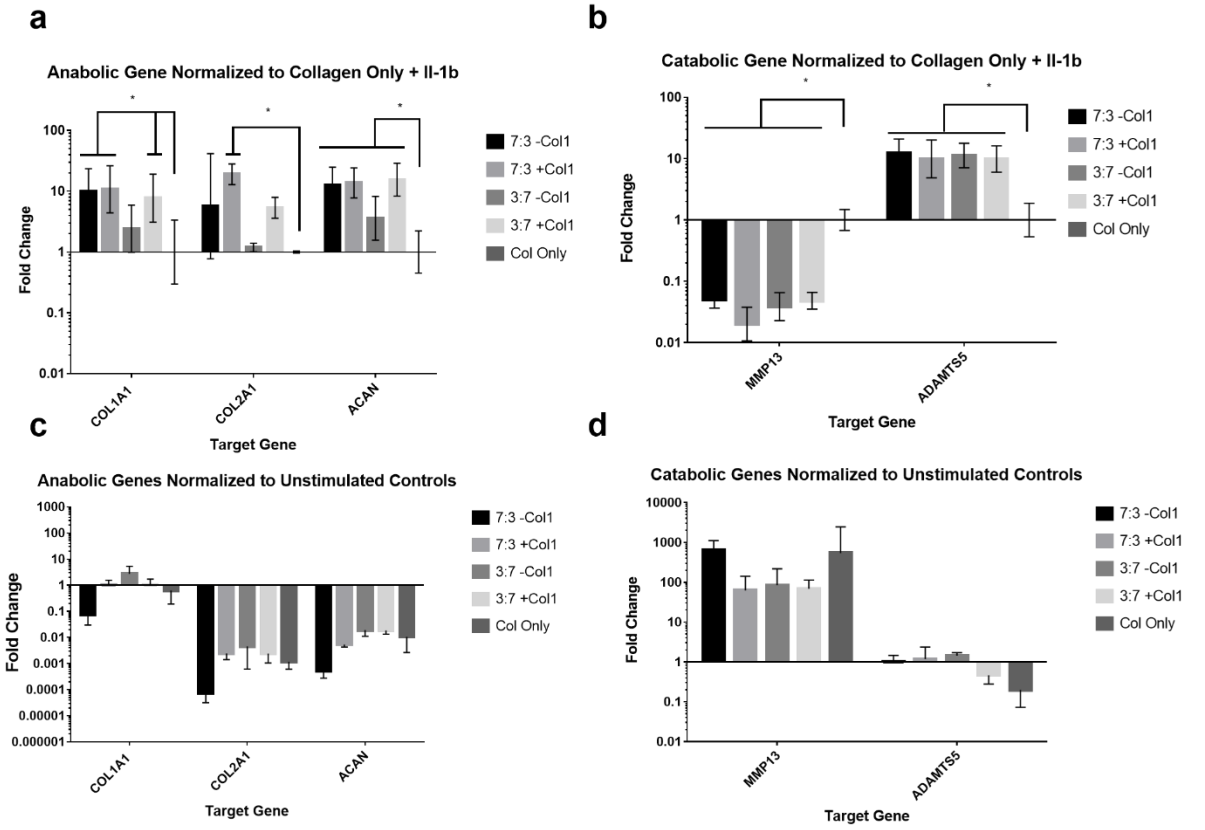


*Figure 3.5: Changes in gene expression after fourteen days of Il-1β stimulated culture. A,C) Changes in anabolic gene expression. B,D) Changes in catabolic gene expression. A,B) Changes in gene expression normalized to Il-1β stimulated collagen only gel. C,D) Changes in gene expression normalized to respective unstimulated group.* Denotes significant differences between groups*

### 3.4. Discussion

Although OA has traditionally been considered a cartilage disease resulting from mechanical wear of the articular cartilage, in contrast with rheumatoid arthritis, recent studies have shown that inflammation is a major component of the pathophysiology of OA. As such, tissue engineering strategies that seek to replace cartilage defects that result from OA should consider the pro-inflammatory

environment that they will be implanted in. While many studies have demonstrated the ability to promote cartilage matrix production and other have demonstrated methods to attune chondrocyte inflammation, few have studied the engineering of cartilage in an inflammatory environment.

In this study, we developed hydrogels based on the GAGs CS and HA to take advantage of their anti-inflammatory and chondrogenic properties. Furthermore, CS and HA were minimally modified to maximize the biological signals they present to the encapsulated cells. In addition to GAGs, collagen type I was added to the some of the gels for two reasons: to incorporate additional cell binding sites within the gel and to provide a tensile force to counteract the swelling of the GAG gels. Using two ratios of CS and HA and collagen, we formulated four hydrogels that had similar initial physical conditions with regard to compressive strength and diffusivity but presented different biological signals to the encapsulated hydrogels. As a control, we opted to use a collagen only gel, as this would be an analogue to the collagen-based scaffolds already being used in OA treatments such as ACI[46].

One hallmark of OA is the increase in catabolic activity, resulting in the enzymatic breakdown of the articular cartilage. However, there was no significant increases in degradation in the GAG hydrogels following the fourteen days of stimulation with Il-1β. Although all gels saw a decrease in compressive strength over the culture period, even greater than the acellular hydrogels, there was no difference in this change between the stimulated and unstimulated gels. This suggests that changes in hydrogel integrity may be due to cellular activity that is not associated with inflammation. This is further evidenced by the lack of differences in hydrogel mass and release of CS into the media, suggesting that chondrocytes encapsulated in these GAG blend gels do not significantly degrade the hydrogels as a result of pro-inflammatory signals. Under pro-inflammatory conditions, it has been demonstrated that chondrocyte hyaluronidase activity is upregulated[40,47,48,48–51]. In OA, this upregulation of83yaluronicdase activity is responsible for the fragmentation of HA and the release of aggrecan from the cartilage. These upregulated hyaluronidases are both cell-membrane bound[49,50] and extracellular[47]. As such, the lack of significant

hydrogel degradation could be due to several factors: the formation of a DPN with CS, leading to reduced hyaluronidase activity due to reduced recognition[44]; the crosslinking of the GAGs, inhibiting the endocytosis of GAGs for degradation in the endosome; or biological signals from the GAGs[27], inhibiting the increased expression of hyaluronidases through anti-inflammatory activity.

Another marker of OA and inflammation is the apoptosis of chondrocytes in the articular cartilage[52]. However, no significant cell death was observed seen with the fbACs encapsulated in the GAG hydrogels nor in the collagen only hydrogel control, though apoptosis itself was not investigated. On the contrary, slight increases in metabolic activity and DNA content were found with the GAG hydrogels, with significant increases in DNA content found within the collagen only hydrogels. While Il-1β mediated apoptosis is a hallmark of osteoarthritis in mature chondrocytes, the findings of the metabolic assays and changes in DNA content over time suggest the opposite is occurring. However, instead of cell death, it has been found that Il-1β stimulation of juvenile chondrocytes can lead to increased proliferation[53–55]. In these cases, increased proliferation of juvenile chondrocytes leads to an increase in the size of the proliferating zone of cartilage and reduced differentiation into hypertrophic chondrocytes[54–56], whereas Il-1β stimulation of adult chondrocytes leads to apoptosis and increased hypertrophic differentiation[57,58].

Because the primary cells used in this study were from bovine fetuses, the findings of this study align well with previously reported studies with juvenile chondrocytes. In this regard, it was found that proliferation of chondrocytes was lower with the GAG containing hydrogels compared to the collagen only gel, suggesting the GAG hydrogels prevented Il-1β mediated proliferation. This is further evidenced by the changes in metabolic rate and DNA content found with rACs from skeletally mature rabbits, where proliferation and metabolic rate decreased following Il-1β stimulation, suggesting an inhibition of proliferation or apoptosis of the cells. Furthermore, among the GAG hydrogels, the smallest increase in metabolism with fbACs was found with the 3:7 + collagen group, with no significant difference in metabolic rate change between the stimulated and unstimulated groups. Although no significant

difference in DNA content was found between the stimulated and unstimulated GAG hydrogels, the smallest increase in DNA content was found again in the 3:7 + collagen gel group. As such, in this case, the 3:7 + collagen hydrogel may be better for long term protection of encapsulated cells from external pro-inflammatory stimuli.

To measure the inflammatory response of the encapsulated chondrocytes, we looked at the production of Il-6 in response to stimulation with Il-1β[59]. As expected, no Il-6 was detected in any unstimulated groups, giving us a baseline for Il-6 production by the chondrocytes in our gels. In all GAG gel groups, when stimulated with Il-1β, there was increased production of Il-6 compared to the unstimulated baseline. However, the Il-1β stimulated collagen gel saw significantly higher Il-6 production, with roughly ten times more Il-6 being produced compared to the GAG gels. Taken together with the change in metabolic rate and DNA content data, this difference in Il-6 production further suggests that the culture in GAG hydrogels can dampen the inflammatory response to Il-1β outside the hydrogel. This may be due to the anti-inflammatory activity of the GAG hydrogel, Il-1β being sequestered away from the cells, or a combination of these two mechanisms. Further analysis will need to be done to determine the interactions between the HA/CS hydrogel and Il-1β.

Furthermore, we measured the catabolic activity of the stimulated chondrocytes through changes in gene expression of catabolic enzymes MMP-13 and ADAMTS5. In this experiment, two points of comparison that were studied with regard to the fbACs cultured in the blended GAG gels to best understand the effect of the pro-inflammatory environment: how gene expression changed compared to an Il-1β stimulated collagen type I gel and how gene expression changed compared to each group's respective unstimulated control. When compared to the collagen type I gel, all GAG gels saw decreased expression of MMP13 but an increased expression of ADAMTS5. However, when compared to their respective unstimulated gel, there was no large change in ADAMTS5 expression, suggesting that increased ADAMTS5 expression was due to culture in a GAG gel versus a collagen only gel. The lack of a change in

ADAMTS5 expression may be explained by the choice of pro-inflammatory cytokine for this model. In OA, increases in ADAMTS5 expression have been correlated to increased TNF-α secretion[60], whereas Il-1β stimulates ADAMTS4 production[61]. However, the Il-1β stimulated GAG gels also saw an increased expression of MMP13, suggesting that although they expressed MMP13 to a lesser degree than the stimulated collagen gel, they were still expressing higher than their respective baseline. Similar to the previously detailed markers of inflammation, the downregulation of MMP13 compared to the collagen only gel but upregulation compared to the unstimulated controls suggest a dampening of inflammation, but not complete protection from it.

Finally, to look at preservation of chondrogenic ability while under pro-inflammatory conditions, we looked at the production of cartilage matrix proteins through changes in gene expression of collagen type II, and aggrecan. Similarly, we looked at changes in gene expression in the stimulated GAG gels compared to both the stimulated collagen gel and their respective unstimulated gels. After fourteen days of culture, we saw increased expression of the genes encoding for the matrix proteins collagen type II and aggrecan, as well as collagen type I in most GAG gel groups, with the 3:7 CS/HA without collagen gel not seeing large increases in the expression of those genes. Similar to the catabolic genes, while there was an increase in the expression of these genes over the collagen type I gel, the expression of collagen type II and aggrecan were still downregulated when compared to their expression in their respective unstimulated controls. Furthermore, the expression of collagen type I did not see a large change between the stimulated gels and their unstimulated controls, again suggesting that collagen type I is not upregulated due to Il-1β stimulation.

Overall, compared to a collagen gel control, our blended GAG hydrogel was able to partially protect against inflammation from relatively high and sustained dose of Il-1β in our culture media over the course of fourteen days[29,37,62,63]. Furthermore, this was accomplished without further soluble factors such as anti-inflammatory peptides[64] or additional cell types such as mesenchymal stromal cells[65–67]. For

these GAG hydrogels, the presence of collagen type I also did not appear to have a large effect on the encapsulated cells while also providing the gels tensile strength in the form of decreased swelling and retention of compressive strength over time. While we were unable to completely prevent inflammation, as seen by the increased Il-6 production and decreased expression of certain cartilage matrix protein genes, the GAG gels still performed better than our collagen only control. These findings are consistent with previously reported studies involving sulfated hydrogels for suppression of inflammation. Arlov et al found that the sulfation of alginate suppressed, but did not completely prevent, Il-1β mediated inflammation over the course of two days[62]. However, their study used a lower concentration of Il-1β and cultured for a shorter period of time. In future studies, this inflammation could be further ameliorated through loading the GAG gels with positively charged anti-inflammatory factors or performing a coculture of chondrocytes and MSCs.

**3.5. Conclusion**

In this study we demonstrated the ability for blended CS/HA hydrogels to dampen the inflammatory response of encapsulated chondrocytes when cultured with a sustained dose of Il-1β over the course of fourteen days, simulating the presence of pro-inflammatory cytokines in the osteoarthritic environment. Under these pro-inflammatory conditions, GAG gels maintained similar robustness as their unstimulated counterparts, and the encapsulated cells showed signs of reduced inflammation induced changes in cell proliferation. Furthermore, although they still produced some levels of Il-6, showed some upregulation of MMP13, and downregulation of cartilage matrix proteins, the chondrocytes cultured in the GAG gels were less susceptible to inflammation compared to our collagen only gel control. Based on the results of this study, the observed anti-inflammatory effects may be due to the bioactive signals from the GAG polymers themselves, the sequestering if Il-1β away from the cells through GAG/protein interactions, or some combination of the two. Altogether, GAG gels possess the potential to allow for

cartilage tissue engineering under pro-inflammatory conditions, allowing for the regeneration of cartilage in the inflammatory osteoarthritis environment.

### 3.6. References


(1) Gage, B. E.; McIlvain, N. M.; Collins, C. L.; Fields, S. K.; Comstock, R. D. Epidemiology of 6.6 Million Knee Injuries Presenting to United States Emergency Departments from 1999 through 2008. *Acad Emerg Med* **2012**, *19* (4), 378–385. https://doi.org/10.1111/j.1553-2712.2012.01315.x.

(2) Arthritis Foundation. Arthritis By The Numbers. *Book of trusted Facts & Figures*. 2019.

(3) Baugé, C.; Legendre, F.; Leclercq, S.; Elissalde, J. M.; Pujol, J. P.; Galéra, P.; Boumédiene, K. Interleukin-1beta Impairment of Transforming Growth Factor Beta1 Signaling by down-Regulation of Transforming Growth Factor Beta Receptor Type II and up-Regulation of Smad7 in Human Articular Chondrocytes. *Arthritis Rheum.* **2007**, *56* (9), 3020–3032. https://doi.org/10.1002/art.22840.

(4) Malemud, C. J.; Islam, N.; Haqqi, T. M. Pathophysiological Mechanisms in Osteoarthritis Lead to Novel Therapeutic Strategies. *CTO* **2003**, *174* (1–2), 34–48. https://doi.org/10.1159/000070573.

(5) Saklatvala, J. Tumour Necrosis Factor α Stimulates Resorption and Inhibits Synthesis of Proteoglycan in Cartilage. *Nature* **1986**, *322* (6079), 547–549. https://doi.org/10.1038/322547a0.

(6) Goldring, M. B.; Otero, M. Inflammation in Osteoarthritis. *Current Opinion in Rheumatology* **2011**, *23* (5), 471–478. https://doi.org/10.1097/BOR.0b013e328349c2b1.

(7) Hügle, T.; Geurts, J. What Drives Osteoarthritis?—Synovial versus Subchondral Bone Pathology. *Rheumatology (Oxford)* **2017**, *56* (9), 1461–1471. https://doi.org/10.1093/rheumatology/kew389.

(8) Haynes, M. K.; Hume, E. L.; Smith, J. B. Phenotypic Characterization of Inflammatory Cells from Osteoarthritic Synovium and Synovial Fluids. *Clinical Immunology* **2002**, *105* (3), 315–325. https://doi.org/10.1006/clim.2002.5283.

(9) Sellam, J.; Berenbaum, F. The Role of Synovitis in Pathophysiology and Clinical Symptoms of Osteoarthritis. *Nature Reviews Rheumatology* **2010**, *6* (11), 625–635. https://doi.org/10.1038/nrrheum.2010.159.

(10) Pap, T.; Korb-Pap, A. Cartilage Damage in Osteoarthritis and Rheumatoid Arthritis—Two Unequal Siblings. *Nat Rev Rheumatol* **2015**, *11* (10), 606–615. https://doi.org/10.1038/nrrheum.2015.95.

(11) Kaneko, S.; Satoh, T.; Chiba, J.; Ju, C.; Inoue, K.; Kagawa, J. Interleukin–6 and Interleukin–8 Levels in Serum and Synovial Fluid of Patients with Osteoarthritis. *Cytokines, Cellular & Molecular Therapy* **2000**, *6* (2), 71–79. https://doi.org/10.1080/13684730050515796.

(12) Glyn-Jones, S.; Palmer, A. J. R.; Agricola, R.; Price, A. J.; Vincent, T. L.; Weinans, H.; Carr, A. J. Osteoarthritis. *The Lancet* **2015**, *386* (9991), 376–387. https://doi.org/10.1016/S0140-6736(14)60802-3.

(13) Hunziker, E. B. Articular Cartilage Repair: Are the Intrinsic Biological Constraints Undermining This Process Insuperable? *Osteoarthritis Cartilage* **1999**, *7* (1), 15–28. https://doi.org/10.1053/joca.1998.0159.

(14) Hunziker, E. B.; Quinn, T. M.; Häuselmann, H.-J. Quantitative Structural Organization of Normal Adult Human Articular Cartilage. *Osteoarthritis and Cartilage* **2002**, *10* (7), 564–572. https://doi.org/10.1053/joca.2002.0814.

(15) Huang, B. J.; Hu, J. C.; Athanasiou, K. A. Cell-Based Tissue Engineering Strategies Used in the Clinical Repair of Articular Cartilage. *Biomaterials* **2016**, *98*, 1–22. https://doi.org/10.1016/j.biomaterials.2016.04.018.

(16) Angele, P.; Fritz, J.; Albrecht, D.; Koh, J.; Zellner, J. Defect Type, Localization and Marker Gene Expression Determines Early Adverse Events of Matrix-Associated Autologous Chondrocyte Implantation. *Injury* **2015**, *46*, S2–S9. https://doi.org/10.1016/S0020-1383(15)30012-7.
(17) Albrecht, C.; Tichy, B.; Zak, L.; Aldrian, S.; Nürnberger, S.; Marlovits, S. Influence of Cell Differentiation and IL-1β Expression on Clinical Outcomes After Matrix-Associated Chondrocyte Transplantation. *Am J Sports Med* **2014**, *42* (1), 59–69. https://doi.org/10.1177/0363546513507543.
(18) Niemeyer, P.; Pestka, J. M.; Salzmann, G. M.; Südkamp, N. P.; Schmal, H. Influence of Cell Quality on Clinical Outcome After Autologous Chondrocyte Implantation. *Am J Sports Med* **2012**, *40* (3), 556–561. https://doi.org/10.1177/0363546511428879.
(19) Campos, Y.; Almirall, A.; Fuentes, G.; Bloem, H. L.; Kaijzel, E. L.; Cruz, L. J. Tissue Engineering: An Alternative to Repair Cartilage. *Tissue Engineering Part B: Reviews* **2019**, *25* (4), 357–373. https://doi.org/10.1089/ten.teb.2018.0330.
(20) Spiller, K. L.; Maher, S. A.; Lowman, A. M. Hydrogels for the Repair of Articular Cartilage Defects. *Tissue Engineering Part B: Reviews* **2011**, *17* (4), 281–299. https://doi.org/10.1089/ten.teb.2011.0077.
(21) Vega, S. L.; Kwon, M. Y.; Burdick, J. A. RECENT ADVANCES IN HYDROGELS FOR CARTILAGE TISSUE ENGINEERING. *Eur Cell Mater* **2017**, *33*, 59–75. https://doi.org/10.22203/eCM.v033a05.
(22) Liu, M.; Zeng, X.; Ma, C.; Yi, H.; Ali, Z.; Mou, X.; Li, S.; Deng, Y.; He, N. Injectable Hydrogels for Cartilage and Bone Tissue Engineering. *Bone Research* **2017**, *5*, 17014. https://doi.org/10.1038/boneres.2017.14.
(23) Shlopov, B. V.; Lie, W. R.; Mainardi, C. L.; Cole, A. A.; Chubinskaya, S.; Hasty, K. A. Osteoarthritic Lesions: Involvement of Three Different Collagenases. *Arthritis Rheum* **1997**, *40* (11), 2065–2074. https://doi.org/10.1002/art.1780401120.
(24) Stanton, H.; Rogerson, F. M.; East, C. J.; Golub, S. B.; Lawlor, K. E.; Meeker, C. T.; Little, C. B.; Last, K.; Farmer, P. J.; Campbell, I. K.; Fourie, A. M.; Fosang, A. J. ADAMTS5 Is the Major Aggrecanase in Mouse Cartilage in Vivo and in Vitro. *Nature* **2005**, *434* (7033), 648–652. https://doi.org/10.1038/nature03417.
(25) Peng, H.; Zhou, J.; Liu, S.; Hu, Q.; Ming, J.; Qiu, B. Hyaluronic Acid Inhibits Nitric Oxide-Induced Apoptosis and Dedifferentiation of Articular Chondrocytes in Vitro. *Inflamm. Res.* **2010**, *59* (7), 519–530. https://doi.org/10.1007/s00011-010-0156-x.
(26) Campo, G. M.; Avenoso, A.; Campo, S.; D'Ascola, A.; Traina, P.; Samà, D.; Calatroni, A. Glycosaminoglycans Modulate Inflammation and Apoptosis in LPS-Treated Chondrocytes. *Journal of Cellular Biochemistry* **2009**, *106* (1), 83–92. https://doi.org/10.1002/jcb.21981.
(27) Campo, G. M.; Avenoso, A.; Nastasi, G.; Micali, A.; Prestipino, V.; Vaccaro, M.; D'Ascola, A.; Calatroni, A.; Campo, S. Hyaluronan Reduces Inflammation in Experimental Arthritis by Modulating TLR-2 and TLR-4 Cartilage Expression. *Biochimica et Biophysica Acta (BBA) - Molecular Basis of Disease* **2011**, *1812* (9), 1170–1181. https://doi.org/10.1016/j.bbadis.2011.06.006.
(28) Topoluk, N.; Steckbeck, K.; Siatkowski, S.; Burnikel, B.; Tokish, J.; Mercuri, J. Amniotic Mesenchymal Stem Cells Mitigate Osteoarthritis Progression in a Synovial Macrophage-Mediated in Vitro Explant Coculture Model. *J Tissue Eng Regen Med* **2018**, *12* (4), 1097–1110. https://doi.org/10.1002/term.2610.
(29) Chen, C.; Zhang, C.; Cai, L.; Xie, H.; Hu, W.; Wang, T.; Lu, D.; Chen, H. Baicalin Suppresses IL-1β-Induced Expression of Inflammatory Cytokines via Blocking NF-KB in Human Osteoarthritis Chondrocytes and Shows Protective Effect in Mice Osteoarthritis Models. *International Immunopharmacology* **2017**, *52*, 218–226. https://doi.org/10.1016/j.intimp.2017.09.017.
(30) Manferdini, C.; Maumus, M.; Gabusi, E.; Paolella, F.; Grassi, F.; Jorgensen, C.; Fleury-Cappellesso, S.; Noël, D.; Lisignoli, G. Lack of Anti-Inflammatory and Anti-Catabolic Effects on Basal Inflamed

Osteoarthritic Chondrocytes or Synoviocytes by Adipose Stem Cell-Conditioned Medium. *Osteoarthritis and Cartilage* **2015**, *23* (11), 2045–2057. https://doi.org/10.1016/j.joca.2015.03.025.
(31) Kawasaki, K.; Ochi, M.; Uchio, Y.; Adachi, N.; Matsusaki, M. Hyaluronic Acid Enhances Proliferation and Chondroitin Sulfate Synthesis in Cultured Chondrocytes Embedded in Collagen Gels. *Journal of Cellular Physiology* **1999**, *179* (2), 142–148. https://doi.org/10.1002/(SICI)1097-4652(199905)179:2<142::AID-JCP4>3.0.CO;2-Q.
(32) Varghese, S.; Hwang, N. S.; Canver, A. C.; Theprungsirikul, P.; Lin, D. W.; Elisseeff, J. Chondroitin Sulfate Based Niches for Chondrogenic Differentiation of Mesenchymal Stem Cells. *Matrix Biol.* **2008**, *27* (1), 12–21. https://doi.org/10.1016/j.matbio.2007.07.002.
(33) Wang, T.; Yang, F. A Comparative Study of Chondroitin Sulfate and Heparan Sulfate for Directing Three-Dimensional Chondrogenesis of Mesenchymal Stem Cells. *Stem Cell Research & Therapy* **2017**, *8* (1), 284. https://doi.org/10.1186/s13287-017-0728-6.
(34) Aisenbrey, E. A.; Bryant, S. J. The Role of Chondroitin Sulfate in Regulating Hypertrophy during MSC Chondrogenesis in a Cartilage Mimetic Hydrogel under Dynamic Loading. *Biomaterials* **2019**, *190–191*, 51–62. https://doi.org/10.1016/j.biomaterials.2018.10.028.
(35) Ialenti, A.; Di Rosa, M. Hyaluronic Acid Modulates Acute and Chronic Inflammation. *Agents Actions* **1994**, *43* (1), 44–47. https://doi.org/10.1007/BF02005763.
(36) Wang, C.-T.; Lin, Y.-T.; Chiang, B.-L.; Lin, Y.-H.; Hou, S.-M. High Molecular Weight Hyaluronic Acid Down-Regulates the Gene Expression of Osteoarthritis-Associated Cytokines and Enzymes in Fibroblast-like Synoviocytes from Patients with Early Osteoarthritis. *Osteoarthritis and Cartilage* **2006**, *14* (12), 1237–1247. https://doi.org/10.1016/j.joca.2006.05.009.
(37) Zhou, P.-H.; Liu, S.-Q.; Peng, H. The Effect of Hyaluronic Acid on IL-1β-Induced Chondrocyte Apoptosis in a Rat Model of Osteoarthritis. *Journal of Orthopaedic Research* **2008**, *26* (12), 1643–1648. https://doi.org/10.1002/jor.20683.
(38) Iovu, M.; Dumais, G.; du Souich, P. Anti-Inflammatory Activity of Chondroitin Sulfate. *Osteoarthritis and Cartilage* **2008**, *16*, S14–S18. https://doi.org/10.1016/j.joca.2008.06.008.
(39) Stabler, T. V.; Huang, Z.; Montell, E.; Vergés, J.; Kraus, V. B. Chondroitin Sulphate Inhibits NF-KB Activity Induced by Interaction of Pathogenic and Damage Associated Molecules. *Osteoarthritis and Cartilage* **2017**, *25* (1), 166–174. https://doi.org/10.1016/j.joca.2016.08.012.
(40) Knudson, W.; Ishizuka, S.; Terabe, K.; Askew, E. B.; Knudson, C. B. The Pericellular Hyaluronan of Articular Chondrocytes. *Matrix Biology* **2019**, *78–79*, 32–46. https://doi.org/10.1016/j.matbio.2018.02.005.
(41) Knudson, C. B.; Knudson, W. Cartilage Proteoglycans. *Seminars in Cell & Developmental Biology* **2001**, *12* (2), 69–78. https://doi.org/10.1006/scdb.2000.0243.
(42) Meghdadi, M.; Pezeshki-Modaress, M.; Irani, S.; Atyabi, S. M.; Zandi, M. Chondroitin Sulfate Immobilized PCL Nanofibers Enhance Chondrogenic Differentiation of Mesenchymal Stem Cells. *International Journal of Biological Macromolecules* **2019**, *136*, 616–624. https://doi.org/10.1016/j.ijbiomac.2019.06.061.
(43) Hegewald, A. A.; Ringe, J.; Bartel, J.; Krüger, I.; Notter, M.; Barnewitz, D.; Kaps, C.; Sittinger, M. Hyaluronic Acid and Autologous Synovial Fluid Induce Chondrogenic Differentiation of Equine Mesenchymal Stem Cells: A Preliminary Study. *Tissue and Cell* **2004**, *36* (6), 431–438. https://doi.org/10.1016/j.tice.2004.07.003.
(44) Nguyen, M.; Liu, J. C.; Panitch, A. Physical and Bioactive Properties of Glycosaminoglycan Hydrogels Modulated by Polymer Design Parameters and Polymer Ratio. *Biomacromolecules* **2021**. https://doi.org/10.1021/acs.biomac.1c00866.
(45) Walimbe, T.; Calve, S.; Panitch, A.; Sivasankar, M. P. Incorporation of Types I and III Collagen in Tunable Hyaluronan Hydrogels for Vocal Fold Tissue Engineering. *Acta Biomater.* **2019**, *87*, 97–107. https://doi.org/10.1016/j.actbio.2019.01.058.

(46) Basad, E.; Wissing, F. R.; Fehrenbach, P.; Rickert, M.; Steinmeyer, J.; Ishaque, B. Matrix-Induced Autologous Chondrocyte Implantation (MACI) in the Knee: Clinical Outcomes and Challenges. *Knee Surg Sports Traumatol Arthrosc* **2015**, *23* (12), 3729–3735. https://doi.org/10.1007/s00167-014-3295-8.
(47) El Hajjaji, H.; Cole, A. A.; Manicourt, D.-H. Chondrocytes, Synoviocytes and Dermal Fibroblasts All Express PH-20, a Hyaluronidase Active at Neutral PH. *Arthritis Res Ther* **2005**, *7* (4), R756–R768. https://doi.org/10.1186/ar1730.
(48) Durigova, M.; Roughley, P. J.; Mort, J. S. Mechanism of Proteoglycan Aggregate Degradation in Cartilage Stimulated with Oncostatin M. *Osteoarthritis and Cartilage* **2008**, *16* (1), 98–104. https://doi.org/10.1016/j.joca.2007.05.002.
(49) Flannery, C. R.; Little, C. B.; Hughes, C. E.; Caterson, B. Expression and Activity of Articular Cartilage Hyaluronidases. *Biochemical and Biophysical Research Communications* **1998**, *251* (3), 824–829. https://doi.org/10.1006/bbrc.1998.9561.
(50) Shimizu, H.; Shimoda, M.; Mochizuki, S.; Miyamae, Y.; Abe, H.; Chijiiwa, M.; Yoshida, H.; Shiozawa, J.; Ishijima, M.; Kaneko, K.; Kanaji, A.; Nakamura, M.; Toyama, Y.; Okada, Y. Hyaluronan-Binding Protein Involved in Hyaluronan Depolymerization Is Up-Regulated and Involved in Hyaluronan Degradation in Human Osteoarthritic Cartilage. *The American Journal of Pathology* **2018**, *188* (9), 2109–2119. https://doi.org/10.1016/j.ajpath.2018.05.012.
(51) Nishida, Y.; D'Souza, A. L.; Thonar, E. J.-M. A.; Knudson, W. Stimulation of Hyaluronan Metabolism by Interleukin-1α in Human Articular Cartilage. *Arthritis & Rheumatism* **2000**, *43* (6), 1315–1326. https://doi.org/10.1002/1529-0131(200006)43:6<1315::AID-ANR14>3.0.CO;2-#.
(52) Kim, J.; Xu, M.; Xo, R.; Mates, A.; Wilson, G. L.; Pearsall, A. W.; Grishko, V. Mitochondrial DNA Damage Is Involved in Apoptosis Caused by Pro-Inflammatory Cytokines in Human OA Chondrocytes. *Osteoarthritis and Cartilage* **2010**, *18* (3), 424–432. https://doi.org/10.1016/j.joca.2009.09.008.
(53) Söder, O.; Madsen, K. Stimulation of Chondrocyte DNA Synthesis by Interleukin-1. *Br J Rheumatol* **1988**, *27* (1), 21–26. https://doi.org/10.1093/rheumatology/27.1.21.
(54) MacRae, V. E.; Farquharson, C.; Ahmed, S. F. The Restricted Potential for Recovery of Growth Plate Chondrogenesis and Longitudinal Bone Growth Following Exposure to Pro-Inflammatory Cytokines. *Journal of Endocrinology* **2006**, *189* (2), 319–328. https://doi.org/10.1677/joe.1.06609.
(55) Simsa-Maziel, S.; Monsonego-Ornan, E. Interleukin-1β Promotes Proliferation and Inhibits Differentiation of Chondrocytes through a Mechanism Involving Down-Regulation of FGFR-3 and P21. *Endocrinology* **2012**, *153* (5), 2296–2310. https://doi.org/10.1210/en.2011-1756.
(56) Samvelyan, H. J.; Madi, K.; Törnqvist, A. E.; Javaheri, B.; Staines, K. A. Characterisation of Growth Plate Dynamics in Surgical and Non-Invasive Loaded Murine Models of Osteoarthritis. *Osteoarthritis and Cartilage* **2021**, *29*, S12. https://doi.org/10.1016/j.joca.2021.05.022.
(57) Cecil, D. L.; Johnson, K.; Rediske, J.; Lotz, M.; Schmidt, A. M.; Terkeltaub, R. Inflammation-Induced Chondrocyte Hypertrophy Is Driven by Receptor for Advanced Glycation End Products. *The Journal of Immunology* **2005**, *175* (12), 8296–8302. https://doi.org/10.4049/jimmunol.175.12.8296.
(58) van der Kraan, P. M.; van den Berg, W. B. Chondrocyte Hypertrophy and Osteoarthritis: Role in Initiation and Progression of Cartilage Degeneration? *Osteoarthritis and Cartilage* **2012**, *20* (3), 223–232. https://doi.org/10.1016/j.joca.2011.12.003.
(59) Guerne, P. A.; Carson, D. A.; Lotz, M. IL-6 Production by Human Articular Chondrocytes. Modulation of Its Synthesis by Cytokines, Growth Factors, and Hormones in Vitro. *J Immunol* **1990**, *144* (2), 499–505.
(60) Song, R.-H.; Tortorella, M. D.; Malfait, A.-M.; Alston, J. T.; Yang, Z.; Arner, E. C.; Griggs, D. W. Aggrecan Degradation in Human Articular Cartilage Explants Is Mediated by Both ADAMTS-4 and ADAMTS-5. *Arthritis Rheum* **2007**, *56* (2), 575–585. https://doi.org/10.1002/art.22334.

(61) Gabay, O.; Sanchez, C.; Salvat, C.; Chevy, F.; Breton, M.; Nourissat, G.; Wolf, C.; Jacques, C.; Berenbaum, F. Stigmasterol: A Phytosterol with Potential Anti-Osteoarthritic Properties. *Osteoarthritis Cartilage* **2010**, *18* (1), 106–116. https://doi.org/10.1016/j.joca.2009.08.019.
(62) Arlov, Ø.; Öztürk, E.; Steinwachs, M.; Skjåk-Bræk, G.; Zenobi-Wong, M. Biomimetic Sulphated Alginate Hydrogels Suppress IL-1B-Induced Inflammatory Responses in Human Chondrocytes. *76-89* **2017**. https://doi.org/10.22203/eCM.v033a06.
(63) Jomphe, C.; Gabriac, M.; Hale, T. M.; Héroux, L.; Trudeau, L.-É.; Deblois, D.; Montell, E.; Vergés, J.; Du Souich, P. Chondroitin Sulfate Inhibits the Nuclear Translocation of Nuclear Factor-KB in Interleukin-1β-Stimulated Chondrocytes. *Basic & Clinical Pharmacology & Toxicology* **2008**, *102* (1), 59–65. https://doi.org/10.1111/j.1742-7843.2007.00158.x.
(64) Deloney, M.; Smart, K.; Christiansen, B. A.; Panitch, A. Thermoresponsive, Hollow, Degradable Core-Shell Nanoparticles for Intra-Articular Delivery of Anti-Inflammatory Peptide. *Journal of Controlled Release* **2020**, *323*, 47–58. https://doi.org/10.1016/j.jconrel.2020.04.007.
(65) Sun, Z.; Nair, L. S.; Laurencin, C. T. The Paracrine Effect of Adipose-Derived Stem Cells Inhibits IL-1β-Induced Inflammation in Chondrogenic Cells through the Wnt/β-Catenin Signaling Pathway. *Regen. Eng. Transl. Med.* **2018**, *4* (1), 35–41. https://doi.org/10.1007/s40883-018-0047-1.
(66) Wang, H.; Yan, X.; Jiang, Y.; Wang, Z.; Li, Y.; Shao, Q. The Human Umbilical Cord Stem Cells Improve the Viability of OA Degenerated Chondrocytes. *Molecular Medicine Reports* **2018**, *17* (3), 4474–4482. https://doi.org/10.3892/mmr.2018.8413.
(67) van Buul, G. M.; Villafuertes, E.; Bos, P. K.; Waarsing, J. H.; Kops, N.; Narcisi, R.; Weinans, H.; Verhaar, J. A. N.; Bernsen, M. R.; van Osch, G. J. V. M. Mesenchymal Stem Cells Secrete Factors That Inhibit Inflammatory Processes in Short-Term Osteoarthritic Synovium and Cartilage Explant Culture. *Osteoarthritis and Cartilage* **2012**, *20* (10), 1186–1196. https://doi.org/10.1016/j.joca.2012.06.003.

# 4. Synthesis and Optimization of Collagen-targeting Peptide-Glycans for Inhibition of Platelets Following Endothelial Injury

This chapter consists of a manuscript by Michael Nguyen, John Paderi, Andrew Wooley, Tanaya Walimbe, and Alyssa Panitch submitted to Biomacromolecules, currently under review.

**Abstract:** Many endothelial complications, whether from surgical or pathological origins, can result in the denudation of the endothelial layer and the exposure of collagen. Exposure of collagen results in the activation of platelets, leading to thrombotic and inflammatory cascades that ultimately result in vessel stenosis. We have previously reported the use of peptide-glycan compounds to target exposed collagen following endothelial injury. In this paper we optimize the spacer sequence of our collagen binding peptide to increase its conjugation to glycan backbones and increase the peptide-glycan collagen binding affinity by increasing C-terminal cationic charge. Furthermore, we demonstrate this molecule's ability to inhibit platelet activation through collagen blocking, as well as its ability to localize to exposed endothelial collagen following systemic delivery. Altogether, optimization of peptide sequence and linkage chemistry can allow for increased conjugation and function, having implications for their use in other clinical applications.

### 4.1: Introduction

Glycans represent a century-old drug class of carbohydrates with wide therapeutic potential. Numerous clinical and preclinical studies have demonstrated the efficacy of glycans in a broad range of

diseases, including oncology, cardiovascular disease, fibrosis, and autoimmune disorders[1,2]. One of the recognized challenges of glycans is their suboptimal pharmacokinetic profile when administered parenterally, thus limiting their use more broadly[3]. Targeted drug delivery strategies can overcome this limitation, however, providing for a novel approach to generate innovative new glycan therapeutics[1,4].

We have identified collagen as a key therapeutic target as collagens are frequently exposed in disease states or during injurious surgical or endovascular procedures. Exposure of collagen to blood triggers a potent platelet activation response and subsequent thrombotic and inflammatory processes[5,6]. During endovascular procedures or in vascular surgeries, for example, the fragile endothelial layer is often denuded, and the platelet-mediated inflammatory response contributes to an adverse hyperplastic healing sequalae that causes vessel stenosis. Endothelial dysfunction can lead to collagen exposure in numerous disease states such as in cancer, autoimmune disorders such as systemic sclerosis[7], infectious diseases including COVID-19[8], and in fibrosis[9]. Collagen is therefore a prime target, as it is both a target for delivery to specific areas of injury or disease, and is also itself a contributing pathomechanism for adverse healing and disease progression.

We have previously designed collagen-binding peptide-modified glycans as therapeutics that target endothelial injury and inhibit platelet activation in the lumen of a blood vessel when delivered locally[10,11]. Systemic delivery of these compounds is limited, however, due to the relatively low affinity of these compounds. We have therefore aimed to improve the binding affinity of these compounds to enable systemic administration with targeted delivery to areas of exposed collagen, as occurs in injury or disease. Generally, optimization strategies include peptide binding affinity, linkage chemistry, spacer optimization between the glycan and the binding domain of the peptide, and conservation of the glycan's therapeutic activity.

Glycans are negatively charged linear carbohydrate chains and include sulfated glycans such as heparin (Hep), dermatan sulfate (DS), and chondroitin sulfate (CS), or non-sulfated carbohydrates

including hyaluronan (HA)[12]. Given the broad therapeutic activity of glycans and their biocompatibility, multiple chemical strategies have been employed for modifying glycans including adding payload[13], immobilizing to surfaces such as vascular grafts[14], generating scaffolds or hydrogels[15], or creating micro- or nano-particle therapeutic agents[16]. The negative charge and charge density of glycans is important for biological activity and the interaction of glycans with numerous biological binding partners[17]. The negative charge also influences modification and purification strategies of glycans, where charged groups can associate[18], lead to precipitation[19], or mask binding regions.

In unpublished studies we identified a modified version of the collagen-binding peptide identified by Chiang and Kang that also binds to collagen, but does not contain thiol or carboxylate groups (GQLYKSILY)[20]. Others have shown that GAG oxidation can affect GAG activity; specifically, heparin oxidation reduces the anticoagulation activity of heparin without affecting its heparinase activity[21]. We have previously reported that there is a balance between GAG modification and preservation of GAG activity[22]. Thus, we focus our efforts on modification through the carboxylate groups on the GAG using peptide-hydrazides, as hydrazides are more reactive under acidic condition than are amines that are present at the N-terminus and on lysines residues present within the peptide. Here we investigated whether inclusion of cationic charge within the spacer region and proximal to hydrazide group would improve peptide-glycan conjugation and optimize collagen-binding potency for the targeted delivery to areas of vascular injury or disease while also preserving the GAG antiplatelet function.

**4.2 Materials and Methods:**

*4.2.1: Synthesis of GQLY Peptide Variants*

The purified peptide SSR-hyd (GQLYKSILYGSGSGSRR-hyd) was purchased from Chinese Peptide Company. GQLY variants SRR-amide (GQLYKSILYGSGSGSRR-amide) and GSG-hyd (GQLYKSILYGSGSG-hyd) were synthesized using solid phase peptide synthesis chemistry, on Rink Amide resin (CEM Corporation)

or hydrazide loaded Cl-TCP(Cl) resin (CEM Corporation) to functionalize the peptide C terminus with an amide or hydrazide group, respectively. Peptide synthesis was performed using a Liberty Blue peptide synthesizer, with post synthesis cleavage of the peptide from the resin being carried out using a cocktail of trifluoracetic acid, triisopropylsilane, phenol, and water. Peptides were purified using fast protein liquid chromatography (FPLC), with the peptide molecular weight in the collected fractions verified using matrix assisted laser desorption/ionization time of flight mass spectrometry (MALDI-TOF MS). Peptides were then frozen, lyophilized, and stored at -80 ºC until later use.

*4.2.2: Synthesis and Analysis of Glycan-GQLY Variants*

The glycans heparin (Bioiberica), hyaluronic acid (Lifecore Biomedical), chondroitin sulfate (Seikigaku Corporation), and dermatan sulfate (Bioiberica) were reacted with GQLY peptide variants using aqueous carbodiimide chemistry. Glycans were dissolved in a solution of 0.1 M 2-(N-morpholino)ethanesulfonic acid (MES), 8M urea, and 0.2 wt% sodium chloride at a concentration of 10 mg/mL. Solid peptide was dissolved in the solution to theoretically functionalize 16% of the glycan disaccharide units present. 1-Ethyl-3-[3-dimethylaminopropyl]carbodiimide (EDC) was then added in a ratio of 0.5:1 EDC to glycan disaccharide units. The reaction was titrated to pH 4.5 and allowed to proceed overnight. Fluorescently labeled compounds were synthesized by reacting a 1:1 molar ratio of fluorophore CF-633-hydrazide (Biotium) to glycan followed by peptide conjugation. To purify the solution, the reaction was first titrated to pH 8.5 to stop the reaction, then purified using a KrosFlo tangential flow filtration system. The reactions were purified against a 10 kDa cutoff membrane at a transmembrane pressure of 25 psi until a permeate volume of 5X the reaction volume had been reached. Solutions were then frozen and lyophilized until further use. Quantification of peptides associated with the glycans was done by analyzing the ultraviolet absorbance of the purified molecules at 280 nm and calculating the peptide content using standard curves for the respective peptide.

*4.2.3: Structural Analysis of GQLY Variants by Circular Dichroism*

The structure of the GQLY variants SRR-hyd and GSG-hyd was analyzed using a Jasco J-715 Circular Dichroism (CD) spectrometer. Samples were dissolved at a concentration of 1 mg/mL in pH 8.5 sodium borate buffer and loaded into a quartz cell. The far-UV spectra of the peptides was measured from 190 to 250 nm, with the structure of the peptides determined from the spectra using BESTSEL.

*4.2.4: Analysis of CS-GQLY Conjugate Association*

To test for the presence of peptides associated with CS through non-covalent interactions, CS reacted with GQLY variants were dissolved in ultrapure water, then analyzed for free peptide using MALDI-TOF MS. To remove any peptide associate with glycans via non-covalent interactions, CS-GQLY variants were dissolved in a solution of 1 M sodium chloride and 8 M urea to disrupt electrostatic interactions between CS and the GQLY variants. Solutions were agitated for 30 minutes, with any disassociated peptide filtered out using Amicon Ultra centrifugal filter units (Millipore) with a 10 kDa molecular weight cut off filter. Following treatment with the salt solution, the salt concentration of the retentate was diluted by replenishing the volume lost with deionized water, then spin filtering three times. The UV absorbance at 280 nm was of the solutions was taken before and after the disassociation process to quantify the amount of peptide removed from the glycan backbone. Dissociation of electrostatically bound peptide was confirmed using MALDI

*4.2.5: Binding Capability of CS-GQLY and Hep-GQLY Variants*

To determine how the C-terminal spacer sequence or glycan backbone affected peptide-glycan binding ability, CS-GQLY and Hep-GQLY variants were biotinylated through reacting with EZ-Link Hydrazide-Biotin (ThermoFisher Scientific) using the same EDC carbodiimide synthesis and purification

process. For collagen binding capability, a Biocoat collagen type I coated plate (Corning) was first blocked with 5% bovine serum albumin for one hour, then washed three times with phosphate buffered saline (PBS). A logarithmic serial dilution of each CS-GQLY and Hep-GQLY variant in PBS was pipetted onto the plate and was incubated at 37 $^{O}$C for 30 minutes. The plate was again washed three times with PBS. Next, a 200X dilution solution of streptavidin-horseradish peroxidase solution (R&D Systems) was added and incubated for 20 minutes. Color was developed with a corresponding substrate solution (R&D Systems) for 20 minutes, with reaction stopped with 2N sulfuric acid. The amount of bound molecule was determined through measuring absorbance at 450 nm, with binding curves constructed using GraphPad Prism.

*4.2.6 Platelet-collagen inhibition studies*

Flow channel slides (Ibidi µ-Slide VI 0.1) were coated with 100 µg/mL of Chrono-Par fibrillar collagen type I for 1 h at room temperature. Channels were flushed three times with 1X PBS pH 7.4 (PBS) to remove any unbound collagen. Following an approved IRB protocol (WIRB protocol # 20,162,858), human blood was collected into citrated vacutainers and was used within 3 h of collection. Whole blood was removed from the vacutainers, pooled and then stained with Calcein-AM at 1 mg/mL in dimethyl sulfoxide (DMSO) for 30 min at 37 ºC. Hep-GQLY-SRR was then added to pre-stained human whole blood at various concentrations. Next, blood was perfused across each channel at a physiological shear rate of 1000 $s^{-1}$. Adherent cells were imaged using EVOS Fluorescence microscope (ThermoFisher Scientific). Platelet adhesion was quantified using NIH ImageJ software.

*4.2.7 Targeted delivery to injured vessels in vivo*

A rabbit artery crush model was used to investigate the ability of compounds to selectively bind to regions of injury. Female New Zealand rabbits (n=3/group) were anesthetized and the carotid artery was

exposed. Blood flow to an artery segment approximately 2 cm was arrested using a non-injurious clamp and blood was subsequently evacuated. Several crush injuries were then created by external clamping for 10 s using a hemostat. Compounds were then administered by ear vein through an IV catheter (1 mL/kg) and blood flow was restored for 2 h. Animals were then euthanized and the arteries were harvested, dissected longitudinally, pinned open to black foam board and fixed with formaldehyde for 1 h before transferring to 1X PBS pH 7.4 and stored at 4° C. The open face of the whole-mount arteries were positioned in a glass coverslip bottom dish (Ibidi μ-Dish) containing PBS and imaged on a LSM780 confocal microscope (Zeiss). Tissue autofluorescence and CF-633-labeled compound were imaged using 488 and 633 lasers, respectively. Maximum-intensity projections of the 3D-tiled confocal data were analyzed qualitatively for targeted binding of the fluorescently tagged molecule.

*4.2.8 Statistical Analysis*

Data are represented as the mean value of replicates, with error bars corresponding to their standard deviation. For the comparison between two groups, statistical significance was determined using a T-Test. For comparisons between three or more groups, a single factor equal variance ANOVA was performed. Differences between specific groups was determined using Tukey's post hoc test. Statistical analysis was performed using Graphpad Prism, with a probability value of 95% ($P < 0.05$) being used to determine statistical significance.

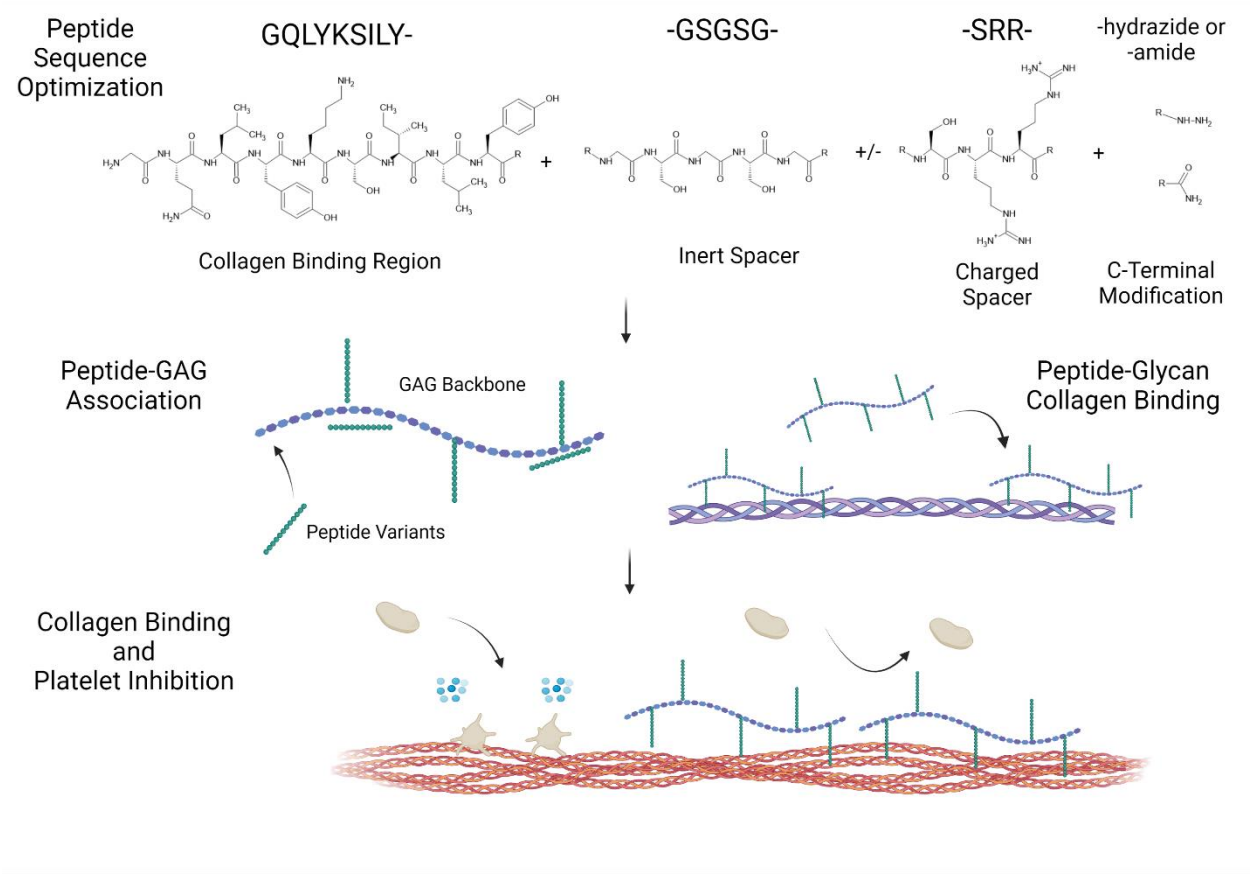


*Figure 4.1: Experiment scheme for GQLY sequence optimization*

**4.3 Results and Discussion:**

*4.3.1: Effect of SRR Spacer on GQLY Conjugation and Collagen Binding Activity*

Peptide conjugation and binding experiments were carried out with CS due to the intermediate degree of sulfation and molecular weight of CS relative to other glycans studied. Next, the importance of the inclusion of cationic charge within the spacer sequence for the GQLY peptide was investigated with regard to molecule synthesis and collagen binding ability. Two variants of the GQLY peptide were synthesized, one with a C-terminal spacer sequence of GSGSG, GQLYKSILYGSGSG-hydrazide (GSG-hyd), and one with C-terminal spacer sequence of GSGSRR, GQLYKSILYGSGSGSRR-hydrazide (SRR-hyd). CD analysis of both variants showed minimal difference in their structure, indicating that the addition of the SRR spacer did not significantly alter the structure of GQLY (Figure 4.2, Table 4.1). Given the negative

charge of the glycan backbone, it was theorized that having the additional positive charge conferred by the arginine residues proximal to C terminus would influence the peptide's association with the sulfated glycan backbone. Following the peptide – glycan reaction in which EDC was used to activate the glycan carbonyl-groups, there was significantly more peptide association with the SRR-hyd variant compared to the GSG-hyd variant (Figure 4.3a). This suggested that the additional positive charge present in the SRR spacer increased the ability of the GQLY peptide to interact with the negatively charged CS backbone.

**Table 4.1: Secondary structure calculations of GQLY variants SRR-hyd and GSG-hyd**

| | Helix | Antiparallel | Parallel | Turn | Others |
|---|---|---|---|---|---|
| SRR-hyd | 5.5 | 21.8 | 0 | 13.5 | 59.2 |
| GSG-hyd | 6.2 | 25.6 | 0 | 14.3 | 53.9 |

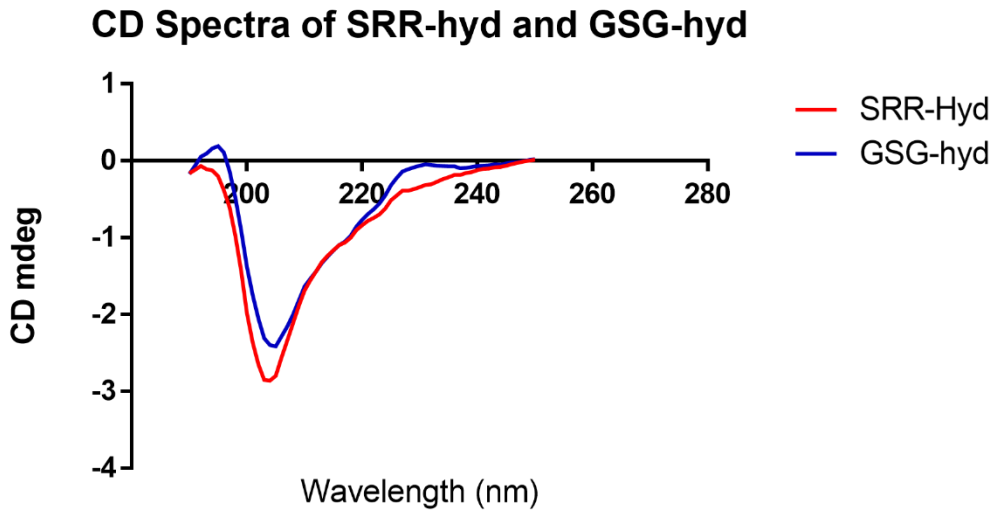


*Figure 4.2: CD Spectra of SRR-hyd and GSG-hyd GQLY variant peptides*

However, the method of peptide detection could not differentiate between covalently bound peptide and electrostatically bound peptide. While the peptide-glycans were purified against a 10 kDa cutoff membrane, it remained possible that peptides complexed with CS via electrostatic charge and were not removed during purification. To determine whether peptide remained bound electrostatically even following initial purification, the peptide-glycans were synthesized in the absence of EDC to eliminate covalent bonds formation. Again, significantly more of the SRR-hyd variant associated with CS compared to the GSG-hyd variant following the initial purification showing that the positive charge conferred by the SRR spacer was driving electrostatic interactions (Figure 4.3a). To probe the difference in covalent and electrostatic association, peptide-glycan that had been reacted with EDC was washed with a concentrated salt and urea solution to disrupt the electrostatic interactions, with the liberated peptide removed through centrifugation against a 10 kDa cutoff membrane. By measuring the associated peptide before and after this second purification, the amount of covalently bound peptide could be determined. Following salt washes, the SRR-hyd reacted peptide-glycan saw a 32% decrease in associated peptides, whereas the GSG-hyd reacted peptide-glycan only saw a 18% decrease in associated peptides (Figure 4.3b, Table 4.2). Furthermore, after electrostatically bound peptides were removed, the SRR-hyd group still exhibited increased association with CS compared the GSG-hyd group, suggesting that the SRR spacer sequence also had a positive effect on covalent conjugation and did not only enhance electrostatic association. The lack of electrostatic interaction following the second high salt purification was confirmed using MALDI-TOF-MS (Figure 4.4,4.5) where following the initial purification, free peptide peaks were seen in the MALDI-TOF-MS; however, following the second purification, no free peptide was observed in the MALDI-TOF-MS spectrum.

**Table 4.2: Average Change (n=3) in SRR-hyd and GSG-hyd association before and after salt and urea wash**

| | Pre-Salt Peptide/Disaccharide Percent | Post-Salt Peptide/Disaccharide Percent | Percent Decrease |
|---|---|---|---|
| CS + SRR-hyd | 16.2% ± 0.09% | 11.1% ± 0.51% | 32% |
| CS + GSG-hyd | 6.7% ± 0.11% | 5.7% ± 0.18% | 15% |

The importance of the SRR spacer on the degree of peptide-glycan binding to collagen was also analyzed. When applied to a collagen type I coated plate, the EC50 of the SRR-hyd conjugated peptide-glycan was an order of magnitude lower than the GSG-hyd conjugated peptide-glycan (Figure 4.3c). There are several possible reasons for this difference in binding capacity. First, the SRR spacer sequence may be responsible for supporting covalent conjugation through the hydrazide thereby orienting the peptide more favorably for collagen binding. Alternatively, the GSG-hyd conjugate peptide-glycan had significantly fewer peptides covalently attached to the glycan backbone, and this difference in peptides per glycan could be responsible for differences in binding. Finally, the addition of this longer peptide spacer and the increased distance between the collagen-binding sequence and the glycan backbone may have also allowed for better interaction with collagen. Regardless, the SRR spacer supports higher peptide-glycan conjugation efficiency and increased collagen binding capability of the peptide-glycan molecules.

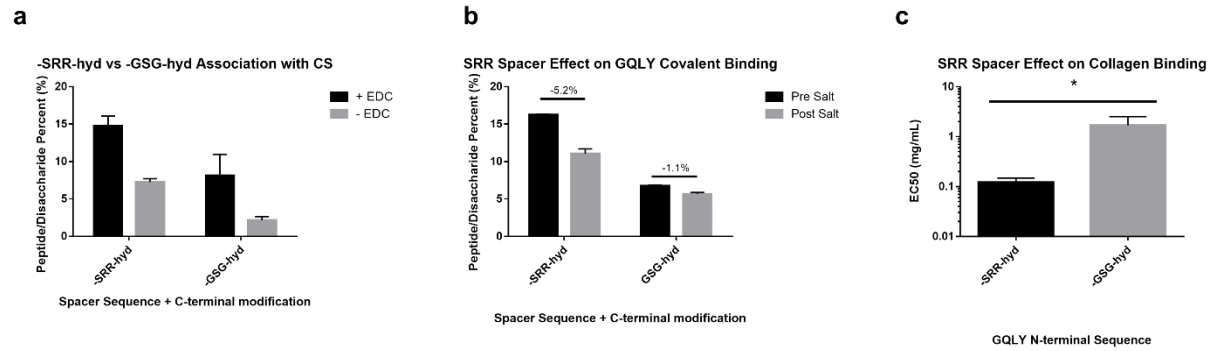

*Figure 4.3: Effect of SRR spacer on peptide-glycan association and collagen binding. A) Associated SRR-hyd or GSG-hyd with CS with and without EDC. B) Associated peptide before and after 1M NaCl and 8M Urea wash and filtration. C) EC50 of CS-GQLY on collagen type I surface with either SRR-hyd or GSG-hyd. * denotes statistical significance between groups.*

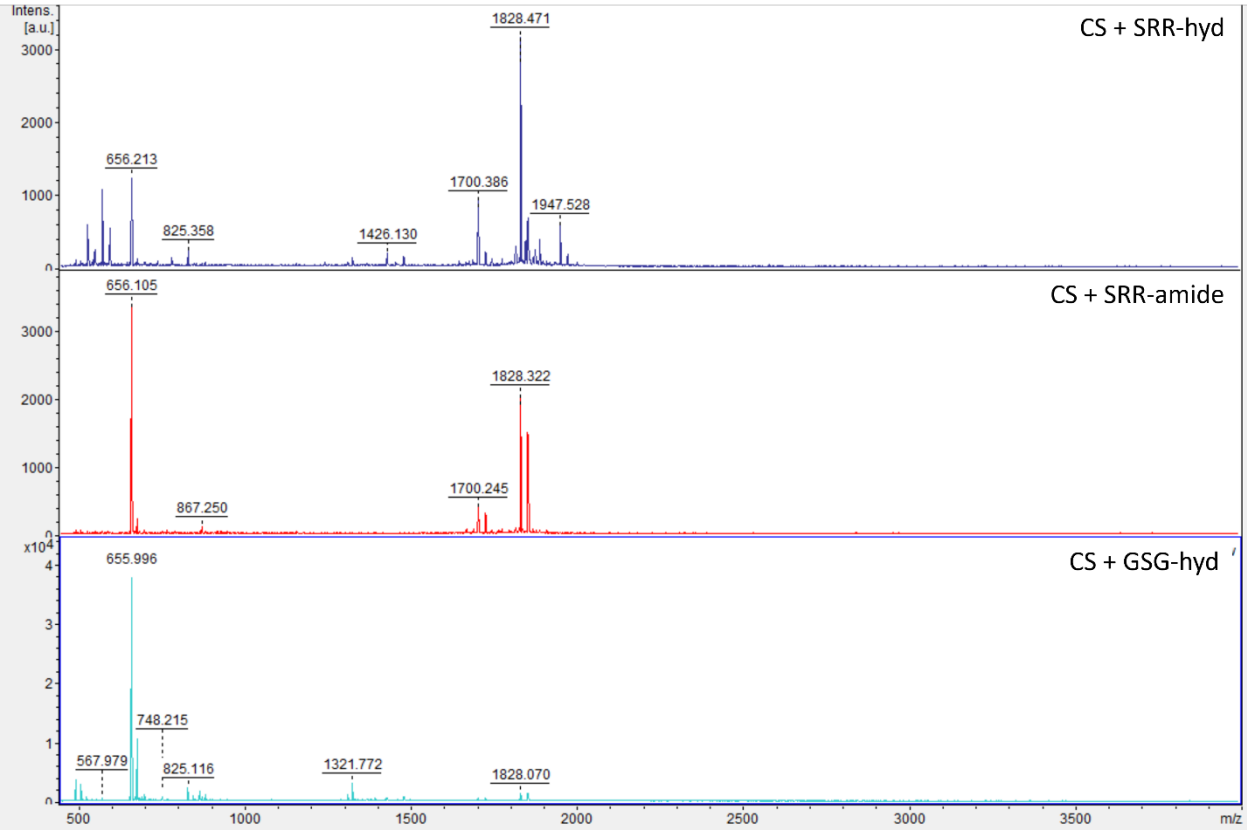


*Figure 4.4. MALDI-TOF MS spectra of CS + SRR-hyd, CS + SRR-SRR-amide, and CS+GSG-hyd before salt and urea wash*

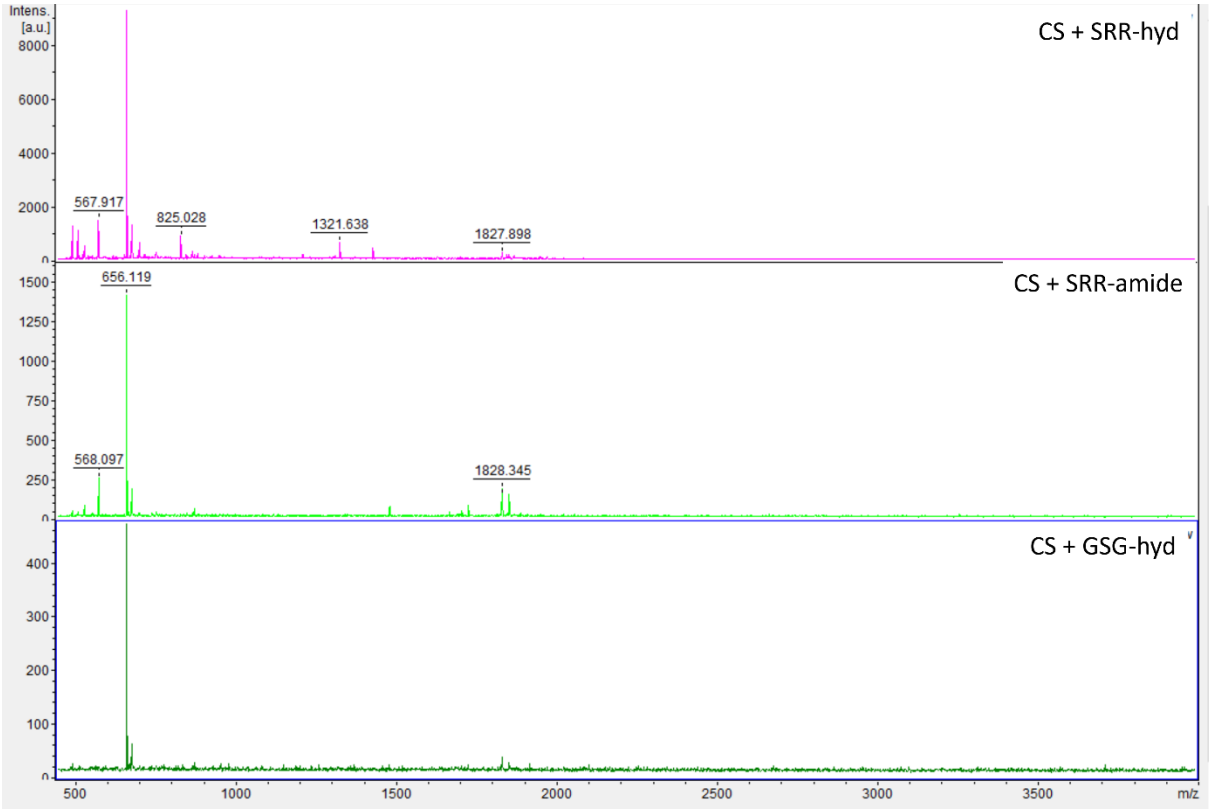


*Figure 4.5. MALDI-TOF MS spectra of CS + SRR-hyd, CS + SRR-SRR-amide, and CS+GSG-hyd after salt and urea wash*

*4.3.2: Effect of C-terminal hydrazide on GQLY Conjugation and Collagen Binding Activity*

The GQLY peptide has internal lysine residues (ε-amine) and an N-terminal amine that could contribute to covalent bonds between the peptide and glycan even though reaction conditions were optimized for hydrazide conjugation to the EDC activated glycan carboxylic acid residues as opposed to amine conjugation to the activated carbonyl. Thus, we tried to understand whether conjugation through the C-terminal hydrazide improved collagen binding. To explore the importance of the C-terminal reaction for collagen binding, a GQLY variant with the SRR spacer but with a non-reactive C-terminal amide, GQLYKSILYGSGSGSRR-amide (SRR-amide) was compared to the SRR-hyd peptide.

Following reaction with EDC, there was more SRR-hyd associated with CS compared to the SRR-amide variant (Figure 4.6a) suggesting that the SRR-hyd increase covalent conjugation, presumably through the more favorable hydrazide-COOH conjugation. In the absence of EDC, the amount of SRR-hyd and SRR-amide that associated with CS was equivalent (Figure 4.6a); which provides further evidence that the SRR spacer sequence promotes association with the glycan through electrostatic interactions. To determine if the difference in association following reaction in the presence of EDC was due to increased covalent conjugation, both peptide-glycan variants were washed with the concentrated salt and urea solution to remove the unbound peptides (Figure 4.4,4.5). Following this purification, both peptide-glycan variants exhibited similar decreases in associated peptides, with the SRR-hyd seeing change of 5.2% and the SRR-amide peptide-glycan seeing a change of 5.7% in the associated peptide to glycan disaccharide ratio suggesting similar levels of peptide-glycan associate driven by electrostatic interactions (Figure 4.6b, Table 4.3). Furthermore, the level of associated peptide was significantly higher for the SRR-hyd variant than for than the SRR-amide variant following salt dissociation (Figure 4.6b), indicating that adding the C-terminal hydrazide allows for increased covalent conjugation over that supported by the N-terminal amine and lysine.

**Table 4.3: Average Change (n=3) in SRR-hyd and SRR-amide association before and after salt and urea wash**

| | Pre-Salt Peptide/Disaccharide Percent | Post-Salt Peptide/Disaccharide Percent | Percent Decrease |
|---|---|---|---|
| CS + SRR-hyd | 16.2% ± 0.09% | 11.1% ± 0.51% | 32% |
| CS + SRR-amide | 13.1% ± 0.19% | 7.3% ± 0.18% | 44% |

Finally, to gain some insight as to whether N-terminal peptide conjugation vs. conjugation through the ϵ-amine of the lysine residues confers improved collagen binding, the collagen binding activity of the SRR-hyd and SRR-amide conjugated glycans was determined. In this case, the EC50 of the SRR-hyd peptide-glycan was again a magnitude lower than that of the SRR-amide peptide-glycan (Figure 4.3c). Although there were still fewer peptides covalently bound to the glycan in the case of the SRR-amide variant, the magnitude of the difference between the two was less than the between the SRR-hyd and GSG-hyd variants. As such, while this difference in binding capacity may be explained by a difference in conjugated peptides, it also plausible, and indeed likely, that the conjugation through the hydrazide over the amines present in the collagen binding sequence of GQLY provides an improved presentation of the peptide to the collagen substrate. Taking the findings from the SRR-amide variant and the GSG-hyd variant together, it appears that having both the SRR spacer sequence and the C-terminal hydrazide are important to the collagen binding capacity of GQLY when conjugated to a glycan backbone.

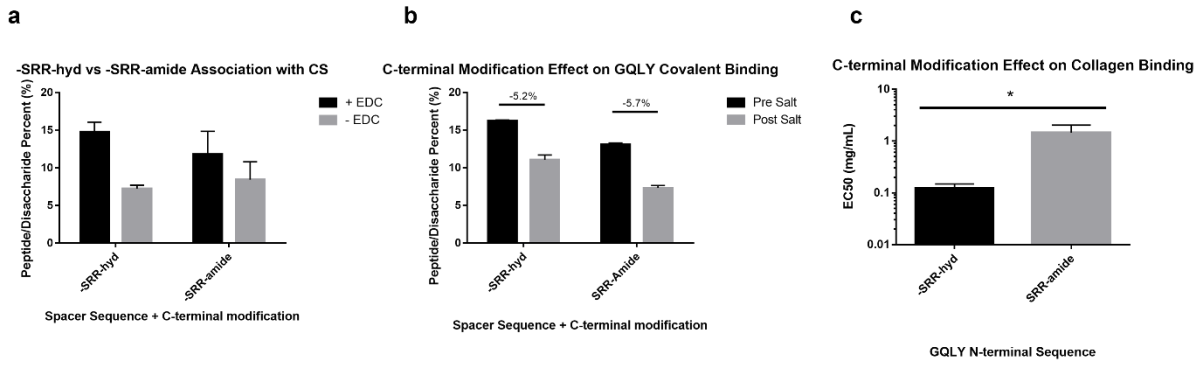


*Figure 4.6: Effect of C-terminal modification of GQLY on peptide-glycan association and collagen binding. A) Associated SRR-hyd or SRR-amide with CS with and without EDC. B) Associated peptide before and after 1M NaCl and 8M Urea wash and filtration. EC50 of CS-GQLY on collagen type I surface with either SRR-hyd or SRR-amide. * denotes statistical significance between groups. n.s. denotes no statistical significance between groups*

*4.3.3: Effect of Glycan choice on GQLY Conjugation and Collagen Binding Activity*

With the new understanding regarding how the SRR spacer and the C-terminal hydrazide affected conjugation to CS, we then sought to determine how the choice of glycan backbone affected the GQLY conjugation. For this, we looked at SRR-hyd conjugation to four glycans: heparin, CS, DS, and HA. Using these four glycans allowed us to investigate SRR-hyd conjugation at three different glycan sulfation levels, with heparin being the most sulfated, HA being unsulfated, and CS and DS having similar, intermediate levels of sulfation. Following salt washing, the conjugation of GQLY to the glycan backbones correlated with this sulfation trend: heparin supported the greatest GQLY conjugation, HA supported the least, and CS and DS supported the same intermediate level of GQLY conjugation (Figure 4.7a). Similar to how the change in positive charge of the peptide affected how it interacted with the glycan backbone, the sulfation, and by extension the negative charge of the glycan, affected the level of glycan-peptide association.

Next, the effect of the glycan backbone on the collagen-binding ability of the peptide-glycans was investigated using both heparin and CS. For this study, HA was not tested due to the significantly lower number of peptides attached. Since the SRR-hyd variant showed significant association with glycan backbone through electrostatic interactions, the peptide-glycans were also washed with the salt and urea solution to look at the collagen binding capacity with and without the electrostatically bound peptides. First, it was found that the collagen binding of the heparin and CS peptide-glycans was equivalent, with the EC50 of both being statistically similar to one another (Figure 4.7b). Furthermore, there was no difference in EC50 before and after the salt and urea washes (Figure 4.7b). This suggests that only covalently bound peptides contributed to the collagen binding of the peptide-glycan. Further, because electrostatically interacting peptide and peptide conjugated through $\varepsilon$-amine likely lie along the glycan backbone rather than extending from the glycan backbone, while the peptide conjugated through the C-

terminal hydrazide is more likely to extend from the backbone, this collagen-binding data suggests that peptide conjugated through the hydrazide shows a greater contribution to collagen binding than does peptide associated electrostatically or conjugated through the internal lysine residues of the peptide.

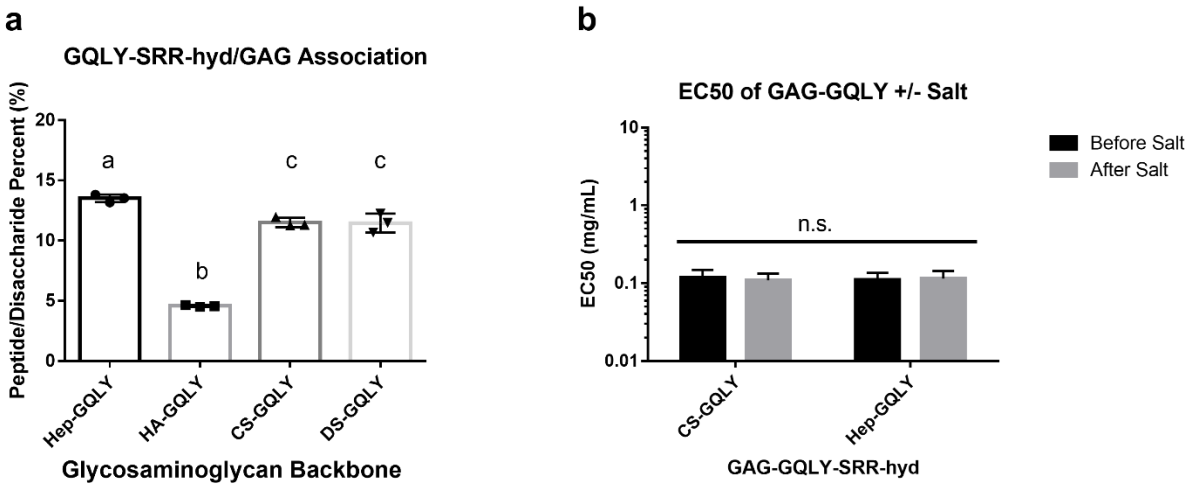


*Figure 4.7: Effect of glycan backbone on peptide-glycan association and collagen binding. A) SRR-hyd conjugation with heparin, HA, CS, and DS. B) EC50 of CS-GQLY and Hep-GQLY on collagen type I. Groups that do not share a letter are statistically significant from one other. n.s. denotes no statistical significance between groups.*

Recent decades of research have seen an increase in the use of conjugated peptides for biomedical uses[23–27]. Compared to proteins, peptides are significantly simpler and cheaper to produce while still providing their intended biological function[28]. However, as therapeutic peptides have yet to be produced on a mass scale, many peptides used still require custom synthesis, adding to their cost and the complexity of the synthesis of the final product[29]. As such, maximizing the reaction efficiency between the peptide and the substrate can improve the clinical translatability of peptide conjugated molecules and materials through reducing the required peptide to achieve desired conjugation targets. From this work, we have demonstrated that relatively simple changes to the non-functional portions of the peptide, the peptide spacer sequence, can have significant effects on the conjugation efficiency of a positively charged

peptide to a negatively charged macromolecule, a glycan backbone. Conversely, the charge properties of the glycan backbone also had an effect on the peptide/glycan conjugation efficiency, demonstrating multiple methods to modulate the peptide conjugation efficiency. As such, modulating the charge between the peptide and the conjunction substrate can be a method to increase the efficiency of conjugation.

*4.3.4 Platelet-collagen inhibition*

The ability of compounds to inhibit collagen-mediated platelet binding was evaluated with hep-GQLY-SRR because heparin and CS both showed maximal conjugation and collagen binding, while heparin is known to suppress platelet binding[14,30]. Strong inhibition of platelet adhesion to immobilized fibrillar collagen was observed with hep-GQLY-SRR in a dose-dependent manner with an IC50 of about 59 µg/mL (or approximately 3 uM). Maximal platelet inhibition was observed at about 0.5 mg/mL, at which more than 90% inhibition was achieved relative to untreated control channels (Figure 4.8). While this does translate to a higher concentration of heparin compared to the effective hourly dosages for preventing platelet adherence in preclinical studies, this molecule would only need to be delivered as a single treatment due to it localizing to the site of injury[31]. As such, no continuous infusion of heparin would be required, reducing the total heparin delivered to the body and alleviating the concern of systemic anti-platelet activity.

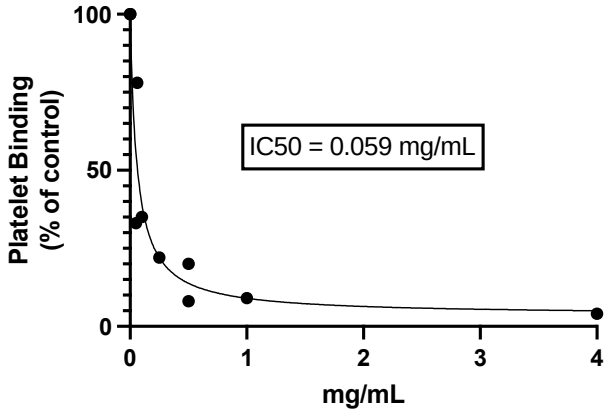

*Figure 4.8: IC50 of hep-GQLY platelet inhibition on collagen coated surface*

*4.3.5 In vivo targeted delivery*

Targeted delivery to areas of vessel injury was evaluated in a rabbit artery crush model with intravenous injection of fluorescently labeled Hep-GQLY-SRR at varying concentrations to investigate the molecule's ability to localize to the site of injury without significant off target binding. The appearance of fluorescence in regions of arterial clamp injuries was observed weakly at 0.16 mg/kg and with a strong signal at 1.6 mg/kg. No signal was observed in the vehicle control group or at 0.016 mg/kg dose level. Representative images from the various Hep-GQLY-SRR concentrations are shown in Figure 4.9. Importantly, no fluorescence signal was observed in areas of the vessel was that were not subject to clamp injury, indicating that targeted delivery only to areas of injury was achieved. Based on unpublished data, a similar collagen targeting peptide-glycan with a DS backbone maintained collagen-binding activity over the course of two weeks, though there was a decrease in binding activity due to hydrolytic degradation of the glycan backbone. As such, further investigation regarding the hydrolytic, as well as enzymatic, degradation of the peptide-glycan *in vivo* is required.

While the artery crush model used for this study best reflects the exposure of endothelial collagen following mechanical injury, such as in the case of balloon angioplasty procedures, the undesired exposure of collagen can occur in a variety of pathologies. As such, collagen-targeting biomolecules have a myriad of potential diagnostic and therapeutic uses given collagen's ubiquity throughout the body[32]. Several collagen binding peptides have been developed from native sources including the platelet collagen binding receptor[33] and the leucine rich repeat units of decorin[34,35]. In this study, we employed a modified version of a previously used platelet derived collagen binding sequence, RRANAALKAGELYKSILYGC, with the benefit of our GQLY sequence being its shorter sequence, resulting in a simpler and quicker synthesis[33]. Furthermore, by using a C-terminal hydrazide we no longer relied on oxidation of the glycan rings[33] or a heterobifunctional crosslinker[11] to conjugate the peptide to the glycan backbone, maintaining

the glycan structure and simplifying the chemistry. Although it is possible for conjugation to occur through other amines present on the peptide, we have demonstrated that the presence of the C-terminal hydrazide potentially drives conjugation through the hydrazide as opposed to the primary amines, improving the collagen binding ability of the molecule.

Additionally, through the addition of additional cationic charge to the spacer sequence of our collagen binding peptide, we were able to increase the binding capability of our peptide-glycan conjugate molecules. With minimal modification to the binding sequence, changes to the peptide spacer sequence resulted in a significant increase in collagen binding activity. This increased binding capability can allow for increased residence time within the body, prolonging the therapeutic life of the molecule. Alternatively, increased binding capability of the peptide can allow for a reduced number of peptides required for effective binding, resulting in reduced modification of the glycan backbone for increased glycan bioactivity[22] or increases in the number of additional therapeutic peptides[36]. Altogether, modulation of the peptide spacer sequence can allow for simplification of the conjugation chemistry, increased conjugation yields, and improved biological activity without the need for modification of the core peptide sequence.

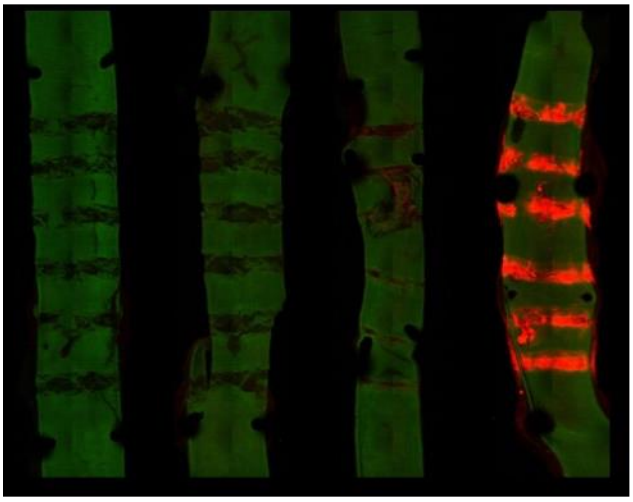

Control 0.016 mg/kg 0.16 mg/kg 1.6 mg/kg

*Figure 4.9: Representative images (n=3) of fluorescently labeled Hep-GQLY-SRR localization to site of artery crush. Maximum intensity projection with tissue autofluorescence shown in green, and fluorescently conjugated molecule shown in red localizing to areas of crush injury.*

**4.4: Conclusions:**

Data obtained through this study demonstrated that the peptide spacer is important to efficient peptide conjugation to glycan. The use of cationic charge proximal to the hydrazide group can improve peptide glycan interaction, which increases conjugation through the hydrazide functional group. Further, C-terminal conjugation appears to be critical in increasing the interaction of the peptide-glycan conjugate with collagen. This work suggests that including cationic charge in the intended bioconjugate can be used to increase the conjugation efficiency of peptides and other chemicals to glycans.

**References:**


(1) Paderi, J.; Prestwich, G. D.; Panitch, A.; Boone, T.; Stuart, K. Glycan Therapeutics: Resurrecting an Almost Pharma-Forgotten Drug Class. *Advanced Therapeutics* **2018**, *1* (8), 1800082. https://doi.org/10.1002/adtp.201800082.

(2) Wang, P.; Chi, L.; Zhang, Z.; Zhao, H.; Zhang, F.; Linhardt, R. J. Heparin: An Old Drug for New Clinical Applications. *Carbohydrate Polymers* **2022**, *295*, 119818. https://doi.org/10.1016/j.carbpol.2022.119818.

(3) Malloy, R. J.; Rimsans, J.; Rhoten, M.; Sylvester, K.; Fanikos, J. Unfractionated Heparin and Low-Molecular-Weight Heparin. In *Anticoagulation Therapy*; Lau, J. F., Barnes, G. D., Streiff, M. B., Eds.; Springer International Publishing: Cham, 2018; pp 31–57. https://doi.org/10.1007/978-3-319-73709-6_3.

(4) Strobel, H. A.; Qendro, E. I.; Alsberg, E.; Rolle, M. W. Targeted Delivery of Bioactive Molecules for Vascular Intervention and Tissue Engineering. *Frontiers in Pharmacology* **2018**, *9*.

(5) Manon-Jensen, T.; Kjeld, N. G.; Karsdal, M. A. Collagen-Mediated Hemostasis. *Journal of Thrombosis and Haemostasis* **2016**, *14* (3), 438–448. https://doi.org/10.1111/jth.13249.

(6) Nording, H. M.; Seizer, P.; Langer, H. F. Platelets in Inflammation and Atherogenesis. *Frontiers in Immunology* **2015**, *6*.

(7) Harifi, G.; Sibilia, J. Pathogenic Role of Platelets in Rheumatoid Arthritis and Systemic Autoimmune Diseases. *Saudi Med J* **2016**, *37* (4), 354–360. https://doi.org/10.15537/smj.2016.4.14768.

(8) D'Agnillo, F.; Walters, K.-A.; Xiao, Y.; Sheng, Z.-M.; Scherler, K.; Park, J.; Gygli, S.; Rosas, L. A.; Sadtler, K.; Kalish, H.; Blatti, C. A.; Zhu, R.; Gatzke, L.; Bushell, C.; Memoli, M. J.; O'Day, S. J.; Fischer, T. D.; Hammond, T. C.; Lee, R. C.; Cash, J. C.; Powers, M. E.; O'Keefe, G. E.; Butnor, K. J.; Rapkiewicz, A. V.; Travis, W. D.; Layne, S. P.; Kash, J. C.; Taubenberger, J. K. Lung Epithelial and Endothelial Damage, Loss of Tissue Repair, Inhibition of Fibrinolysis, and Cellular Senescence in

Fatal COVID-19. *Science Translational Medicine* **2021**, *13* (620), eabj7790. https://doi.org/10.1126/scitranslmed.abj7790.
(9) Karsdal, M. A.; Nielsen, S. H.; Leeming, D. J.; Langholm, L. L.; Nielsen, M. J.; Manon-Jensen, T.; Siebuhr, A.; Gudmann, N. S.; Rønnow, S.; Sand, J. M.; Daniels, S. J.; Mortensen, J. H.; Schuppan, D. The Good and the Bad Collagens of Fibrosis – Their Role in Signaling and Organ Function. *Advanced Drug Delivery Reviews* **2017**, *121*, 43–56. https://doi.org/10.1016/j.addr.2017.07.014.
(10) Paderi, J. E.; Stuart, K.; Sturek, M.; Park, K.; Panitch, A. The Inhibition of Platelet Adhesion and Activation on Collagen during Balloon Angioplasty by Collagen-Binding Peptidoglycans. *Biomaterials* **2011**, *32* (10), 2516–2523. https://doi.org/10.1016/j.biomaterials.2010.12.025.
(11) Scott, R. A.; Paderi, J. E.; Sturek, M.; Panitch, A. Decorin Mimic Inhibits Vascular Smooth Muscle Proliferation and Migration. *PLOS ONE* **2013**, *8* (11), e82456. https://doi.org/10.1371/journal.pone.0082456.
(12) Vallet, S. D.; Clerc, O.; Ricard-Blum, S. Glycosaminoglycan–Protein Interactions: The First Draft of the Glycosaminoglycan Interactome. *J Histochem Cytochem.* **2021**, *69* (2), 93–104. https://doi.org/10.1369/0022155420946403.
(13) Han, H. D.; Lee, A.; Song, C. K.; Hwang, T.; Seong, H.; Lee, C. O.; Shin, B. C. In Vivo Distribution and Antitumor Activity of Heparin-Stabilized Doxorubicin-Loaded Liposomes. *International Journal of Pharmaceutics* **2006**, *313* (1), 181–188. https://doi.org/10.1016/j.ijpharm.2006.02.007.
(14) Biran, R.; Pond, D. Heparin Coatings for Improving Blood Compatibility of Medical Devices. *Advanced Drug Delivery Reviews* **2017**, *112*, 12–23. https://doi.org/10.1016/j.addr.2016.12.002.
(15) Liang, Y.; Kiick, K. L. Heparin-Functionalized Polymeric Biomaterials in Tissue Engineering and Drug Delivery Applications. *Acta Biomaterialia* **2014**, *10* (4), 1588–1600. https://doi.org/10.1016/j.actbio.2013.07.031.
(16) Das Kurmi, B.; Tekchandani, P.; Paliwal, R.; Rai Paliwal, S. Nanocarriers in Improved Heparin Delivery: Recent Updates. *Current Pharmaceutical Design* **2015**, *21* (30), 4509–4518.
(17) Capila, I.; Linhardt, R. J. Heparin–Protein Interactions. *Angewandte Chemie International Edition* **2002**, *41* (3), 390–412. https://doi.org/10.1002/1521-3773(20020201)41:3<390::AID-ANIE390>3.0.CO;2-B.
(18) Schick, B. P.; Maslow, D.; Moshinski, A.; Antonio, J. D. S. Novel Concatameric Heparin-Binding Peptides Reverse Heparin and Low-Molecular-Weight Heparin Anticoagulant Activities in Patient Plasma in Vitro and in Rats in Vivo. *Blood* **2004**, *103* (4), 1356–1363. https://doi.org/10.1182/blood-2003-07-2334.
(19) Cho, Y.-S.; Han Ahn, K. Molecular Interactions between Charged Macromolecules : Colorimetric Detection and Quantification of Heparin with a Polydiacetylene Liposome. *Journal of Materials Chemistry B* **2013**, *1* (8), 1182–1189. https://doi.org/10.1039/C2TB00410K.
(20) Chiang, T. M.; Kang, A. H. A Synthetic Peptide Derived from the Sequence of a Type I Collagen Receptor Inhibits Type I Collagen-Mediated Platelet Aggregation. *J Clin Invest* **1997**, *100* (8), 2079–2084. https://doi.org/10.1172/JCI119741.
(21) Naggi, A.; Casu, B.; Perez, M.; Torri, G.; Cassinelli, G.; Penco, S.; Pisano, C.; Giannini, G.; Ishai-Michaeli, R.; Vlodavsky, I. Modulation of the Heparanase-Inhibiting Activity of Heparin through Selective Desulfation, Graded N-Acetylation, and Glycol Splitting. *J Biol Chem* **2005**, *280* (13), 12103–12113. https://doi.org/10.1074/jbc.M414217200.
(22) Nguyen, M.; Liu, J. C.; Panitch, A. Physical and Bioactive Properties of Glycosaminoglycan Hydrogels Modulated by Polymer Design Parameters and Polymer Ratio. *Biomacromolecules* **2021**. https://doi.org/10.1021/acs.biomac.1c00866.
(23) Park, S. H.; Seo, J. Y.; Park, J. Y.; Ji, Y. B.; Kim, K.; Choi, H. S.; Choi, S.; Kim, J. H.; Min, B. H.; Kim, M. S. An Injectable, Click-Crosslinked, Cytomodulin-Modified Hyaluronic Acid Hydrogel for Cartilage

Tissue Engineering. *NPG Asia Mater* **2019**, *11* (1), 1–16. https://doi.org/10.1038/s41427-019-0130-1.
(24) Yao, Y.; Zeng, L.; Huang, Y. The Enhancement of Chondrogenesis of ATDC5 Cells in RGD-Immobilized Microcavitary Alginate Hydrogels. *J Biomater Appl* **2016**, *31* (1), 92–101. https://doi.org/10.1177/0885328216640397.
(25) Akkiraju, H.; Srinivasan, P. P.; Xu, X.; Jia, X.; Safran, C. B. K.; Nohe, A. CK2.1, a Bone Morphogenetic Protein Receptor Type Ia Mimetic Peptide, Repairs Cartilage in Mice with Destabilized Medial Meniscus. *Stem Cell Res Ther* **2017**, *8* (1), 82. https://doi.org/10.1186/s13287-017-0537-y.
(26) Deloney, M.; Garoosi, P.; Dartora, V. F. C.; Christiansen, B. A.; Panitch, A. Hyaluronic Acid-Binding, Anionic, Nanoparticles Inhibit ECM Degradation and Restore Compressive Stiffness in Aggrecan-Depleted Articular Cartilage Explants. *Pharmaceutics* **2021**, *13* (9), 1503. https://doi.org/10.3390/pharmaceutics13091503.
(27) Hao, D.; Liu, R.; Fernandez, T. G.; Pivetti, C.; Jackson, J. E.; Kulubya, E. S.; Jiang, H.-J.; Ju, H.-Y.; Liu, W.-L.; Panitch, A.; Lam, K. S.; Leach, J. K.; Farmer, D. L.; Wang, A. A Bioactive Material with Dual Integrin-Targeting Ligands Regulates Specific Endogenous Cell Adhesion and Promotes Vascularized Bone Regeneration in Adult and Fetal Bone Defects. *Bioactive Materials* **2023**, *20*, 179–193. https://doi.org/10.1016/j.bioactmat.2022.05.027.
(28) Hosoyama, K.; Lazurko, C.; Muñoz, M.; McTiernan, C. D.; Alarcon, E. I. Peptide-Based Functional Biomaterials for Soft-Tissue Repair. *Frontiers in Bioengineering and Biotechnology* **2019**, *7*.
(29) Collier, J. H.; Segura, T. Evolving the Use of Peptides as Biomaterials Components. *Biomaterials* **2011**, *32* (18), 4198–4204. https://doi.org/10.1016/j.biomaterials.2011.02.030.
(30) Linhardt, R. J.; Murugesan, S.; Xie, J. Immobilization of Heparin: Approaches and Applications. *Current Topics in Medicinal Chemistry* **2008**, *8* (2), 80–100. https://doi.org/10.2174/156802608783378891.
(31) Hoover, R. L.; Rosenberg, R.; Haering, W.; Karnovsky, M. J. Inhibition of Rat Arterial Smooth Muscle Cell Proliferation by Heparin. II. In Vitro Studies. *Circ Res* **1980**, *47* (4), 578–583. https://doi.org/10.1161/01.res.47.4.578.
(32) Wahyudi, H.; Reynolds, A. A.; Li, Y.; Owen, S. C.; Yu, S. M. Targeting Collagen for Diagnostic Imaging and Therapeutic Delivery. *Journal of Controlled Release* **2016**, *240*, 323–331. https://doi.org/10.1016/j.jconrel.2016.01.007.
(33) Stuart, K.; Paderi, J.; Snyder, P. W.; Freeman, L.; Panitch, A. Collagen-Binding Peptidoglycans Inhibit MMP Mediated Collagen Degradation and Reduce Dermal Scarring. *PLOS ONE* **2011**, *6* (7), e22139. https://doi.org/10.1371/journal.pone.0022139.
(34) Federico, S.; Pierce, B. F.; Piluso, S.; Wischke, C.; Lendlein, A.; Neffe, A. T. Design of Decorin-Based Peptides That Bind to Collagen I and Their Potential as Adhesion Moieties in Biomaterials. *Angewandte Chemie International Edition* **2015**, *54* (37), 10980–10984. https://doi.org/10.1002/anie.201505227.
(35) Hunter, G. K.; Poitras, M. S.; Underhill, T. M.; Grynpas, M. D.; Goldberg, H. A. Induction of Collagen Mineralization by a Bone Sialoprotein–Decorin Chimeric Protein. *Journal of Biomedical Materials Research* **2001**, *55* (4), 496–502. https://doi.org/10.1002/1097-4636(20010615)55:4<496::AID-JBM1042>3.0.CO;2-2.
(36) Walimbe, T.; Dehghani, T.; Casella, A.; Lin, J.; Wang, A.; Panitch, A. Proangiogenic Collagen-Binding Glycan Therapeutic Promotes Endothelial Cell Angiogenesis. *ACS Biomater. Sci. Eng.* **2021**, *7* (7), 3281–3292. https://doi.org/10.1021/acsbiomaterials.1c00336.

# 5. Conclusions and future work

## 5.1 Conclusions

GAGs play an important role in nearly every tissue throughout the body[1]. Given their bioactivity[2–5], easily accessible reactive moieties, and relatively widespread commercial availability[6–9], many have sought to use them for a variety of therapeutic purposes. The aim of this thesis was to engineer GAGs to leverage their bioactive properties through chemical modification, balancing functionalization of the GAG backbone with leaving the polymer intact for biorecognition. As such, chapter two first looked at how modification affected recognition, with the subsequent chapter building off of this to utilize engineered GAGs for two clinical needs.

In chapter two, the interplay between chemical modification and the biorecognition of GAGs was investigated. GAGs have been widely used in the field of tissue engineering as components of cell scaffolds[10] or as parts of proteoglycan mimetic molecules[1]. Because of their repeating linear structure and many reactive moieties, GAGs possess some of the benefits of synthetic polymers, in that they're easy to chemically modify, while also possessing the potent bioactive signals like other biopolymers including collagen and fibrin. However, it was found that increased chemical modification of these polymers can reduce their biorecognition. This was demonstrated though decreased susceptibility to enzymatic degradation by hyaluronidase and decreased binding with CS and HA targeting peptides, two analogues for how proteins can interact with GAGs in the body, when the chemical modification of the GAGs was increased. For the purposes of forming hydrogels for tissue engineering scaffolds, a balance between functionalization and maintaining biorecognition is required, as too few crosslinks in a material yields a material too weak to support growth. This balance was found for a 1.5 GAG wt% hydrogel, with 17% modification, which formed a robust hydrogel while leaving the majority of the GAG unmodified to retain

native biological activity. Other aspects of GAG hydrogels were investigated, including the molecular weight of the HA incorporated and how the blending of CS and HA affected the hydrogel properties. Although HA molecular weight did not appear to have a large effect on stiffness or degradation, the blending of CS and HA changed these properties. Surprisingly, although CS was found to be less susceptible to degradation by hyaluronidase, the blending of CS and HA resulted in a hydrogel that less susceptible to degradation than were both the CS and HA homopolymer hydrogels, most likely due to the interplay of increased swelling pressure conferred by the higher anionic charge of CS homopolymer and the decreased CS susceptibility to hyaluronidase. Finally, hydrogels that contained CS resulted in increased MSC viability over the course of one week compared to the HA homopolymer hydrogel, though the amount of CS had no effect on cell viability. In all, this chapter demonstrates the need to balance chemical modification of GAGs with maintaining bioactivity, as well as how blending of CS and HA can modulate hydrogel properties.

In chapter three, the blended CS/HA hydrogel was used to suppress the inflammatory response of encapsulated chondrocytes from pro-inflammatory cytokines. This was investigated as a method to engineer cartilage in a pro-inflammatory environment, as the progression of cartilage degradation that occurs during osteoarthritis is caused by secreted pro-inflammatory cytokines from the cartilage and synovial cells[11,12]. fbACs were encapsulated in CS/HA DPN hydrogels as well as IPN hydrogels made from a blend of crosslinked CS and HA and uncrosslinked collagen type I to modulate hydrogel mechanical properties and possibly provide additional binding sites for encapsulated cells. Despite differences in polymer composition, the initial mechanical properties of the hydrogels were the same, though the long-term material properties differed. Following fourteen days of pro-inflammatory culture, hydrogels with cells encapsulated within them saw no significant differences in material compressive strength or mass, signifying there was no significant enzymatic degradation due to Il-1β mediated hyaluronidase activity. Small increases in metabolic activity, DNA content, and Il-6 production were observed, though this was to

a lesser degree when compared to a collagen only hydrogel control. Similarly, genes for MMP13 were upregulated and genes for collagen type II and aggrecan were downregulated when compared to unstimulated controls. However, the chondrocytes in GAG hydrogels expressed MMP13 to a lesser degree and anabolic genes to a greater degree when compared to a collagen only hydrogel. These data suggest that culturing in GAG hydrogels can suppress inflammation in encapsulated chondrocytes when compared to a collagen hydroge118oweverver, inflammation was not completely prevented, leaving room for additional work to completely protect the encapsulated cells.

In chapter four, the spacer sequence of the collagen-binding peptide GQLY was optimized for improved binding ability when conjugated to a GAG backbone. In all variants of the GQLY peptide, the original binding sequence was unchanged, with only the spacer sequence and the C-terminal modification seeing change. The addition of two C-terminal arginines significantly increased the association of GQLY to a CS backbone. Following disassociation of the electrostatically bound peptides, the SRR-hyd variant still had increased conjugation efficiency over the GSG-hyd variant, demonstrating that the additional C-terminal positive charge improved covalent conjugation, not just electrostatic association. Furthermore, the CS-SRR-hyd molecule showed improved collagen binding over the CS-GSG-hyd variant, demonstrating the importance of the C-terminal spacer in collagen binding function. Focusing on the C-terminal modification, there was increased conjugation with the the SRR-hyd variant compared to the SRR-amide variant, though the SRR-amide variant still had a significant amount of chemical conjugation to the CS backbone. This suggests, despite the acidic reaction environment, that the peptide can conjugate to the backbone through the primary amines present on the peptide, including the N-terminal amine and the lysine $\varepsilon$-amine. However, the CS-SRR-hyd molecule still had improved collagen binding ability over the CS-SRR-amide molecule, demonstrating the importance of the C-terminal conjugation point for peptide function. The GAG backbone also had a significant effect on the conjugation efficiency, with the most sulfated GAG, heparin, having improved conjugation compared to CS and DS, which had higher

conjugation efficiency over the unsulfated GAG HA. However, between CS and heparin, there were no differences in collagen binding. For the purposes of blocking collagen mediated platelet activation, Hep-SRR-hyd blocked platelet activation from a collagen coated surface at an IC50 of 59 μg/mL and reached maximum inhibition at 0.5 mg/mL. Following *in vivo* delivery to a crushed rabbit artery, Hep-SRR-hyd showed localization to the exposed collagen surfaces. From this study, it was demonstrated that the reaction efficiency and function of peptides conjugated to GAGs can be modulated through the non-functional portions of the sequence, reducing the need for excess peptide during the reaction and improving the efficacy of peptide-glycan therapeutic molecules.

**5.2 Future Work**

From chapters three and four, two paths can be taken with regard to future work. For the anti-inflammatory activity of the GAG/collagen IPN hydrogels, full prevention of inflammation was not obtained. To further reduce inflammation and protect the chondrogenic phenotype, additional anti-inflammatory factors can be introduced into the hydrogel. For example, a previously used cell penetrating MK2 inhibitor peptide can be incorporated into the negatively charged GAG hydrogel[13]. Because of the high positive charge of the peptide, the residence time of the peptide would likely be increased. Furthermore, one significant weakness of using chondrocytes for tissue engineering applications is their source, as they have to be used autologously to prevent a host rejection response. Harvesting autologous chondrocytes can result in donor site morbidity[14] and the culture of chondrocytes on two-dimensional tissue culture plastic will result in dedifferentiation[15]. As such, replacing the chondrocytes in these GAG hydrogels with a co-culture of MSCs and autologous chondrocytes can reduce the number of chondrocytes needed while also providing anti-inflammatory cues from the secretome of the MSCs, improving tissue engineering outcomes.

From chapter four, future work would look at applying these spacer modifications to other peptides to see if this can also improve their conjugation efficiency. One potential target for this would be the LXW7 peptide, a cyclic RGD proangiogenic peptide that has been conjugated onto a DS backbone[16]. However, some significant issues with this peptide are its low conjugation efficiency and low synthesis yields. This may stem from its negative charge from the aspartic acid residues or its cyclic structure. The addition of C-terminal arginines and the associated increase in the C-terminal charge may be able to overcome the forces that prevent its conjugation to a GAG backbone, improving the clinical translatability of LXW7-glycan molecules.

GAGs lie in an overlap between synthetic polymers and other bioactive polymers, where they possess some of the tunability of synthetic polymers like poly(ethylene glycol) while having bioactive properties like ECM derived proteins such as collagen and elastin. While already well used for a variety of biomedical applications, GAGs based therapeutics still possess the potential for further development in many applications. As fabrication strategies such as 3D printing and microfluidics mature, because of their ease of tunability, GAG based materials stand to balance the tunability requirements that these fabrications require with potent bioactive signals. This can allow for previse control over material shape and mechanical properties, properties important to the direction of cell fate, while also providing the biological signals from GAGs. Additionally, the field of glycan therapeutics still has much room to develop, with GAGs and other glycan based therapeutics only recently seeing an increase in interest. Tuning the presentation of these molecules through chemical modification can provide improved efficacy of these molecules, though this modification must be balanced with preservation of the molecules bioactivity. Altogether, whether in the form of a material or as a soluble therapeutic, much work has been done with GAGs to apply them to biomedical applications, with many potential applications for these polymers still remaining.

**5.3 References**

(1) Nguyen, M.; Panitch, A. Proteoglycans and Proteoglycan Mimetics for Tissue Engineering. *American Journal of Physiology-Cell Physiology* **2022**. https://doi.org/10.1152/ajpcell.00442.2021.
(2) Altman, R.; Bedi, A.; Manjoo, A.; Niazi, F.; Shaw, P.; Mease, P. Anti-Inflammatory Effects of Intra-Articular Hyaluronic Acid: A Systematic Review. *CARTILAGE* **2019**, *10* (1), 43–52. https://doi.org/10.1177/1947603517749919.
(3) Iovu, M.; Dumais, G.; du Souich, P. Anti-Inflammatory Activity of Chondroitin Sulfate. *Osteoarthritis and Cartilage* **2008**, *16*, S14–S18. https://doi.org/10.1016/j.joca.2008.06.008.
(4) Aisenbrey, E. A.; Bryant, S. J. The Role of Chondroitin Sulfate in Regulating Hypertrophy during MSC Chondrogenesis in a Cartilage Mimetic Hydrogel under Dynamic Loading. *Biomaterials* **2019**, *190–191*, 51–62. https://doi.org/10.1016/j.biomaterials.2018.10.028.
(5) Amann, E.; Wolff, P.; Breel, E.; van Griensven, M.; Balmayor, E. R. Hyaluronic Acid Facilitates Chondrogenesis and Matrix Deposition of Human Adipose Derived Mesenchymal Stem Cells and Human Chondrocytes Co-Cultures. *Acta Biomater.* **2017**, *52*, 130–144. https://doi.org/10.1016/j.actbio.2017.01.064.
(6) Van der Meer, J.-Y.; Kellenbach, E.; Van den Bos, L. J. From Farm to Pharma: An Overview of Industrial Heparin Manufacturing Methods. *Molecules* **2017**, *22* (6), 1025. https://doi.org/10.3390/molecules22061025.
(7) Garnjanagoonchorn, W.; Wongekalak, L.; Engkagul, A. Determination of Chondroitin Sulfate from Different Sources of Cartilage. *Chemical Engineering and Processing: Process Intensification* **2007**, *46* (5), 465–471. https://doi.org/10.1016/j.cep.2006.05.019.
(8) Schiraldi, C.; Cimini, D.; De Rosa, M. Production of Chondroitin Sulfate and Chondroitin. *Appl Microbiol Biotechnol* **2010**, *87* (4), 1209–1220. https://doi.org/10.1007/s00253-010-2677-1.
(9) Woo, J. E.; Seong, H. J.; Lee, S. Y.; Jang, Y.-S. Metabolic Engineering of Escherichia Coli for the Production of Hyaluronic Acid From Glucose and Galactose. *Frontiers in Bioengineering and Biotechnology* **2019**, *7*.
(10) Sodhi, H.; Panitch, A. Glycosaminoglycans in Tissue Engineering: A Review. *Biomolecules* **2021**, *11* (1), 29. https://doi.org/10.3390/biom11010029.
(11) Goldring, M. B.; Otero, M. Inflammation in Osteoarthritis. *Current Opinion in Rheumatology* **2011**, *23* (5), 471–478. https://doi.org/10.1097/BOR.0b013e328349c2b1.
(12) Lieberthal, J.; Sambamurthy, N.; Scanzello, C. R. Inflammation in Joint Injury and Post-Traumatic Osteoarthritis. *Osteoarthritis Cartilage* **2015**, *23* (11), 1825–1834. https://doi.org/10.1016/j.joca.2015.08.015.
(13) Deloney, M.; Smart, K.; Christiansen, B. A.; Panitch, A. Thermoresponsive, Hollow, Degradable Core-Shell Nanoparticles for Intra-Articular Delivery of Anti-Inflammatory Peptide. *Journal of Controlled Release* **2020**, *323*, 47–58. https://doi.org/10.1016/j.jconrel.2020.04.007.
(14) Andrade, R.; Vasta, S.; Pereira, R.; Pereira, H.; Papalia, R.; Karahan, M.; Oliveira, J. M.; Reis, R. L.; Espregueira-Mendes, J. Knee Donor-Site Morbidity after Mosaicplasty – a Systematic Review. *J EXP ORTOP* **2016**, *3* (1), 31. https://doi.org/10.1186/s40634-016-0066-0.
(15) Duan, L.; Ma, B.; Liang, Y.; Chen, J.; Zhu, W.; Li, M.; Wang, D. Cytokine Networking of Chondrocyte Dedifferentiation in Vitro and Its Implications for Cell-Based Cartilage Therapy. *Am J Transl Res* **2015**, *7* (2), 194–208.
(16) Walimbe, T.; Dehghani, T.; Casella, A.; Lin, J.; Wang, A.; Panitch, A. Proangiogenic Collagen-Binding Glycan Therapeutic Promotes Endothelial Cell Angiogenesis. *ACS Biomater. Sci. Eng.* **2021**, *7* (7), 3281–3292. https://doi.org/10.1021/acsbiomaterials.1c00336.